CHEMICAL REVIEWS

Review

pubs.acs.org/CR

Heterogeneously Catalyzed Hydrothermal Processing of C_5–C_6 Sugars

Xingguang Zhang, Karen Wilson, and Adam F. Lee*

European Bioenergy Research Institute, Aston University, Birmingham B4 7ET, United Kingdom

ABSTRACT: Biomass has been long exploited as an anthropogenic energy source; however, the 21st century challenges of energy security and climate change are driving resurgence in its utilization both as a renewable alternative to fossil fuels and as a sustainable carbon feedstock for chemicals production. Deconstruction of cellulose and hemicellulose carbohydrate polymers into their constituent C_5 and C_6 sugars, and subsequent heterogeneously catalyzed transformations, offer the promise of unlocking diverse oxygenates such as furfural, 5-hydroxymethylfurfural, xylitol, sorbitol, mannitol, and gluconic acid as biorefinery platform chemicals. Here, we review recent advances in the design and development of catalysts and processes for C_5–C_6 sugar reforming into chemical intermediates and products, and highlight the challenges of aqueous phase operation and catalyst evaluation, in addition to process considerations such as solvent and reactor selection.

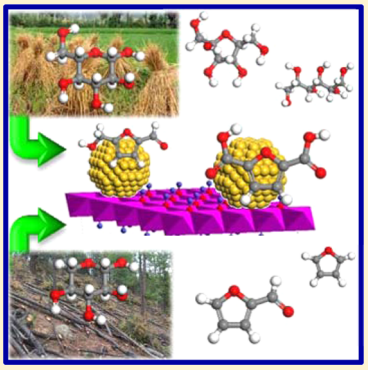

CONTENTS

1. INTRODUCTION

1.1. Biomass Conversion and Hydrothermal Processing of Sugars

The quest for sustainable resources to meet the energy, food, and materials nexus of needs for a rising global population, set against the backdrop of climate change and dwindling ecodiversity, necessitates new chemical technologies. Global

Received: May 16, 2016
Published: September 28, 2016

DOI: 10.1021/acs.chemrev.6b00311
Chem. Rev. 2016, 116, 12328–12368

energy demand is expected to rise 2% per annum, with 2050 energy consumption predicted to be twice that of 2001, with associated CO_2 emissions increasing from 6.6 to 11.0 GtC yr^{-1}.[1] The Copenhagen Accord stated that greenhouse gas concentrations in the atmosphere should be stabilized at a level that would prevent dangerous anthropogenic interference with the climate system, with the ensuing scientific consensus that the global temperature rise by the end of the 21st century should be <2 °C relative to preindustrial levels.[2] In 2015, the Paris COP21 UN conference on climate change culminated in 195 countries adopting the first universal commitment to cut greenhouse gases, affirming the prior aspirational goal to limit warming <2 °C and indeed strive to keep global temperature rises <1.5 °C, heralding what some considered the dawn of the postfossil fuel era.[3] Realizing these ambitious targets will require a transition from traditional fossil fuel resources to renewables, notably nuclear, solar, wind, and wave power, and biomass.[4] Biomass is a generic term describing biogenic organic matter, typically formed through photosynthesis, with the potential to replace fossil feedstocks for the production of biobased transportation fuels, heat, power, and biomaterials, in addition to underpinning new chemical platforms (Figure 1).[5−8]

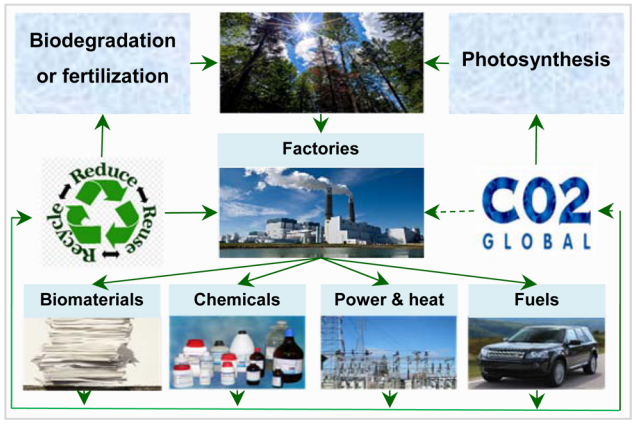

Figure 1. Carbon neutral circular framework for biomass.

Recent decades have witnessed an inauspicious beginning to global biomass utilization, with large-scale diversion of edible plant crops toward bioethanol and first-generation biodiesel manufacture impacting upon food supply and prices. The ensuing "food versus fuel" debate highlighted the importance of identifying inedible and waste biomass feedstocks, in tandem with the biorefinery concept for the coproduction of high volume/low value fuels and low volume/high value chemicals. In 2004, The U.S. Department of Energy (DOE) identified a range of such sugar-derived platform chemicals accessible through the chemical or biochemical transformation of lignocellulosic biomass (Figure 2) that would be potential target products from biorefineries, several of which are featured in this Review.

Lignocellulose is the most abundant biomass source inedible to humans, prevalent in plant walls, and comprises a mixture of cellulose and hemicellulose carbohydrate polymers embedded in a lignin matrix.[9,10] Lignin is a three-dimensional network of polyaromatic alcohols, whose catalytic upgrading is now viewed as an important source of renewable value added chemicals.[11] Hemicellulose comprises pentose (xylose predominantly) and hexose units connected by different glycosidic bonds. Cellulose

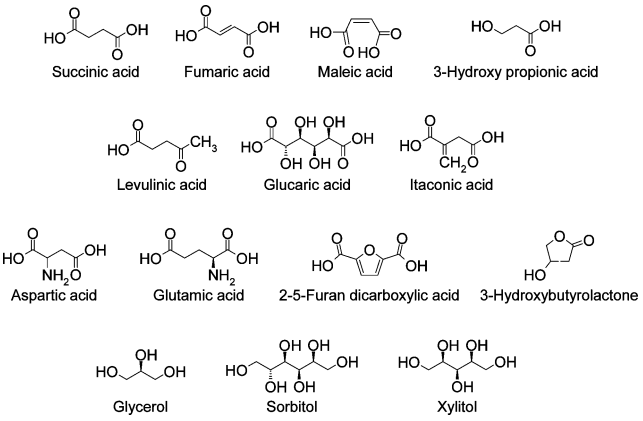

Figure 2. 2004 DOE top biobased products from biorefinery carbohydrates.

is a water insoluble, linear polysaccharide formed from glucose units linked via β-1,4-glycosidic bonds (Figure 3).[12] Ligno-

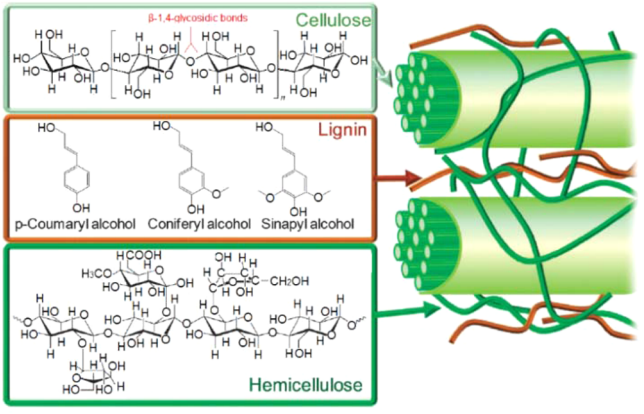

Figure 3. Schematic of cellulose, hemicellulose, and lignin components of lignocellulosic biomass and associated molecular building blocks. Reproduced with permission from ref 12. Copyright 2012 The Royal Society of Chemistry.

cellulose from different sources, regions, and seasons exhibits significant variations in the proportions of the aforementioned components; however, the combined hemicellulose and cellulose content generally exceeds 60 wt %.[13]

Popular approaches to lignocellulosic biomass conversion to fuels and chemicals, via noncatalytic thermochemical and enzymatic biochemical platforms, including gasification[14−19] to produce syngas (CO/H_2) or H_2, fast pyrolysis[20−24] or liquefaction[25−27] to produce bio-oils, or sugar fermentation to bioethanol,[28−32] butanol,[33−35] or other high value chemicals,[36−38] have been comprehensively reviewed. Thermochemical methods such as gasification are rather crude, unselective routes to the production of platform chemicals from highly functional biomass components, and syngas production from high-quality biomass as a route to subsequent hydrocarbon (e.g., Fischer−Tropsch) synthesis cannot therefore be rationalized unless the biomass feedstock is particularly recalcitrant and unsuitable for processing via more economic methods. Biomass fast pyrolysis offers a potential route to drop-in liquid hydrocarbon fuels, but is limited by the poor quality of the resulting bio-oils (high oxygen content, low heating value of typically 16−19 MJ kg^{-1}, i.e., one-half that of petroleum-

DOI: 10.1021/acs.chemrev.6b00311
Chem. Rev. 2016, 116, 12328−12368

derived fuels, corrosive nature, high viscosity, immiscibility with conventional fuels, and poor chemical stability), which hence require costly and energy intensive upgrading treatments prior to use as a biofuel. Fast pyrolysis also requires predried biomass feeds, compromising the potential economic advantage of important wet feedstocks such as algae.[39,40] Hydrothermal liquification is a moderate temperature/high pressure process to depolymerize solid biomass and yields higher energy density (5−20 wt % oxygen content) bio-oils and chemicals, but is also unselective and requires high capital investment in robust reactor construction materials and energy intensive operation.[25] Biocatalytic processes generally offer superior activity and selectivity than chemical catalysts; however, while widely investigated in the context of biorefineries[41] for bioalcohol production,[42] processes become less viable when the target products are involatile and/or in low concentration, making their isolation economically prohibitive.[43]

C_5−C_6 sugar monomers derived from nonfood (hemi)-cellulose have risen in prominence as key building blocks of biofuels and platform chemicals for either drop-in or new applications. However, obtaining such sugars from lignocellulosic biomass for chemical (or biochemical) processes is particularly challenging due to the difficulty of separating (hemi)cellulose from lignin, and hemicellulose from cellulose in turn. Hence, while enzymatic transformation of sugars to chemicals and fuels is an attractive prospect, this requires extensive processing of raw biomass.[31,44] Fractionation to isolate cellulose, lignin, and hemicellulose is typically performed via acid or base hydrolysis, steam explosion,[45] or organosolv treatments[46] to separate the polysaccharide from lignin.[47] Biomass pretreatment is an area of intensive research wherein greener methods are sought, and is expected to play an increasingly important role in biorefinery viability.[48] Such greener strategies have been the subject of reviews spanning supercritical fluids[49] (with CO_2 showing promise as both solvent and acid to hydrolyze biomass in subcritical pressurized water[50]) to ionic liquids (ILs)[51−56] or deep eutectic solvents (DESs) whose properties can be tuned to dissolve lignin or cellulose selectively.[57−60] Once separated, cellulose fractions are typically hydrolyzed to fermentable sugars for further processing into fuels and/or chemicals via enzymatic,[61] chemical (acid or base),[62,63] supercritical water,[64] or more recently IL-based treatments.[65]

ILs and DESs have similar properties, and are based on salts with poorly coordinated ions present in the liquid phase at normal operating temperatures (typically <150 °C), but differ in the properties of their ionic components. ILs comprise a single discrete anion and cation pair, often based upon tetraalkylammonium, 1,3-dialkylimidazolium, tetraalkylphosphonium, and alkylpyridinium cations with a range of anions. ILs have essentially no vapor pressure at chemically relevant temperatures, and are thermally stable as liquids at temperatures exceeding 300 °C. In contrast, DESs are mixtures of various anionic and/or cationic species formed when Lewis or Brønsted acids and bases are mixed.[59] The combination of ILs and CO_2 in the presence of a solid acid catalyst has been reported for phenolics extraction from lignocellulose.[66] Despite the advantages of ILs as reaction media for biomass conversion, their industrial uptake has been limited for several reasons: (i) the high cost of some ILs; (ii) energy intensive product separation and purification from ILs; (iii) lack of data regarding their toxicity and biodegradability; and (iv) IL contamination by oligomeric species and humins produced as byproducts during biomass processing,[67] which render these processes economically unfavorable on a commercial scale. Low-cost ILs have been developed ($\lesssim$\$2.50 kg^{-1}), which enable competition with conventional solvents.[55] DESs are promising alternatives to ILs, which allow the use of benign Lewis acids and/or bases of general formula Cat^+X^-zY, where Cat^+ is cationic ammonium, phosphonium, or sulfonium species and X^- is a Lewis base (typically a halide anion). DESs have been reviewed in detail,[59,60] and in the context of biomass fractionation DESs based on choline chloride with urea, malonic acid, lactic, malic, or oxalic acid[68] offer process advantages similar to those of ILs, while mitigating toxicity of the cationic (e.g., imidazolium, pyridinium, or pyrrolidinium) components.[69−71] Despite progress in this area of "green solvents", much research is required for their large-scale application to biomass fractionation, specifically to minimize solvent use, improve energy/atom economies, and minimize wastewater production during acid/base neutralization.[72,73] Water recovery and reuse remains a challenge in biorefineries, and the cost of removing trace organic contaminants may be prohibitive,[74] with product separation hindered by physical and chemical barriers such as polarity and azeotropy. Imidazolium-based ILs have been advanced as a means to separate target components from biorefinery streams,[75] with examples spanning the extractive separation of ethanol−water mixtures or the removal of ethanol, butanol, or lactic acid from fermentation broths. Tuning ILs polarity and thermal properties by altering the cation−anion combination[76] makes them attractive alternatives to volatile organic solvents for separation/extraction processes.[77−79] Imidazolium-based ILs can aid the separation and dehydration of ethanol from azeotropic water mixtures by enhancing the relative volatility of ethanol;[80] efficacy for ethanol separation via extractive distillation follows the order [BMIM]Cl > [EMIM][BF_4] > [BMIM][BF_4].[81] ILs such as trihexyltetradecylphosphonium dicyanamide ($P_{666,14}$[$N(CN)_2$]) are also promising for aromatics extraction from aqueous sugar solutions obtained from biomass pyrolysis, permitting their subsequent fermentation or catalytic upgrading. ILs have also shown particular promise as a medium for biomass conversion, with the catalytic transformation of glucose and fructose to 5-HMF receiving particular attention.[82,83] Soluble Lewis acid catalysts such as $SnCl_4$ are particularly effective for glucose conversion into 5-HMF in 1-ethyl-3-methylimidazolium tetrafluoroborate ([EMIM]BF_4). [EMIM]BF_4/$SnCl_4$ alone is also effective for the conversion of fructose, sucrose, inulin, cellobiose, and even starch to 5-HMF, demonstrating the generality of ILs as reactive solvents.[84] The IL catalytic performance can also be fine-tuned by varying the alkyl chain length of the cation, as observed in the direct conversion of glucose to 5-HMF in dialkylimidazolium chlorides with germanium(IV) chloride, where 5-HMF yields decreased from 38.4% to 23.3% when the alkyl group changed from butyl to decyl.[85]

Mechanocatalysis offers an intriguing opportunity for solvent-free biomass processing.[86,87] For example, H_2SO_4 impregnated lignocellulosic substrates offer a clean and efficient route to one-pot biomass depolymerization, in which mechanical forces and mineral acids convert dry lignocellulose into water-soluble products comprising oligosaccharides and lignin fragments.[86,88] Heterogeneous analogues, employing clays and simple metal oxides, have also been exploited in mechanocatalysis of cellulose to glucose, in addition to

DOI: 10.1021/acs.chemrev.6b00311
Chem. Rev. 2016, 116, 12328−12368

Scheme 1. Core Catalytic Technologies and Biorefinery Concept Underpinning This Review

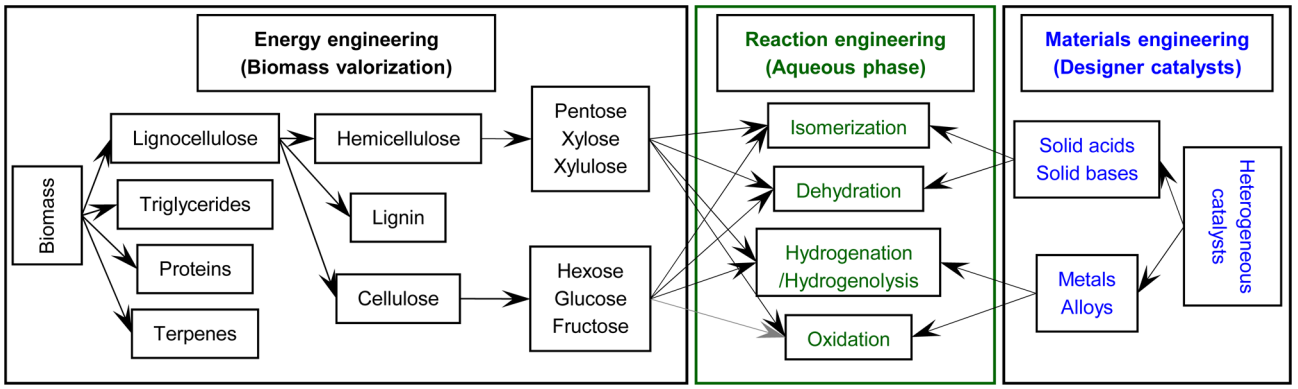

levoglucosan, levoglucosenone, and 5-hydroxymethyfurfural (5-HMF).[87]

Catalysis underpins the development of sustainable technologies for the green chemical transformation of sugars and their reforming,[6,9,89] with biocatalysis, homogeneous catalysis, and heterogeneous catalysis each presenting theoretical, technical, and economic challenges for biomass utilization. Biocatalysis has delivered several successful industrial processes for bioderived chemicals production, generally in the food sector. Notable examples include xylitol (an artificial sweetener) from xylose using microorganisms,[90] and glucose isomerization to fructose using glucose isomerase.[91] It is also advantageous in applications where a societal desire for sustainable consumer products permits less economical routes to the manufacture of renewable chemicals for biopolymers based upon, for example, 1,3-propanediol, polylactic acid, or polyhydroxyalkanoate.[92] Bioprocesses to produce chemicals such as succinic acid, 1,4-butanediol, and isoprene are also being commercialized;[92] however, the market for these drop-in products remains volatile because they are competing against existing petrochemical routes whose cost is linked to (currently low) oil prices.[93] Challenges facing large-scale biocatalytic biomass processing include[94−96] (i) purification of low-cost waste biomass-derived feed streams, which may otherwise compromise enzyme activity; (ii) the necessity for buffered solutions to maintain an optimal environment, for example, pH 7−8; (iii) low operating temperatures to protect enzyme lifetime and maximize product selectivity, which afford lower activity; and (iv) high operational costs from frequent enzyme replacement due to irreversible deactivation.

Heterogeneous catalysts offer opportunities to selectively transform a wide range of biomass-derived sugar-containing feed streams into chemical and fuels over a wide operational regime (typically 25−300 °C and 1−80 bar) and with a good tolerance to impurities and consequent long lifetimes. With respect to aqueous phase processing of waste-derived C_5−C_6 sugars from cellulosic sources,[97] heterogeneous catalysts may complement biocatalysts.[98] Accessing key platform chemicals from xylose and glucose (the primary C_5−C_6 sugars obtained from lignocellulose) requires a range of transformations,[99] including isomerization to xylulose/lyxose or fructose/mannose, hydrogenation to xylitol or sorbitol, dehydration to furanic species such as furfural and 5-HMF, and selective oxidation to xylonic acid and gluconic acid, all of which may be heterogeneously catalyzed.[94,100,101] Catalytic approaches have also been adopted to upgrade the preceding sugar-derived chemicals through, for example, hydrodeoxygenation (HDO) or deoxydehydration.[23] Although a number of the preceding reactions may be catalyzed by soluble acids/bases,[102−105] such approaches suffer the same drawbacks common to homogeneous catalysis, difficult product separation and catalyst recovery/reuse and accompanying high volumes of waste, problematic storage/handling of hazardous materials, and process issues related to scale-up and continuous operation. Solid catalysts circumvent many of the preceding limitations, facilitating (i) low-cost recovery and recycling through centrifugation, filtration, or fixed-bed operation (rendering them suited to large-scale continuous industrial process units); (ii) robust performance under challenging reaction environments; (iii) safe storage/handling/operation within reactors constructed from conventional materials, extending the lifetime of operation units; and (iv) tunable physical and chemical properties allowing tailoring to individual reactions.[106−108]

1.2. Scope of the Current Review

Despite a plethora of original research on heterogeneous catalysts for the transformation of (hemi)cellulose-derived C_5−C_6 sugars into oxygenates, aliphatic, and cyclic compounds over the past five years, there have been no comprehensive reviews encompassing the range of associated acid, base, and metal catalysis reported. This Review focuses primarily on the aqueous phase reforming of such sugars, highlighting promising heterogeneously catalyzed isomerization, dehydration, hydrogenation/hydrogenolysis, and selective oxidation pathways, with a view to identifying structure−function relationships, and exploring the role of active phase and (where applicable) catalyst support in controlling overall activity, selectivity, and reusability. Throughout, we will try to unify diverse performance indicators (e.g., conversion, selectivity, yield, turnover frequency, and initial reaction rate) to permit quantitative benchmarking of disparate systems, and to assess the reliability of literature data in the light of analytical methods employed and the extent to which, for example, mass balances and reuse tests have been utilized. The impact of process engineering (e.g., reactor design, solvent effects, and cost issues) on catalysis and scale-up is also discussed, and emergent areas for aqueous phase sugar reforming identified. Indicative cost estimates for earth scarce catalyst components (e.g., platinum group metals) provide additional metrics for readers to assess the utility of competing catalyst technologies.

We hope that this Review will provide a useful resource for guiding academic and industrial researchers toward informed judgments regarding the selection of the most appropriate technology for platform chemicals production from biomass, and in turn encourage greater awareness of biobased trans-

DOI: 10.1021/acs.chemrev.6b00311
Chem. Rev. 2016, 116, 12328−12368

formations and communication between catalytic scientists and biotechnologists. The overall framework of this Review is summarized in Scheme 1.

2. C_5–C_6 SUGAR TRANSFORMATIONS

Prior to a detailed account of catalytic systems developed for the aqueous reforming of C_5–C_6 sugars, we introduced the most common reaction classes (isomerization, dehydration, hydrogenation/hydrogenolysis, and selective oxidation) and their interrelations.

2.1. Isomerization

Xylose, mainly derived from xylan hemicelluloses by acid/base hydrolysis, is a five-carbon sugar with lower calorific value than glucose. It can exist as a pyranose ring, a furanose ring, or an open-chain structure in water.[109] Glucose also exhibits three conformers in water: a pyranose ring, a furanose ring, and an open-chain (aldohexose) structure.[96] Although most popularly known for their use as sweeteners, xylose/xylulose and glucose/fructose are important chemical intermediates; the higher reactivity of xylulose and fructose as compared to xylose and glucose rendering the former more easily valorized, and hence targets for the heterogeneously catalyzed isomerization of the latter. The overall reaction network is more complicated than first appears due to side reactions such as the epimerization of xylose to lyxose and of glucose to mannose, the retroaldolization of fructose to glyceraldehyde and dihydroxyacetone, and glucose conversion to glycolaldehyde and erythrose, as illustrated in Figure 4.[96,109,110] Furthermore, all four sugar reactants (and their intermediates) can irreversibly react to form solid humins or other degradation products, which are intractable for valorization. The maximum reported xylulose yield from xylose isomerization is therefore 27%, with a corresponding lyxose yield of 11%, at a xylose conversion of 60% (albeit after only 7 min at 110 °C).[109] For glucose

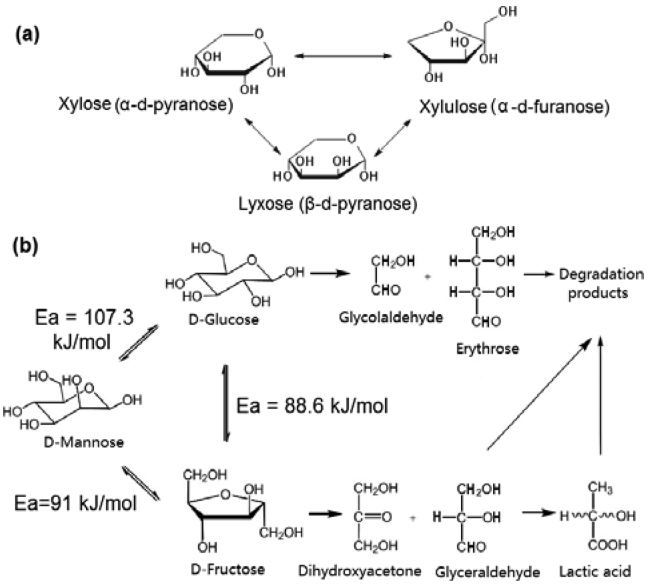

Figure 4. Main reaction pathway for the isomerization of (a) xylose over Sn-beta zeolites. Adapted with permission from ref 109. Copyright 2011 American Chemical Society. Main reaction pathway for the isomerization of (b) glucose over Mg–Al hydrotalcites and Sn-BEA zeolites. Adapted with permission from ref 110. Copyright 2014 The Royal Society of Chemistry. Apparent activation energies taken from ref 96.

isomerization, kinetic studies reveal that the energy barrier from glucose to fructose is 17% lower than that to mannose, and hence fructose is the dominant isomeric product under appropriate kinetic control.[96]

2.2. Dehydration

Fructose dehydration yields 5-HMF, which features in the top 10 list of valuable biobased chemicals according to the U.S. DOE,[111] and is a hot topic of both academic and commercial research[112] due to its potential as a versatile platform chemical from which to access 12 important furan derivatives and nonfuranic compounds.[82,113,114] However, 5-HMF production direct from glucose is more challenging than from fructose due to the additional (slow) isomerization that must precede fructose dehydration, and this multistep process often results in poor 5-HMF yields (Figure 5).[115] The analogous dehydration

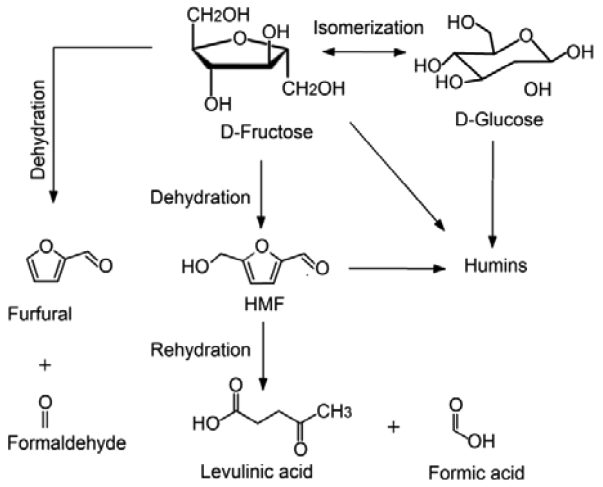

Figure 5. Reaction network for glucose/fructose dehydration catalyzed by solid acids/bases. Adapted with permission from ref 115. Copyright 2014 Elsevier.

product from xylose is furfural, itself an important chemical feedstock for furfuryl alcohol, THFA, and pentanediols production. Unfortunately, the typical temperatures required for xylose and fructose dehydration of 120–200 °C are significantly higher than those for xylose/glucose isomerization of 100–120 °C,[115,116] and consequently xylulose and lyxose formation compete with furfural (Figure 6).[117] Furfural can subsequently fragment into organic acids, or oligomerize into furilic species (not shown). Complete dehydration of organic acids yields carbonaceous deposits, while xylose and its isomers readily form dark colored solid humins, and such side reactions result in low selectivity toward furfural and significant deficits in carbon mass balance. Humins are common byproducts of higher temperature catalytic sugar transformations, formed notably alongside furfural, formaldehyde, formic acid, and levulinic acid synthesis, and whose undesired production is always favored at higher reaction temperatures, driving the quest for more active catalysts.

2.3. Hydrogenation/Hydrogenolysis

Xylitol is a five-carbon artificial sweetener with unusual anticarcinogenic properties whose sweetening capacity exceeds that of sucrose, yet offers lower insulin requirements, and hence is especially suited to diabetics. Demand for xylitol has thus risen within the food, cosmetic, and pharmaceutical sectors.[118–120] Its six-carbon analogue, sorbitol, finds direct

DOI: 10.1021/acs.chemrev.6b00311
Chem. Rev. 2016, 116, 12328–12368

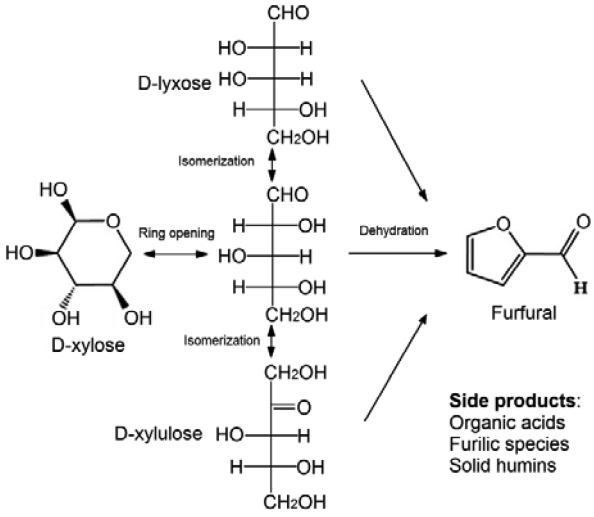

Figure 6. Reaction network of xylose dehydration catalyzed by solid acids/bases. Adapted with permission from refs 116 and 117. Copyright 2011 and 2013 Elsevier and Springer, respectively.

application as a sweetener, laxative, and cosmetic thickener, and can be valorized through dehydration to sorbitan and isosorbide, or by hydrogenolysis to other polyols. Sorbitan and isosorbide are used in medical therapies, while their esters are important emulsifiers and food stabilizers; moreover, isosorbide can be further deoxygenated to yield light ($<C_6$) alkanes for the production of second-generation biofuels suitable for the gasoline pool.[121,122] Catalytic routes to both xylitol and sorbitol from bioderived feedstocks are thus of growing interest, with xylose and glucose hydrogenation, respectively, considered promising pathways, although the associated reaction temperatures of 100−140 °C promote competing isomerization and dehydration side reactions (Figure 7).[123,124] Hydrogenolysis offers an alternative route from biomass-derived carbohydrates to a range of sugar alcohols,[101] but occurs through more complex reaction networks than hydrogenation. Glucose hydrogenolysis, for example, features competing hydrogenation to sorbitol, dehydration to 5-HMF, and carbon chain fragmentation and subsequent cascade reactions (Figure 8), and hence necessitates multifunctional catalysts or combinations of different catalyst classes to achieve the desired product;[125,126] the development of selective hydrogenolysis catalyst systems remains a challenge.[127]

2.4. Selective Oxidation

In the aerobic selective oxidation (selox) of C_5−C_6 sugars, most reports focus on glucose oxidation to gluconic acid, with other monosaccharides largely neglected. Gluconic acid finds widespread use in the food, detergent, and pharmaceutical industries, and it is produced commercially by fermentation (enzymatic oxidation) of glucose, presenting problematic enzyme separation, wastewater removal, and a narrow window of reaction conditions.[129] There is hence an opportunity for heterogeneously catalyzed routes.

Gluconic and glucaric acid are expected major products of glucose selox; however, glucose possesses both aldehyde and primary and secondary alcohol functions, all of which are oxidizable, resulting in a wide product distribution (Figure 9). Moreover, as an isomer of glucose, fructose can also be oxidized to 2-keto-D-gluconic acid and D-threo-hexo-2,5-diulose ("5-

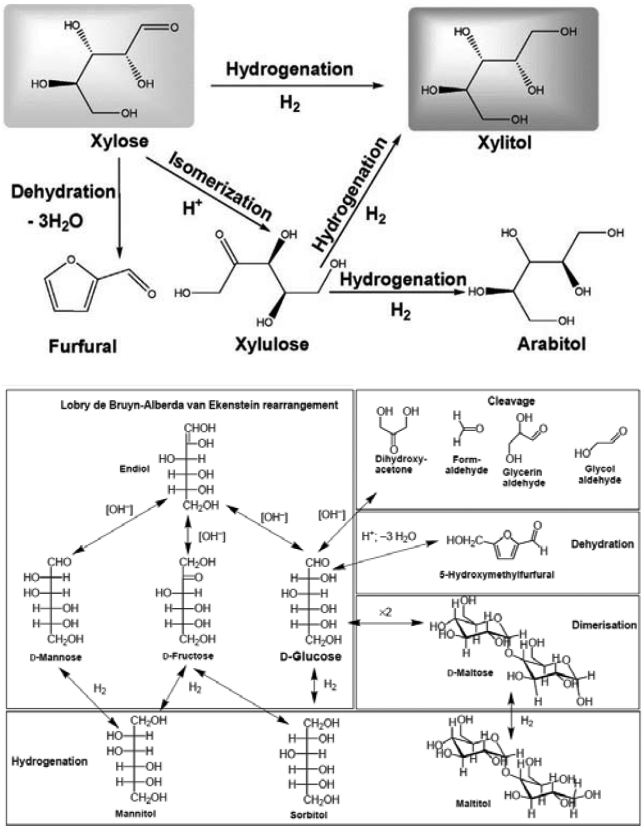

Figure 7. (top) Hydrogenation of xylose with possible side reactions over Ru/Y catalysts. Reproduced with permission from ref 123. Copyright 2013 Elsevier. (bottom) Hydrogenation of glucose with possible side reactions over oxides supported Ni and Ru catalysts. Reproduced with permission from ref 124. Copyright 2003 John Wiley & Sons.

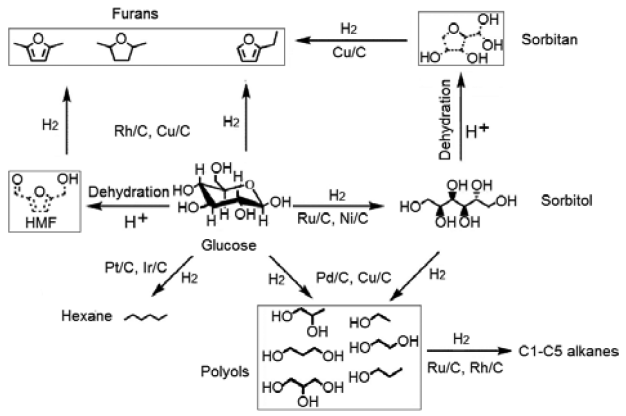

Figure 8. Reaction network for glucose hydrogenolysis. Adapted with permission from ref 128. Copyright 2015 Elsevier.

ketofructose"), although for simplicity this reaction network is omitted.[130−132]

Selox of the fructose dehydration product, 5-HMF, also produces 2,5-furandicarboxylic acid,[133] a valuable monomer proposed as a potential renewable replacement for terephtalic acid. Another problem in glucose oxidation is the common requirement for an alkaline medium (pH = 9−10),[134,202] which poses an additional constraint on the catalyst stability. Nevertheless, the oxidation of glucose has the advantage of operating under mild temperatures (40−80 °C), and hence

DOI: 10.1021/acs.chemrev.6b00311
Chem. Rev. 2016, 116, 12328−12368

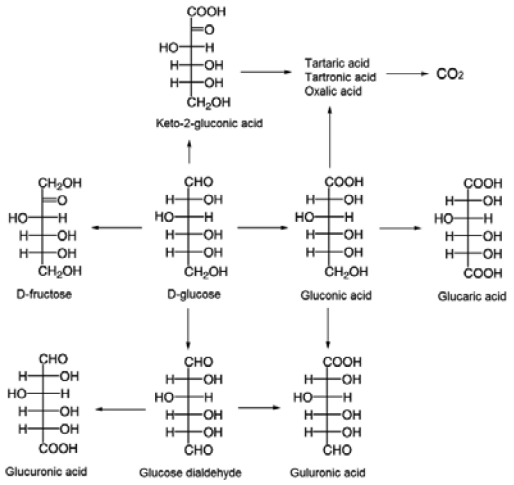

Figure 9. Possible products of glucose oxidation. Adapted with permission from ref 132. Copyright 2002 Elsevier.

suppressing isomerization and undesired solid humin formation reactions, as compared to dehydration and hydrogenation/hydrogenolysis pathways.

3. HETEROGENEOUS CATALYSTS FOR SUGAR TRANSFORMATIONS

The preceding overview of xylose and glucose transformations highlights the complexity of associated reaction networks and hence requirement for both active and selective heterogeneous catalysts to direct reforming of C_5–C_6 sugars from biomass. Such catalysts are now discussed according to their classification and associated applications.

3.1. Solid Acids/Bases for Isomerization

Since the pioneering work of Lobry de Bruyn and Alberda van Ekenstein (LBAE) in 1895 on hexose isomerization in alkaline medium,[135] extensive research has been undertaken to improve the isomerization efficiency in terms of conversion, selectivity, and yield through heterogeneous catalysis. Solid Lewis acids and solid bases have been explored in most detail for the isomerization of C_5–C_6 sugars (Table 1), exemplified by zeolitic Lewis acids,[136−138] hydrotalcite solid bases,[139] and metallosilicate solid bases.[140]

3.1.1. Zeolitic Solid Lewis Acids. Zeolites are well-known crystalline aluminosilicates, with rigid microporous structures and well-defined channels of molecular dimensions. The nanoporous nature of zeolites offers high surface areas, shape-selective reactions, and efficient mass/heat transfer.[141] Zeolite frameworks comprise $[SiO_4]$ and $[AlO_4]^-$ tetrahedra, with the negative charge on the $[AlO_4]^-$ tetrahedra necessitating extra-framework cations (e.g., Na^+ and K^+) to provide electroneutrality. These cations are ion-exchangeable, permitting the introduction of new charge-balancing cations (e.g., H^+, Ag^+, Ca^{2+}, and Ce^{3+}) with attendant modification of the zeolite acid/electronic properties; for instance, charge compensation with protons imparts strong Brønsted acidity. The zeolite framework may also be modified to incorporate heteroatoms (e.g., Fe, Mn, and Sn) and thereby create new porous structures and impart Lewis acidity.[109,142,143]

The heteroatomic Sn-beta zeolite, first synthesized by Corma and co-workers, has successfully been employed as a catalyst for the Meerwein–Ponndorf–Verley (MPV) reduction of carbonyl compounds,[144] and has also found application to xylose isomerization, giving a 27% xylulose yield at 100 °C at 60% conversion (entry 1, Table 1). Sn-beta (possessing 0.8 nm pores, entry 2, Table 1) has also been investigated for glucose isomerization in comparison with a related Ti-beta (0.8 nm pores), and mesoporous Sn-MCM-41 and Ti-MCM-41.[145] Sn-beta and Ti-beta offered the highest fructose yields of 32% and 14%, respectively, from a 10 wt % glucose solution at 110 °C, with the former maintaining good activity even when a 45 wt % glucose solution was employed. The catalytic performance was partly attributed to the unique environment within large pore β-zeolites, with no reaction observed over a TS-1 zeolite (0.5–0.6 nm pores). Isomerization activity was reduced considerably for Sn-MCM-41, possibly reflecting a lower degree of Sn incorporation into the MCM framework. The active sites were identified as Sn atoms coordinated within the zeolite framework because neither $SnCl_4{\cdot}5H_2O$ nor SnO_2 alone catalyzed isomerization. Key factors influencing glucose isomerization

Table 1. Solid Acid/Base-Catalyzed Xylose and Glucose Isomerization to Xylulose and Fructose, Respectively, in Water

entry	catalyst	conversion/%	selectivity/%	yield/%	initial rate/ mmol g_{cat}^{-1} h^{-1}	TOF[a]/h^{-1}	reaction conditions	ref
1	zeolite Sn-β	60	45	27	22.2	200	10 wt % xylose, 0.072 g of catalyst, 100 °C, 25–60 h, 1 mL	109
2	zeolite Sn-β	80	29	23		34	10 wt % glucose, 140 °C, 1.5 h, 1.5 mL	145
3	zeolite Sn-β	65	66	43			10 wt % glucose, 0.03 g of catalyst, 120 °C, 2 h, 0.4 mL	160
4	zeolites NaX	20	86	17	7.0		10 wt % glucose, 1 g of catalyst, 95 °C, 50 mL	138
5	hydrotalcites $Mg_{4.5}Al_2(OH)_{13}CO_3$	29	83	24	49.6		5 wt % glucose, 1 g of catalyst, 90 °C, 1 h, 50 mL	151
6	hydrotalcites $Mg_6Al_2(CO_3)(OH)_{16}{\cdot}4H_2O$	41	75	31			1 wt % glucose, 1 g of catalyst, 90 °C, 2 h, 30 mL	110
7	$Mg_{0.75}Al_{0.25}(OH)_2(CO_3)_{0.125}{\cdot}0.71H_2O$	29	89	25	7.8	23	10 wt % glucose, 0.1 g of catalyst, 110 °C, 1.5 h, 5 mL	152
8	hydrotalcites $Mg_6Al_2(CO_3)(OH)_{16}{\cdot}4H_2O$	39.1	78.6	31			3 wt % glucose, 0.1 g of catalyst, 100 °C, 3 h, 10 mL	161
9	$Na_9Si_{12}Ti_5O_{38}(OH)$	48	84	39	3.3		5 wt % glucose, 0.02 g of catalyst, 100 °C, 2 h, 1 mL	140
10	zirconium carbonate	45	76	34			10 wt % glucose, 0.3 g of catalyst, 120 °C, 1–3 h, 3 mL	162

[a]Per acid or base site.

DOI: 10.1021/acs.chemrev.6b00311
Chem. Rev. 2016, 116, 12328–12368

are (i) framework or extra-framework active sites;[146] (ii) the solvent (e.g., water or methanol);[147] and (iii) the nature of exchange cations.[136] Davis and co-workers demonstrated that framework tin sites in Sn-beta catalyzed the isomerization of glucose to fructose via a Lewis acid-mediated intramolecular hydride shift in water (Figure 10a),[133] whereas the former

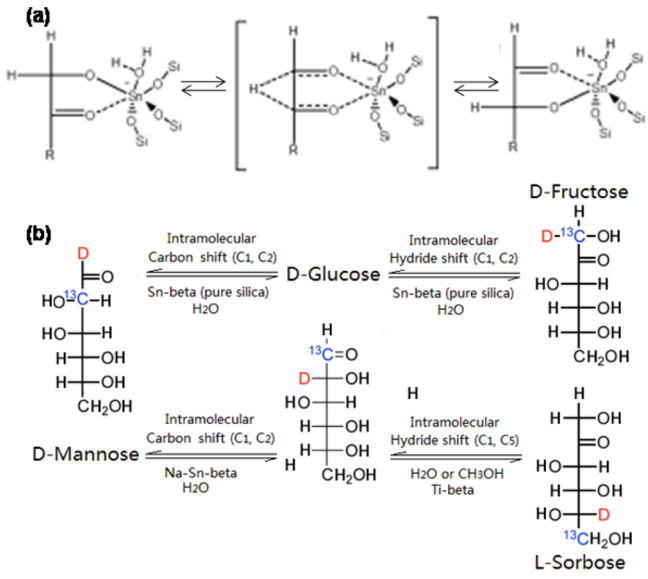

Figure 10. (a) Proposed glucose coordination to Sn during isomerization to fructose. Adapted with permission from ref 148. Copyright 2010 John Wiley & Sons. (b) Principal reaction pathways for glucose isomerization catalyzed by Sn-beta or Ti-beta in water or methanol. Adapted with permission from refs 136, 146, and 147 . Copyright 2014, 2012, and 2013 American Chemical Society, respectively.

epimerization into mannose occurs by a Lewis acid-mediated intramolecular carbon shift. Extra-framework Sn located within the hydrophobic zeolite channels isomerized glucose to fructose in water and methanol through a base-catalyzed H^+ transfer mechanism. Isotope labeling (^2H and ^{13}C) of glucose highlights that its isomerization products are formed through either hydrogen or carbon shifts, varying with the catalyst and solvent as summarized in Figure 10b.

Cation-exchanged zeolites X, Y, and A are also active for glucose isomerization. Ca- and Ba-exchanged A, X, and Y zeolites exhibited low selectivity to fructose, whereas moderate basicity NaX and KX achieved 86% fructose selectivity (entry 4, Table 1), albeit only for glucose conversions <25% and potentially accompanied by cation leaching.

3.1.2. Hydrotalcite Solid Bases. Hydrotalcites (HTs), a subset of layered double hydroxides and found in nature as anionic clays, are important solid base catalysts that exhibit high catalytic activity and robustness in water.[149,150] With a general formula of $[M(II)_{1-x}M(III)_x(OH)_2]^{x+}(A_{x/n}{}^{n-})\cdot mH_2O$, hydrotalcites comprise brucite-like hydroxide sheets containing octahedrally coordinated M^{2+} (e.g., Mg^{2+}) and M^{3+} (e.g., Al^{3+}) cations, separated by interlayer A^{n-} charge-balancing anions, where x is the fraction of M^{3+} (typically $0.17 < x < 0.34$ for aluminum) and m denotes the water of crystallization. HTs exhibit an unusual so-called "memory effect", in which their calcination results in the formation of high area mixed metal oxides, whose subsequent rehydration can restore the original layered double hydroxide structure. HTs can function as strong Lewis bases, with basicity dependent upon the M(II):M(III) ratio within the hydrotalcite sheets. The chemical composition, and textural properties, of HTs can hence be tuned to modify their catalytic performances.

A variety of commercial Mg−Al hydrotalcites, prepared as the hydroxide, carbonate, and mixed carbonate−hydroxide anionic forms, have been explored for glucose isomerization.[151] Hydroxide-containing structures were both more active and somewhat more selective than the carbonate form [entry 5, Table 1]; however, all of these HTs deactivated after only 15% glucose conversion, concomitant with a rapid fall in their initial high (90%) selectivity to fructose. The initial activity and selectivity were claimed to return upon recycling, presumably due to the removal of reversibly adsorbed products during regeneration.

The hydrophobic/hydrophilic nature of commercial Mg−Al HTs was also investigated in batch and continuous aqueous phase glucose isomerization.[110] Hydrophobic materials exhibited lower conversion but superior selectivity toward fructose, exceeding 92% at 30% glucose conversion in 24 h. The main byproducts were from fructose retroaldolization to glyceraldehyde and dihydroxyacetone (and glucose conversion to glycolaldehyde and erythrose) (Figure 4), whose strong adsorption was ascribed to catalyst deactivation. Acidic degradation products such as lactic acid were also responsible for neutralizing the hydrotalcites and magnesium leaching; however, hot filtration tests on these materials suggested that isomerization occurred exclusively via heterogeneous catalysis. Structure−performance relations of Mg−Al hydrotalcites were examined recently for glucose isomerization, employing different Mg:Al molar ratios, textural properties, and morphologies (shown in Figure 11).[152] Catalysts were prepared by coprecipitation, employing a range of pH, Mg:Al ratios, aging temperatures, and solvents to tune their basicity and structure. Isomerization was catalyzed by weak base sites, specifically interlayer anions accessible at the edges of primary particles and defects on the basal planes of the hydrotalcite, with glucose conversion scaling with base site density. Dimensions of coherent crystallographic domains and primary particles, and their agglomeration, are both strong influences on catalytic activity, and may explain the higher activity and selectivity of the porous $Mg_{0.75}Al_{0.25}(OH)_2(CO_3)_{0.125}\cdot 0.71H_2O$ (HT1-10-RT in Figure 11) [entry 7, Table 1]. These HTs were recyclable without loss of activity or selectivity, although some magnesium leaching due to the presence of lactic acid byproduct was again reported. These catalysts were precipitated by a $NaOH/Na_2CO_3$ solution, and hence the possibility of homogeneous catalysis by leached/residual Na^+ cannot be discounted in this study.

3.1.3. Other Solid Base Catalysts. In comparison with zeolitic Lewis acids and hydrotalcites, the solid bases of metallosilicates and zirconium compounds are less studied for sugar isomerization. Lima and co-workers investigated glucose isomerization in water at 100 °C catalyzed by a variety of metallosilicates such as $Na_9Si_{12}Ti_5O_{38}(OH)$, finding fructose yields of between 20% and 40% after only 2 h (entry 9, Table 1).[140] Catalytic performances were comparable or superior to those achievable with a commercial NaX zeolite or NaOH under these reaction conditions, although deactivation occurred after two recycles due to a combination of sodium/potassium leaching, loss of crystallinity, and surface passivation. Zirconium salts such as zirconium carbonate and zirconium phosphate are also active for glucose isomerization, with the carbonate best

DOI: 10.1021/acs.chemrev.6b00311
Chem. Rev. 2016, 116, 12328−12368

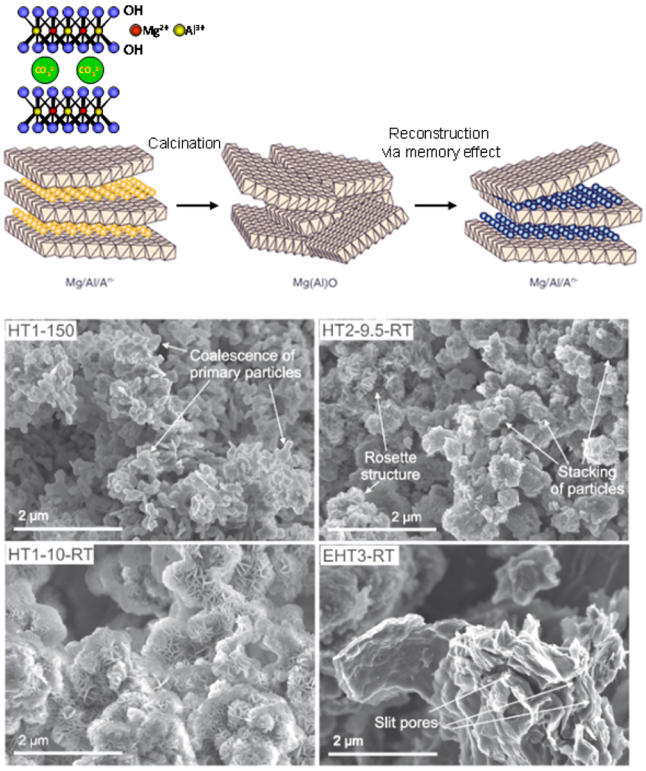

Figure 11. (top) Hydrotalcite structure and memory effect in their synthesis. Adapted with permission from ref 153. Copyright 2003 Springer. (bottom) SEM micrographs of selected hydrotalcites with different morphologies and structures: HT1-150 $[Mg_{0.78}Al_{0.22}(OH)_2(CO_3)_{0.11}\cdot 0.57H_2O]$, HT2-9.5-RT $[Mg_{0.76}Al_{0.24}(OH)_2(CO_3)_{0.12}\cdot 0.85H_2O]$, HT1-10-RT $[Mg_{0.75}Al_{0.25}(OH)_2(CO_3)_{0.125}\cdot 0.71H_2O]$, and EHT3-RT $[Mg_{0.69}Al_{0.31}(OH)_2(CO_3)_{0.155}\cdot 0.79H_2O]$. Adapted with permission from ref 152. Copyright 2015 Elsevier.

performing with a maximum conversion of 45% and 76% selectivity to fructose at 120 °C, and exhibiting excellent stability over five recycles (entry 10, Table 1). Sulfated zirconia, synthesized in both bulk form[154] and as ultrathin conformal monolayers over mesoporous SBA-15,[155] exhibits modest glucose conversions up to 20%, but high fructose selectivity >85% (with 5-HMF as a significant byproduct of fructose dehydration), with the latter thin film system exhibiting excellent hydrothermal stability.

3.1.4. Process Considerations. Glucose isomerization to fructose is equilibrium-limited; thus innovative reactor designs are required to facilitate fructose removal and thereby drive the forward reaction and also minimize side reactions of fructose, which are problematic in water.[138] Equilibrium-limited reactions, or reactions wherein the catalyst deactivates and requires periodic reactivation, are well-suited to a moving bed reactor design such as those employed in immobilized enzymatic glucose–fructose isomerization accompanied by quasi-continuous chromatographic separation,[156] and could be readily extended to improve heterogeneously catalyzed isomerization. Figure 12a illustrates this reactor concept, in which six reactive chromatographic fixed-bed reactors are interconnected to form a closed-loop. Three functional zones have different roles in the process: zone I between the desorbent and the extract line is for regeneration of the solid, zone II is for reaction/separation, and zone III between the feed and the eluent line is for reaction/separation and recycling of solvent.

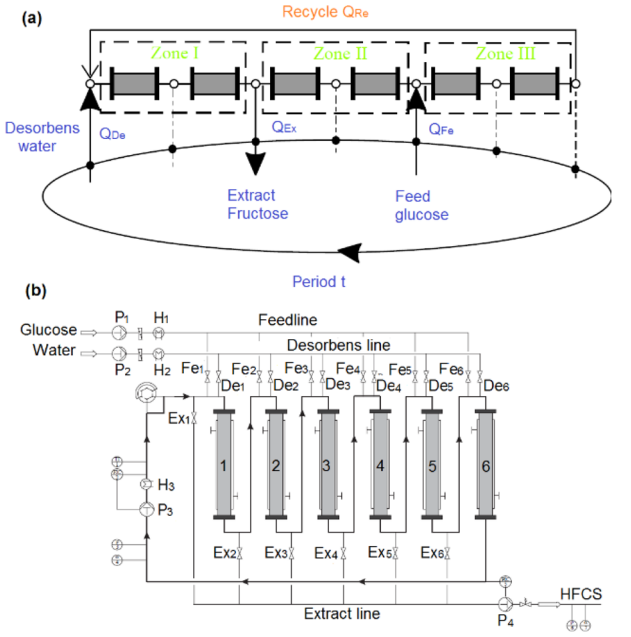

Figure 12. (a) Illustration of a three-zone reactive simulated moving bed reactor system for glucose isomerization to fructose. (b) Process flowsheet of the reactive simulated moving bed reactors. Adapted with permission from ref 156. Copyright 2004 Elsevier.

Three different lines (feed, desorbent, and extract) are fed by three different pumps, as shown in Figure 12b. An additional fourth pump closes the loop and recycles flow from the last column to the first. At any time, only one valve associated with a given line is open. Port switching is achieved by simultaneously closing the open valve (e.g., De1) and opening the next valve in the direction of the flow (e.g., De2). In this design, the integration of reaction and separation in one unit operation is advantageous for glucose isomerization, where it enables product removal from the reaction zone and displacement of the equilibrium.[157]

Enhanced yields of fructose from glucose have also been achieved through the use of aqueous alcohol cosolvents over Si/Al zeolite catalysts. Reactively formed fructose in methanol immediately reacts to form methyl fructoside. In a subsequent step, water is added to hydrolyze the methyl fructoside back to fructose.[158] Lewis acidic Sn-beta also shows enhanced glucose conversion and fructose yield with a methanol solvent;[136] Density Functional Theory (DFT) calculations suggest this results from a differing solvation behavior of water versus methanol in the hydrophobic pores of Sn-beta.[159]

3.1.5. Summary of Solid Base Isomerization Catalysts. A relatively narrow range of catalysts have been assessed for xylose/glucose isomerization, typically operating between 90 and 110 °C and offering modest sugar conversion albeit with notably high fructose selectivity. Few studies quantify catalyst performance in terms of either initial rates of sugar conversion, per site turnover frequency (TOF), or isomer productivity, hampering accurate benchmarking. Catalyst characterization is also rather restricted to either acid/base site densities and/or classification as Brønsted/Lewis, with acid/base strength distributions rarely reported. The apparent activation energy for glucose isomerization over NaX zeolites of 104 kJ mol^{-1}[138] is around 22 kJ mol^{-1} lower than that over the hydroxyl form of hydrotalcites,[151] indicative of a different reaction mechanism, although there is little fundamental work in this regard; over

DOI: 10.1021/acs.chemrev.6b00311
Chem. Rev. 2016, 116, 12328–12368

Table 2. Solid Acid-Catalyzed Xylose Dehydration to Furfural and Glucose/Fructose Dehydration to 5-HMF in Water

entry	catalyst	conv./%	sele./%	yield/%	initial rate/ mmol g_{cat}^{-1} h^{-1}	TOF/h^{-1}	typical reaction conditions	ref
1	H-ZSM-5 (1.2 nm in pore diameter)	96	55	52.5	10		10 wt % xylose, 3 g of catalyst, 200 °C, 0.5 h, 800 rpm, 100 mL, 50 bar	207
2	H-ZSM-5, dealuminated(2)	50	66	33	1	1.6	3 wt % xylose, 0.6 g of catalyst, 140 °C, 10 h, 500 rpm, 60 mL, 30 bar	169
3	ITQ-2 (Si/Al = 24)	73	70	51	3.3		10 wt % xylose, 1 g of catalyst, 170 °C, 16 h, 700 rpm, 1 mL	170
4	H-beta (Al/fructose = 0.03)	12	26	31			10 wt % fructose, 130 °C, 5 h	173
5	H-USY (hierarchical)	70	10	7.0			10 wt % fructose, 0.08 g of catalyst, 130 °C, 10 h, 60 mL	171
6	SO_3H-MCM-41	37	65	23.8			3 wt % xylose, 0.1 g of catalyst, 170 °C, 1 h, 30 mL	116
7	sulfonated GO (SGO)	83	75	62		2.5	3 wt % xylose, 0.45 g of catalyst, 200 °C, 35/60 h, 300 rpm, 75 mL	183
8	SO_3H-hybrid silica	53	50	27			3 wt % xylose, 0.02 g of catalyst, 140 °C, 24 h, 500 rpm, 1 mL	181
9	SO_4/ZrO_2 (surface S: 4.0%)	25	33	8.3	1.2	0.8	0.5 wt % fructose, 0.1 g of catalyst, 100 °C, 6 h, 20 mL	154
10	poly(4-styrenesulfonic acid)/SiO_2	80	34	27			6.5 wt % fructose, 0.1 g of catalyst, 120 °C, 6 h, 3.5 mL	182
11	carbon treated by H_2SO_4 and HNO_3	40	70	28			5 wt % fructose, 0.1 g of catalyst, 200 °C, 1000 rpm, 90 mL	117
12	zirconium phosphate (hydrothermal method, organic amine, calcination)	52	51.9	27		1.1	10 wt % xylose, 0.1 g of catalyst, 140 °C, 2 h, 500 rpm, 40 mL	197
13	niobium phosphate (NbPO)	58	22	13	1.3	3.7	20 wt % glucose, 2 g of catalyst, 135 °C, 5 h, 500 rpm, 60 mL	196
14	vanadyl phosphate $VOPO_4{\cdot}2H_2O$ (VOP)	45.1	73.0	32.9		274	6 wt % fructose, 0.1 g of catalyst, 80 °C, 0.5 h	192
15	alkaline earth phosphate, α-$Sr(PO_3)_2$	89	39	35			10 wt % fructose, 0.01 g of catalyst, 200 °C, 1 mL	194
16	copper phosphate, α-$Cu_2P_2O_7$-900	82.2	43.6	35.8		34.0	10 wt % fructose, 0.01 g of catalyst, 200 °C, 5−60 h, 1 mL	193
17	heteropolyacid ionic crystal $Cs_2Cr_3SiW_{12}$	73.2	45.6	33.4			30 wt % fructose, 0.007 mmol of catalyst, 120 °C, 1 h, 10 mL	206
18	solid heteropolyacid salt $Ag_3PW_{12}O_{40}$	98	87	86			1 wt % fructose, 0.08 g of catalyst, 120 °C, 2 h, 26 mL	204
19	TiO_2	63.8	29.2	18.6		84	2 wt % glucose, 0.05 g of catalyst, 200 °C, 5−60 h, 5 mL	201
20	25% CeO_2/75% Nb_2O_5	68	47	32.0		67.7	1 wt % fructose, 0.08 g of catalyst, 130 °C, 6 h, 60 mL	203
21	tungstated zirconia (WO_X/ZrO_2)	90	15	13.5			10 wt % xylose, 0.5 mmol of acid sites, 160 °C, 1 h, 30 mL	208

NaA zeolites, isomerization is reported as first order in glucose for concentrations <1 wt %, but zero order >5 wt %; in contrast, over NaX zeolites the transition from first to zero order only occurs at glucose concentrations >10 wt %.[138] The work of Davis and co-workers is notable, revealing that Sn-beta zeolite maintains activity and selectivity under acidic conditions. This is significant because it unlocks the possibility for one-pot transformations compatible with acid pretreatments employed to isolate carbohydrate components of biomass.[145] Catalyst deactivation during isomerization is generally attributed to a loss of active sites through leaching, or site-blocking by strongly adsorbed products, although the origin is rarely investigated, with Sn-beta[145] and Sn−Al-beta[160] exhibiting the best stability over repeated reuse.

Despite efforts to develop new catalysts, isomerization efficiency is constrained by virtue of its slight endothermicity (ΔH = 3 kJ mol^{-1}) and reversibility ($K_{eq} \approx 1$ at 25 °C), restricting the maximum attainable fructose yield (according to Moliner et al., the equilibrium conversion of glucose at 90 °C is 55%[145]). However, Paniagua and co-workers have designed a two-step process utilizing different commercial zeolites to enhance xylose isomerization, through its initial conversion to xylulose and subsequent reaction with methanol to form methyl xyluloside (step 1), which could in turn be hydrolyzed back to xylulose (step 2), affording a 47% xylulose yield over H-USY(6) at 100 °C. The same process translated to glucose, resulting in a remarkable 55% fructose yield at 120 °C, higher than for any single catalytic step in Table 1. Scale-up of this two-step reaction may prove a challenge for commercial development. Hot-compressed (hydrothermal and supercritical) water, which is known to fragment or hydrolyze cellulose within woody biomass,[163] has also been harnessed to initiate ionic and radical isomerization. However, the resulting reaction networks are complicated by competing dehydration, condensation, and degradation of fructose. Future chemical technologies would be better focused at lower temperature and neutral reaction media to reduce side reactions.

3.2. Solid Acids for Dehydration

Catalytic dehydration of C_5−C_6 sugars is conventionally catalyzed by liquid acids, such as H_2SO_4, HCl, H_3PO_4, oxalic, and maleic acid, in aqueous solution.[164,165] Lewis acid metal halides (e.g., $CrCl_3$) have also been investigated in conjunction with a liquid Brønsted acid (e.g., HCl).[166,167] However, liquid acid processes are associated with corrosion, toxicity, and separation and product recovery issues (and associated high

DOI: 10.1021/acs.chemrev.6b00311
Chem. Rev. 2016, 116, 12328−12368

volumes of contaminated aqueous waste from quench and neutralization steps). Solid acid catalysts are thus promising alternatives for dehydration.

3.2.1. Zeolitic Materials. Proton-exchanged zeolites are popular solid Brønsted acids for sugar dehydration.[168] In xylose dehydration, H-form ferrierite, ZSM-5, mordenite, beta, and Y zeolites possessing similar acid densities, and external and specific surface areas, were compared to determine the impact of zeolite structure (entry 2, Table 2).[169] Pore channel size influenced both conversion and selectivity to furfural, with conversion linearly proportional to channel diameter as shown in Figure 13, while H-ZSM-5 exhibited the highest furfural

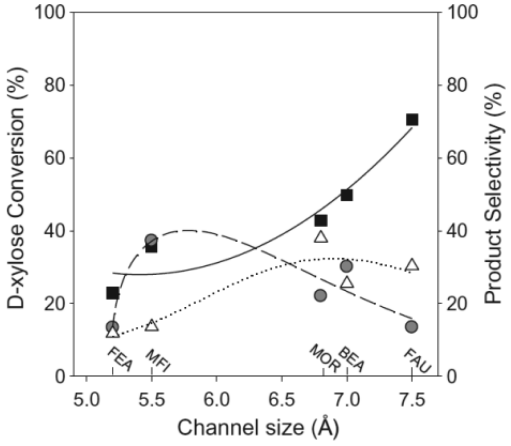

Figure 13. Xylose conversion and selectivity as a function of zeolite pore size: conversion (■, solid line), furfural selectivity (●, dashed line), and isomer selectivity (△, dotted line). Adapted with permission from ref 169. Copyright 2014 Elsevier.

selectivity due to the similarity of its channel size to the product dimensions (size selectivity). However, mass balances were not reported, an important omission for such microporous materials wherein slow in-pore diffusion may favor side reactions leading to humins, although in this instance furfural selectivity appeared time-independent. Dealumination and desilication also improved the catalytic activity of H-ZSM-5 due to the resulting change in solid acidity, with dealuminated H-ZSM-5 exhibiting higher furfural selectivity than the parent H-ZSM-5 due to an increase in Brønsted acid sites (entry 2, Table 2).[169]

The effect of Si:Al ratio has also been explored in H-MCM-22-catalyzed xylose dehydration.[170] Decreasing the Si:Al ratio enhanced dehydration activity without adversely affecting furfural selectivity. The delaminated analogue ITQ-2 has a significantly higher external surface area than H-MCM-22, but a similar acid loading, and hence both exhibit comparable performances (for Si:Al = 24). ITQ-2 was however easier to regenerate, suggesting differences in the nature of carbonaceous deposits formed during reaction suppressed deactivation by coking. Acid loading and strength were both shown to influence the catalytic performance of hierarchical USY, beta, and ZSM-5 zeolites (entry 5, Table 2)[171] prepared by alkaline treatment, and whose acid strength, density, and distribution were quantified (Figure 14). When applied to fructose dehydration, these modified zeolites offered higher 5-HMF selectivity than their parent materials (Figure 15). As mentioned in section 3.1.1, framework-substituted Sn-beta zeolite is an efficient catalyst for xylose and glucose isomerization,[109,136] and has

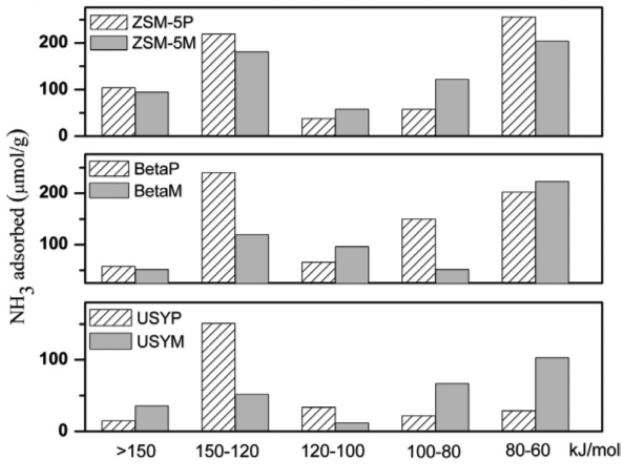

Figure 14. Acid site distribution in parent (P) and modified (M) zeolites. Adapted with permission from ref 171. Copyright 2014 Elsevier.

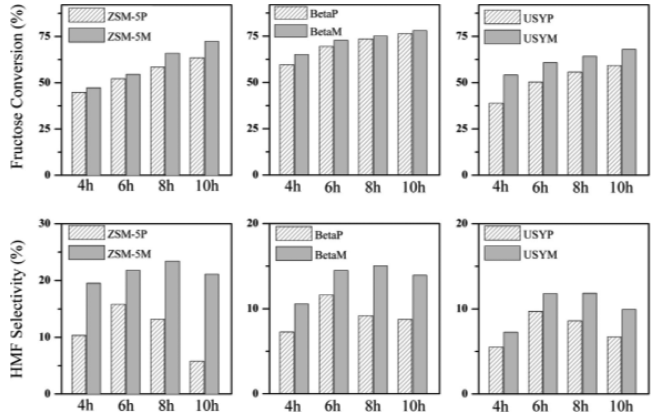

Figure 15. Fructose conversion and 5-HMF selectivity of parent (P) and modified (M) zeolites. Adapted with permission from ref 171. Copyright 2014 Elsevier.

been explored in conjunction with HCl as a Brønsted acid catalyst for one-pot xylose conversion to furfural in water at low temperature; catalyst stability in such an acidic environment remains difficult, and the use of corrosive mineral acids undesirable.

Microporous zeolites exhibit poor hydrothermal stability at high reaction temperatures (>150 °C)[112] and weaker mechanical strengths as compared to dense metal oxides. Moreover, dissolved zeolitic species formed in water can catalyze homogeneous reactions of fructose and 5-HMF.[172,173] NMR, FTIR, DLS, and XRD analyses indicate that oligomeric aluminosilicate fragments are probably the dissolved active species; hence more robust and stable solid acid/base catalysts are required for sugar dehydration in acidic aqueous media.

3.2.2. Sulfonic Acid and Sulfated Metal Oxides. *3.2.2.1. Sulfonic Acid Derivatized Solid Acids.* Sulfonic (SO_3H) solid acids are attractive catalysts because of their strong acidity, high stability, low cost, and broad application as a replacement for H_2SO_4 in acid-catalyzed reactions.[174−179] Early studies show that the sulfonic acid resin Amberlyst-15 catalyzed fructose dehydration at 80 °C in an IL and dimethyl sulfoxide (DMSO) solvent mixture.[180] Mesoporous SO_3H-MCM-41 silica and SO_3H-hybrid-organic-silica also showed activity for xylose dehydration in DMSO or water, biphasic

DOI: 10.1021/acs.chemrev.6b00311
Chem. Rev. 2016, 116, 12328−12368

toluene/water, or MIBK/water solvents.[181] Poorly ordered microporous hybrid materials prepared via co-condensing 3-mercaptopropyl-trimethoxysilane with bis-trimethoxysilylethylbenzene exhibited lower furfural selectivity as compared to the mesoporous MCM-41 silica functionalized postsynthesis (entry 8, Table 2), with selectivity increasing strongly with reaction temperature.

More recently, silica nanoparticles with a mesoporous silica shell and dense silica core (MSHS) have been developed for the catalytic dehydration of xylose to furfural in water. These were modified by sulfonic acids as Brønsted acids (SO_3H-MSHS), or by aluminum as Lewis acids (Al-MSHS) (Figures 16 and 17).[116] SO_3H-MSHS outperformed Al-MSHS in respect

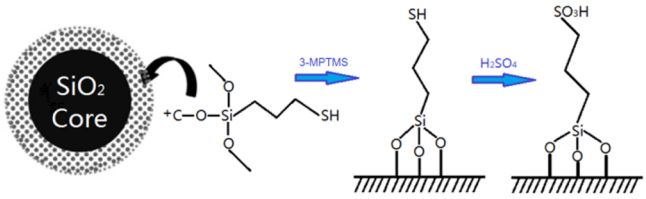

Figure 16. Synthesis of MSHS catalysts modified by SO_3H groups. Adapted with permission from ref 116. Copyright 2011 Elsevier.

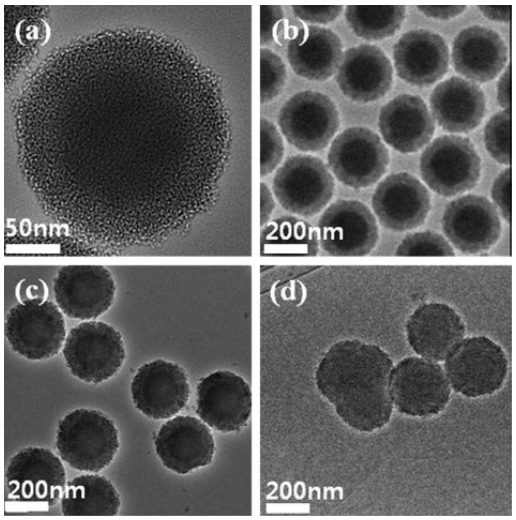

Figure 17. TEM images of (a,b) MSHS, (c) SO_3H-MSHS, and (d) Al-MSHS. Adapted with permission from ref 116. Copyright 2011 Elsevier.

of selectivity to furfural due to the latter driving xylose isomerization to lyxose. The hydrothermal stability of SO_3H-MSHS was superior to other mesoporous silica materials such as MCM-41 (entry 6, Table 2), although the forcing reaction conditions (170−190 °C) and associated lack of reported humin formation are surprising. Nevertheless, these MSHS materials suffer from relatively low surface areas and consequent low acid site densities.

In an effort to address the issue of low active site loadings, "hairy" solid acid catalysts have been designed by outward growth of poly(sodium 4-styrenesulfonate) brushes from the surface of silica core particles (Figure 18). Subsequent acidification resulted in poly(4-styrenesulfonic acid) (PSSH) brushes (entry 10, Table 2).[182] Such PSSH catalysts displayed improved 5-HMF yields from fructose dehydration in water than the free homopolymer acid, attributed to a unique solvation microenvironment formed by the densely grafted

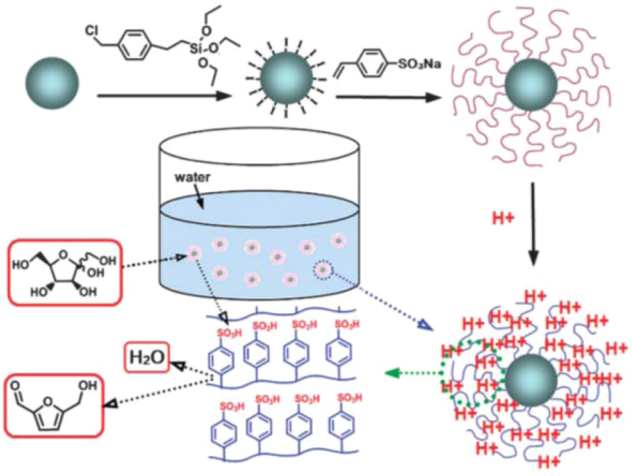

Figure 18. Synthetic route to poly(4-styrenesulfonic acid) silica particles for fructose dehydration to 5-HMF. Reproduced with permission from ref 182. Copyright 2013 The Royal Society of Chemistry.

PSSH chains in the brush structures. The sulfonic acid hybrid catalysts could be reused several times with a minimal decrease in the 5-HMF yield (entry 8, Table 2).

Sulfonated graphene and graphene oxides have also been tested for xylose dehydration;[183] sulfonated graphene oxide proved an active and water-tolerant solid acid catalyst even at very low catalyst loadings down to 0.5 wt % (relative to xylose), and able to sustain its initial activity for 12 reuses at 200 °C, with an average furfural yield of 61% versus 44% for the uncatalyzed system (entry 7, Table 2).

Glucose dehydration to 5-HMF is economically more attractive than from fructose because the former can be obtained directly from cellulose hydrolysis. Nevertheless, glucose conversion is more challenging because it requires a tandem catalytic process involving a Lewis acid- or base-catalyzed isomerization and subsequent Brønsted acid catalyzed dehydration. Glucose is also susceptible to side reactions such as condensation and mutarotation,[184,185] and the mechanism of its isomerization to fructose and associated active sites remains debated.[146,186,187] The design of efficient catalysts for glucose dehydration to 5-HMF remains problematic for low temperature aqueous operation.[188]

3.2.2.2. Sulfated Metal Oxides. Bifunctional sulfated zirconia (SZ) has been investigated in detail for one-pot 5-HMF production from glucose (entry 9, Table 2).[154] A comparison of acidic properties and associated reactivity toward glucose and fructose revealed that submonolayer SO_4 coverages provide the optimal balance between base sites on the exposed zirconia responsible for glucose isomerization to fructose, and polydentate Brønsted acid sulfoxy species coordinated to the underlying tetragonal zirconia support efficient for fructose dehydration to 5-HMF (Figure 19). TOFs for fructose dehydration evidenced that this transformation was catalyzed solely by Brønsted acidic sulfoxy groups. However, these materials possessed low surface areas, and hence sulfation of high surface area ZrO_2/SBA-15 prepared via a conformal ZrO_2 coating method was developed to create high area analogues over a mesoporous SBA-15 template.[155] Resulting bilayer SZ/SBA-15 exhibited excellent hydrothermal stability, and a 3-fold enhancement in 5-HMF productivity from both glucose and fructose as compared to nonporous SZ counterparts. SZ/SBA-

DOI: 10.1021/acs.chemrev.6b00311
Chem. Rev. 2016, 116, 12328−12368

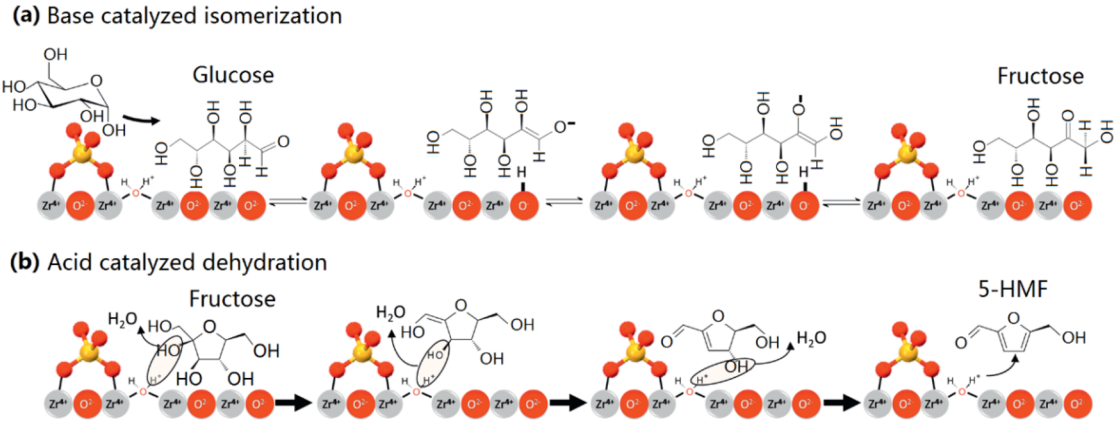

Figure 19. Proposed bifunctional surface-catalyzed mechanism of direct glucose conversion to 5-HMF: (a) base-catalyzed isomerization of glucose to fructose (note that O^{2-}sites of monoclinic ZrO_2 provide the basic sites, and the Lewis acidic Zr^{4+} may stabilize enolate intermediates); and (b) Brønsted acid-catalyzed dehydration of fructose to 5-HMF over sulfoxy species. Reproduced with permission from ref 154. Copyright 2014 The Royal Society of Chemistry.

15 is also a promising catalyst for the one-pot cascade synthesis of alkyl levulinates from glucose.[189] The hydrothermal stability of this material is particularly interesting as this is one of the key desirable properties for catalysts in aqueous phase biomass processing.

3.2.3. Metal Phosphates. Metal phosphates have been widely investigated in academia and industry as heterogeneous catalysts.[190,191] Early studies reveal niobium phosphate as active for the aqueous phase dehydration of fructose to 5-HMF,[190] although little correlation was reported between acidic properties and performance with conversions of between 30% and 60% and high initial 5-HMF selectivity, although in all cases selectivity declined sharply over the course of reaction to unidentified (presumably polymeric) secondary products.

Doped and oxide supported vanadyl phosphates ($VOPO_4 \cdot 2H_2O$) with Brønsted and Lewis acid sites have also been studied for fructose dehydration. Doped vanadyl phosphates were prepared by isomorphic substitution of VO^{3+} groups with trivalent metals Fe^{3+}, Cr^{3+}, Ga^{3+}, Mn^{3+}, and Al^{3+} (entry 14, Table 2).[192] In the case of supported vanadyl phosphates, the support acidity was also important in promoting dehydration. For the doped samples, Fe-$VOPO_4 \cdot 2H_2O$ offered the best activity and selectivity, and was able to convert concentrated aqueous fructose solutions with a 5-HMF productivity of 376 mmol g_{cat}^{-1} h^{-1} at 80 °C, with minimal insoluble polymers or 5-HMF rehydration reported. Fructose dehydration over copper phosphates was dependent on their surface acidity (Brønsted/Lewis character) and morphology (Figure 20) (entry 16, Table 2).[193] Heat treatment of $CuHPO_4 \cdot H_2O$ nanoneedles transformed it into α-$Cu_2P_2O_7$ nanocrystals at 600 °C and rod-like nanostructures at 900 °C. The thermally processed phosphates exhibited weak acidity ($+3.3 \leq H_0 \leq +4.8$) but enhanced productivity as compared to H_3PO_4, with the α-$Cu_2P_2O_7$-900 giving up to a 36% 5-HMF yield.

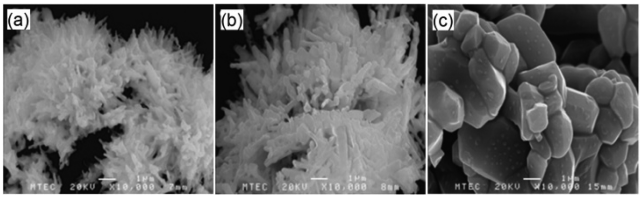

Figure 20. SEM images of (a) $CuHPO_4 \cdot H_2O$ (parent copper phosphates), (b) α-$Cu_2P_2O_7$-600 (calcined at 600 °C), and (c) α-$Cu_2P_2O_7$-900 (calcined at 900 °C). Adapted with permission from ref 193. Copyright 2012 Elsevier.

Calcium and α-strontium phosphates have been investigated for glucose, fructose, and cellulose conversion in hot compressed water (entry 15, Table 2).[194] These catalysts were prepared by a modified coprecipitation method, resulting in worm-like SEM morphologies as shown in Figure 21. Although

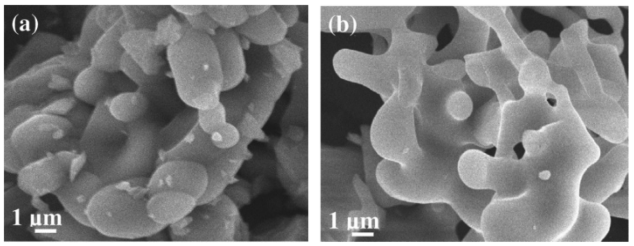

Figure 21. SEM images of (a) CaP_2O_6 and (b) a-$Sr(PO_3)_2$. Reproduced with permission from ref 194. Copyright 2012 Elsevier.

they are nonporous with very low (0.5 g m^{-2}) surface areas, high activity was observed for glucose and fructose dehydration, and the hydrolysis and dehydration of cellulose (Figure 22), with CaP_2O_6 and α-$Sr(PO_3)_2$ phosphate favoring 5-HMF formation from glucose and fructose.

In comparison with the preceding niobium, vanadium, copper, and alkaline earth phosphates, zirconium phosphates (ZrPO) are more extensively investigated. Crystalline ZrPO, precipitated from $ZrCl_2$, was explored for fructose dehydration in subcritical water at 240 °C, achieving around 80% fructose conversion after 120 s with 61% selectivity to 5-HMF.[195] However, these aggressive conditions resulted in a high background rate of dehydration to 5-HMF. Metal phosphates of aluminum (AlPO), titanium (TiPO), zirconium (ZrPO), and niobium phosphates (NbPO) have also been compared for glucose dehydration,[196] with a view to examine the effect of different phosphate species and associated acidity. Acid strength and activity both increased with decreasing electronegativity of the metal cation, with NbPO > ZrPO > TiPO > AlPO. The Brønsted:Lewis acid site distribution also influenced 5-HMF selectivity, with excess Lewis acidity driving unselective glucose

DOI: 10.1021/acs.chemrev.6b00311
Chem. Rev. 2016, 116, 12328−12368

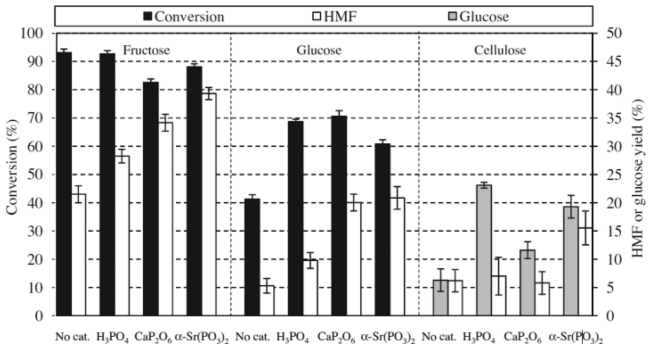

Figure 22. Fructose, glucose, and cellulose conversion, and 5-HMF yields for H_3PO_4, CaP_2O_6, or a-$Sr(PO_3)_2$. Reproduced with permission from ref 194. Copyright 2012 Elsevier.

transformation into humins (see entry 13, Table 2). The modification of NbPO and ZrPO through silylation to eliminate unselective Lewis acid sites afforded a drastic increase in 5-HMF selectivity, which reached 60% (albeit at 135 °C).

Porous metal phosphates have also attracted interest with a view to enhancing their catalytic performance. Cheng et al. reported mesoporous zirconium phosphates (Figure 23)

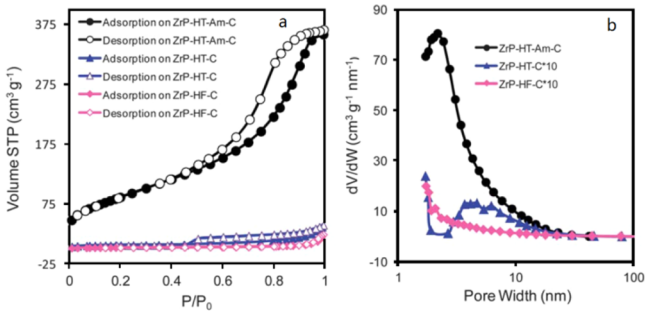

Figure 23. (a) N_2 adsorption−desorption isotherms. (b) Pore size distribution curves of the as-synthesized zirconium phosphate catalysts. Reproduced with permission from ref 197. Copyright 2013 The Royal Society of Chemistry.

obtained by hydrothermal synthesis using organic amine (dodecylamine and hexadecylamine) templates, which exhibited high conversion (up to 96%) for xylose dehydration in water and corresponding high furfural yields reaching 52% (entry 12, Table 2).[197] This was attributed to their open internal structures and abundant Brønsted/Lewis acid sites; the mesoporous ZrPO catalyst showed good stability and was easily regenerated by calcination.

While (transition) metal phosphates show promise for C_5−C_6 sugar dehydration, control over their textural properties is limited due to restructuring under high temperature calcination to remove structure-directing agents,[198,199] while mild calcination or solvent extraction (e.g., acid and ethanol) is insufficient to completely remove organic templates. Synthesis of porous metal phosphates is also restricted currently to a limited range of metals: zirconium, titanium, and niobium.[200] Continued effort should be devoted to preparing porous and ordered metal phosphates with improved active site accessibility.

3.2.4. Composite Metal and Nonmetal Oxides. Metal oxides are extensively used in catalysis as active components or supports, and have been investigated in the aqueous phase reforming of C_5−C_6 sugars. A comparison of TiO_2 and ZrO_2 with homogeneous mineral acids (H_2SO_4 and HCl) highlighted their advantages for both glucose and fructose dehydration during microwave irradiation (and sand bath heating to 200 °C).[201] ZrO_2 promoted glucose isomerization to fructose, whereas TiO_2 drove both glucose isomerization and subsequent dehydration of reactively formed fructose to 5-HMF. TiO_2 and ZrO_2 were both efficient for 5-HMF production from fructose (entry 19, Table 2), suppressing levulinic and formic acid products of 5-HMF rehydration.

Supported metal oxides have also been utilized; for example, TiO_2 (8−9 nm anatase) carbon nanocomposites were prepared by a microwave-assisted method for the catalytic dehydration of xylose into furfural (Figure 24).[202] TiO_2/RGO (reduced

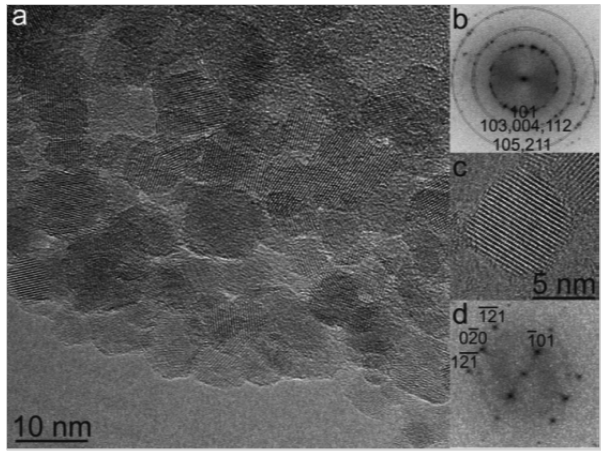

Figure 24. (a) HRTEM and (b) electron diffractogram of TiO_2/RGO, and (c) HRTEM image and (d) electron diffractogram of an individual 8 nm TiO_2 nanoparticle on RGO. Reproduced with permission from ref 202. Copyright 2013 The Royal Society of Chemistry.

graphene oxide) and TiO_2/CB (carbon black) exhibited high furfural yields (67−69%) under identical conditions, and showed excellent stability with negligible Ti leaching over 3 cycles. This synthetic approach could be generalized to a variety of metal oxides and composites.

Mixed metal oxides offer interesting opportunities to tune Brønsted and Lewis acidity relative to their oxide constituents. CeO_2−Nb_2O_5 mixed oxides prepared by coprecipitation were tested for fructose dehydration;[203] although no crystalline mixed phases were observed, the CeO_2:Nb_2O_5 ratio influenced the strong acid site density and associated conversion and selectivity (Figure 25). Higher Nb_2O_5 loadings favored fructose dehydration and 5-HMF selectivity; however, there was no clear evidence of any synergy, with pure niobia superior to any of the ceria composites.

Nonmetal oxides are also sporadically reported for the catalytic dehydration of sugars. For instance, graphene oxides have been examined in xylose conversion to furfural, in comparison with graphene, sulfonated graphene, and sulfonated graphene oxides (Figure 26).[183] Although sulfated graphene oxides showed the best 5-HMF selectivity and yield, this study does show the potential of nonmetal oxides for the C_5−C_6 sugar dehydration.

3.2.5. Other Solid Acid Catalysts. Heteropolyacids are an important class of catalysts due to their superacidity and strong redox properties for which they have found application in selox. Heteropolyacid salts have also been investigated in catalytic sugar transformations, with Fan et al. reporting that $Ag_3PW_{12}O_{40}$ catalyzed 5-HMF production from fructose and

DOI: 10.1021/acs.chemrev.6b00311
Chem. Rev. 2016, 116, 12328−12368

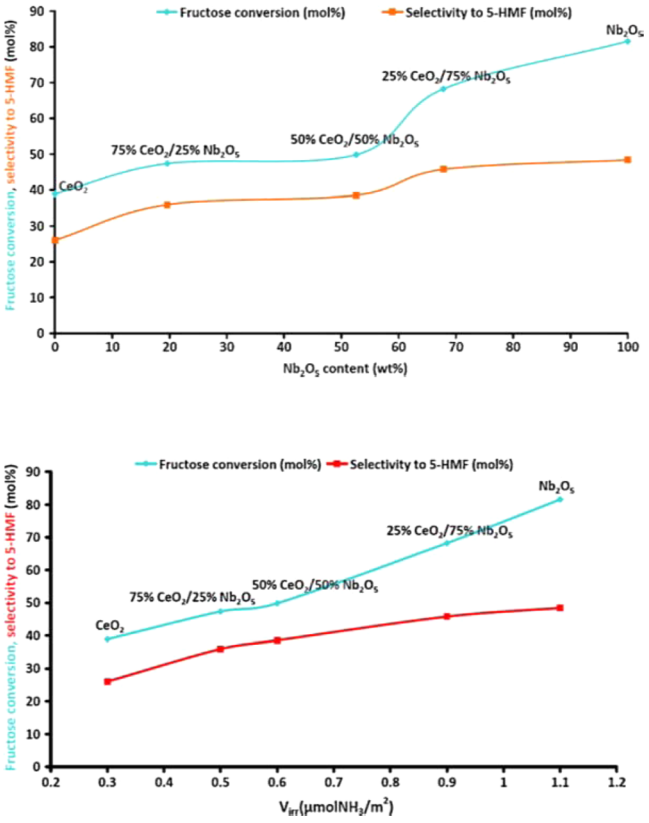

Figure 25. Influence of (top) Nb_2O_5 loading and (bottom) the density of strong acid sites, on fructose conversion and selectivity toward 5-HMF over CeO_2–Nb_2O_5 composites. Reproduced with permission from ref 203. Copyright 2012 Elsevier.

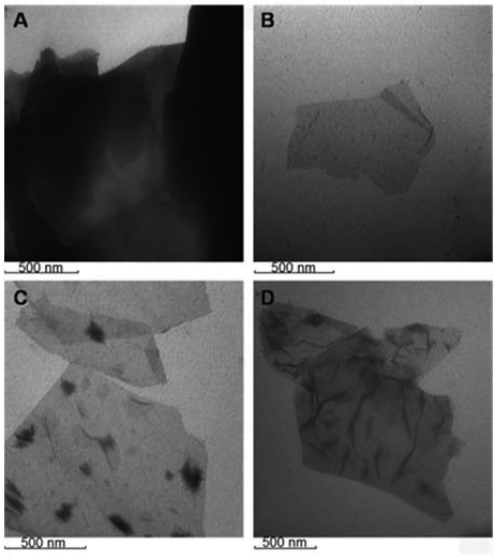

Figure 26. TEM images of (A) graphene, (B) graphene oxide, (C) sulfated graphene oxide, and (D) sulfated graphene. Reproduced with permission from ref 183. Copyright 2012 Elsevier.

glucose;[204] it was claimed that fructose could be dehydrated to 5-HMF with 94% selectivity and 78% yield within only 1 h at 120 °C (entry 18, Table 2). Silver ion-exchanged silicotungstic acid $Ag_4[Si(W_3O_{10})_4]\cdot nH_2O$ has also been proven an effective catalyst for fructose and sucrose dehydration to 5-HMF in superheated water,[205] achieving 98% fructose conversion and an 86% 5-HMF yield. However, the cost of such high loading (10 wt %) Ag-exchanged catalysts would likely be prohibitive for scale-up as compared to, for example, acidified carbons.[117] A Cr-substituted silicotungstic acid, $Cs_2[Cr_3O(OOCC_2H_5)_6(H_2O)_3]_2[\alpha\text{-}SiW_{12}O_{40}]$, possessing dual Brønsted–Lewis acidity, was also reported for monosaccharide dehydration to 5-HMF in water (entry 17, Table 2),[206] with a yield of 86% from fructose in DMSO (versus 56% in water, this difference is significant because DMSO is itself an effective Brønsted acid catalyst for this dehydration[206]). Somewhat lower yields of 48% 5-HMF were obtained from glucose (Figure 27). The authors claimed that the "low polar" 5-HMF product may be stabilized in the hydrophobic channels of the ionic crystals.

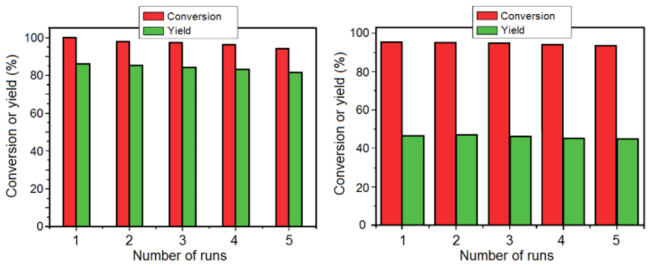

Figure 27. Catalyst performance in (left) DMSO and (right) water over five reaction cycles at 130 °C over $Cs_2Cr_3SiW_{12}$. Reproduced with permission from ref 206. Copyright 2015 The Royal Society of Chemistry.

3.2.6. Process Considerations. A continuous process for fructose dehydration to 5-HMF has been developed around water tolerant niobia catalysts using a fixed-bed tubular flow reactor,[209] in which both the preheater and the reactor are held isothermal via a hot air circulating oven (Figure 28). The reactor design enabled efficient temperature control between

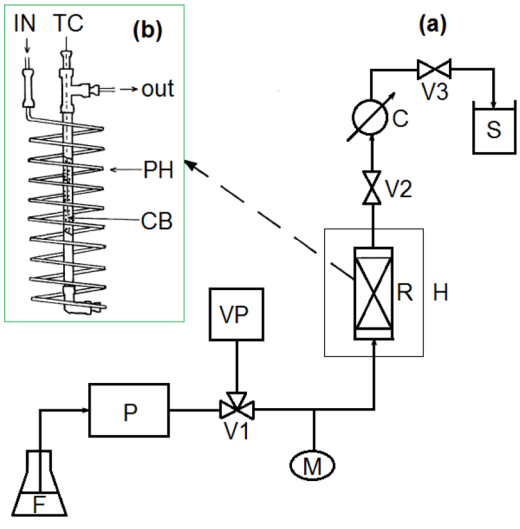

Figure 28. (a) Schematic of the continuous reaction line used for the catalytic experiments: feed reservoir (F); dosing pump (P); vacuum pump (VP); manual three-ways valve (V1); manometer (M); catalytic reactor (R); oven (H); manual two ways-valve (V2); cooler (C); manual precision valve (V3); and autosampler collector (S). (b) Schematic of the catalytic reactor with preheater (PH), thermocouple (TC), and catalytic bed (CB). Reproduced with permission from ref 209. Copyright 2006 Elsevier.

DOI: 10.1021/acs.chemrev.6b00311
Chem. Rev. 2016, 116, 12328–12368

90 and 110 °C. Pressure control between 2 and 6 bar was achieved using a micrometric valve at the end of the reaction line to avoid water evaporation and the formation of gas bubbles in the catalyst bed. 5-HMF selectivity increased with fructose conversion under continuous flow conditions, contrary to observations in batch, wherein 5-HMF selectivity normally decreases with conversion. Short residence times accessible in continuous flow operation allow rapid product removal and suppression of undesired side reactions.

A major limitation to the development of economic C_5-C_6 sugar dehydration in pure water is the accompanying poor selectivity to 5-HMF or furfural due to product degradation.[210] Use of a biphasic continuous reactor is recognized as one of the most promising methods to improve the yield of 5-HMF, whereby a water-immiscible organic solvent is used for continuous 5-HMF extraction from the aqueous phase, thereby facilitating efficient product separation and limiting degradation reactions.[211−215] Xylose and fructose conversion to furfural or 5-HMF, respectively, is reported to proceed with improved selectivity (up to 90%) when conducted in such biphasic reactors, which also permit continuous product extraction.[59,214] A continuous flow, biphasic fixed-bed reactor for furfural production from xylan and xylose has been reported[216] utilizing a mixed catalytic bed of a Lewis acid gallium-containing USY zeolite for xylose isomerization and a Brønsted acid ion-exchanged resin (Amberlyst-36) for hemicellulose hydrolysis and xylulose dehydration (Figure 29). High product selectivity was achieved via efficient extraction of furfural to the organic phase, with furfural yields of 72% from xylose and 69% from xylan obtained.

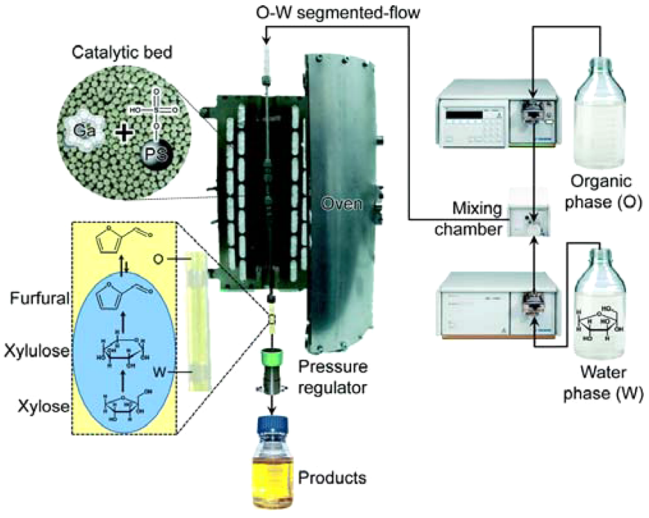

Figure 29. Continuous flow biphasic reactor used for the conversion of C_5 carbohydrates to furfural. Reproduced with permission from ref 216. Copyright 2015 The Royal Society of Chemistry.

Addition of solvent modifiers including DMSO,[217,218] 1-methyl-2-pyrrolidinone (NMP), poly(1-vinyl-2-pyrrolidinone) (PVP), and alcohols[218−220] is reported to inhibit aqueous phase side reactions and increase 5-HMF productivity. While the use of aprotic solvents such as DMSO can improve 5-HMF yields, separation from the high-boiling point solvent is difficult due to attendant product decomposition; hence there is growing interest in molecular simulation to obtain fundamental insight into the design of such mixed solvent systems. Desirable solvent features include (i) nonmiscibility of the cosolvents; (ii) high partition coefficients for extracting the desired compound from water without extracting the catalyst; and (iii) higher boiling points than the product to aid distillation and final product separation. MD simulations to investigate the solubility of 5-HMF in 2-butanol/MIBK biphasic systems[221] demonstrate the potential of in silico screening of organic solvent mixtures to assist process design. 2-*sec*-Butylphenol (SBP), propyl guaiacol (PG), and propyl syringol (PS), which can be derived from lignin, have also proven viable renewable cosolvents[222] for furfural, 5-HMF, levulinic acid, and γ-valerolactone production from C_5-C_6 sugars. Process optimization also necessitates the development of heterogeneous catalysts, which selectively partition within the aqueous phase.[223,224]

As discussed in section 1.1, ILs, DES, and CO_2 are potential cosolvents for use in aqueous phase catalysis to enhance the dissolution of nonpolar substrates and/or provide a second phase to extract products into. DESs are becoming a popular green solvent for catalytic reactions;[222] however, there are few reports on catalytic processing of sugars in biphasic DES/H_2O or IL/H_2O systems, with most studies concentrating on enzymatic transformations in which DESs enhance substrate solubility and increase reaction rates and in some cases regio- or enantioselectivity.[66] One promising example of a chemocatalytic transformation concerns the mixed solvent systems of betaine hydrochloride (BHC) and choline chloride (ChCl) in water for fructose and inulin dehydration to 5-HMF.[225] MIBK addition enabled the continuous extraction of 70% 5-HMF from the ChCl/BHC/H_2O system, which could be recycled seven times. Alternatively, addition of an $AlCl_3$ Lewis acid catalyst to ChCl/BHC/H_2O promoted glucose isomerization to fructose, with a 40% 5-HMF yield. ZrO_2-catalyzed 5-HMF production from glucose proceeded more effectively in IL−water mixtures (10−50 wt % water in 1,3-dialkylimidazolium chloride) than pure water or IL; a 50 wt % 1-hexyl-3-methyl imidazolium chloride mixture offered 53% 5-HMF in only 10 min at 200 °C.[226]

3.2.7. Summary of Solid Acid Dehydration Catalysts.

The catalytic performances of the preceding solid acids are summarized in Table 2, and represent a more diverse collection than employed for xylose and glucose isomerization (which reflected principally zeolites and hydrotalcites). Reaction temperatures for dehydration are generally higher (120−200 °C) than employed for isomerization (90−120 °C), with the attendant possibility of side reactions of reactants, intermediates, and products. Wide variations are observed in sugar conversions; however, product yields were relatively low, with the highest yield observed over the sulfonated graphene oxide and $Ag_3PW_{12}O_{40}$ (entries 7 and 18, Table 2). Although few studies provide kinetic data or mass balances, the latter is extremely important because the xylose, glucose, or fructose dehydration may be accompanied by a range of side reactions and require detailed HPLC analysis.[154] Catalyst reusability has only been explored for select systems, notably the sulfated graphene oxide[183] and heteropolyacids[206] highlighted above. A high density of accessible and medium-strong acid sites is required for low temperature (<150 °C) sugar dehydration, with Brønsted acidity generally considered a key factor for high activity and selectivity to furfural (Figure 30)[208] and 5-HMF, with the latter also favored by porous structures. Water is both the reaction media of choice in biomass conversion, and byproduct of dehydration; hence competing rehydration and hydrolysis pathways are inevitable, limiting selectivity and presenting a challenge to most solid acids; metal oxide−water

DOI: 10.1021/acs.chemrev.6b00311
Chem. Rev. 2016, 116, 12328−12368

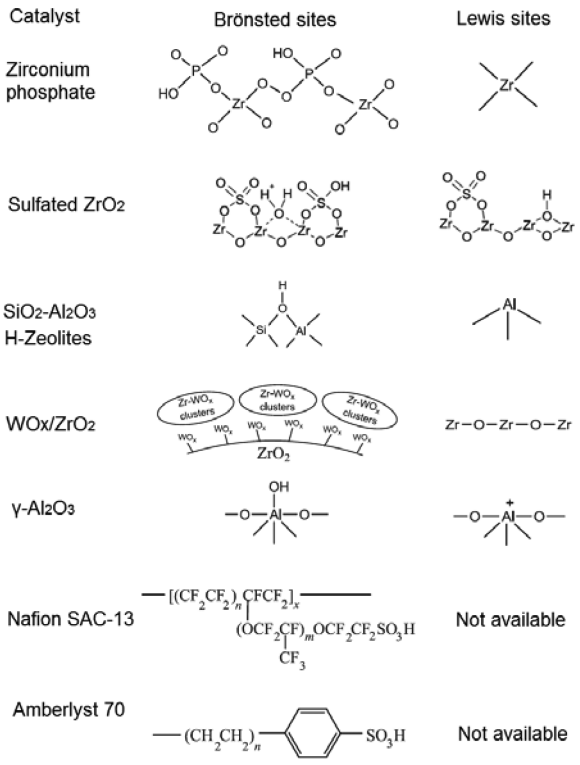

Figure 30. Typical solid acids and the origin of acid types. Adapted with permission from ref 208. Copyright 2011 Elsevier.

interfaces drive a range of chemistries, including acid−base, ligand exchange, and/or redox processes,[227,228] and require further study in the context of sugar dehydration. Water is also a common poison of solid acids, either through leaching of active sites or strong adsorption and site-blocking, and water-tolerant solid acids would thus represent a key development for commercialization.[229]

3.3. Metal Catalysts for Hydrogenation

Early studies revealed Raney nickel and ruthenium, platinum, cobalt, copper, and rhodium as promising catalysts for selective hydrogenation of xylose, glucose, and fructose.[230−232] Although the hydrogenation of keto or aldose carbonyls should be routine, selectivity is hampered by the tendency for sugars to undergo competitive isomerization, polymerization, degradation, and dehydration (Figure 6). This challenge has largely been addressed through the use of promoters and cocatalysts, or modification of support structure or electronic properties.

3.3.1. Amorphous Alloys. *3.3.1.1. Raney Ni Catalysts.* Raney Ni is prepared from Ni−Al alloys, with some or all of the aluminum removed by alkaline leaching to deliver a porous structure. Mo, Cr, Fe, and Sn promoters (M) have been used in $Ni_{40-x}Al_{60}M_x$ Raney-catalyzed glucose hydrogenation (entry 1, Table 3),[233] enhancing activity 7-fold (Figure 31) for Fe-promoted Raney Ni. The promoter type, distribution, and the oxidation state also influenced performances, with low valent species acting as Lewis sites binding glucose through the oxygen of the C═O group, polarizing the bond to favor hydrogenation via nucleophilic attack by surface hydrogen. Promoter stability remains to be addressed.

3.3.1.2. Ni−P Amorphous Alloys. Inspired by Raney Ni, a skeletal Ni−P amorphous alloy catalyst (Raney Ni−P) was prepared by alkali leaching of a Ni−Al−P precursor,[234] which exhibited higher TOFs (per surface Ni) than Raney Ni catalyst in glucose hydrogenation to sorbitol, attributed to P promotion of active Ni sites (entry 2, Table 3). The Raney Ni−P catalyst outperformed conventional Ni−P alloys due to a higher surface area and density of surface Ni atoms.

3.3.1.3. Ni−B Amorphous Alloys. Silica supported amorphous Ni−B was also investigated in glucose hydrogenation.[235] The as-prepared Ni−B/SiO_2 catalyst was more active than other Ni catalysts, such as crystalline Ni−B/SiO_2, Ni/SiO_2, and commercial Raney Ni (entry 3, Table 3), attributed to the high dispersion of Ni and electronic perturbation of metallic Ni by B, which was proposed to induce stronger C═O adsorption to Ni atoms. The addition of Cr, Mo, and W promoters further improved activity (Figure 31). High promoter concentrations resulted in site-blocking of active Ni sites. The question of selectivity was largely neglected in the preceding Ni alloy studies, with sorbitol implicit as the major product even though Lewis acid promoters are also expected to drive glucose isomerization.[236]

3.3.1.4. Co−B and Ru−B Amorphous Alloys. Co−B[237,238] and Ru−B[239,240] amorphous alloys have been explored in glucose hydrogenation. Amorphous Co−B (entry 5, Table 3) exhibited higher activity than crystalline Co and Ni analogues, with Cr, Mo, and W further increasing conversion, attributed to enhanced dispersion of the Co active species (and hence carbonyl adsorption). Ultrafine Ru−B particles in amorphous Ru−B alloys likewise conferred higher activity in glucose hydrogenation than crystalline Ru−B and pure Ru powders. In another study,[240] addition of trace Cr in the form of Cr_2O_3 similarly promoted glucose hydrogenation by increasing Ru−B alloy dispersion.

3.3.2. Ni. Raney Ni was employed historically for the hydrogenation of sugar compounds due to its low cost; however, supported nickel catalysts often offer higher activity. Kusserow et al. investigated Ni over SiO_2, TiO_2, Al_2O_3, and carbon supports in comparison with commercial Raney Ni for the aqueous phase hydrogenation of glucose in batch and flow,[124] prepared by impregnation, sol−gel, precipitation, and templated syntheses (Figure 32). Impregnated alumina proved the best (entry 6, Table 3), with a conversion comparable to that of an industrial Ni68T catalyst (despite containing only 5 wt % Ni versus 66 wt %) and similar sorbitol selectivities of around 90%. Ni on TiO_2 and SiO_2 exhibited lower conversions, with carbon providing poor activity. Specific sorbitol productivities followed Al_2O_3 > TiO_2 > SiO_2 > C. Prereduction temperature strongly influenced performance, with catalysts reduced at 500 °C more active than those reduced at 300 °C. Further investigations of catalyst pretreatment for Ni/SiO_2 in glucose hydrogenation[241] revealed that calcination prior to reduction gave higher conversion and selectivity than direct reduction due to improved decomposition of the nickel precursor.

Recently, Ni/Cu/Al hydrotalcite precursors and Ni/Cu/Al/Fe hydrotalcite-like catalysts were developed for the hydrogenation of glucose and fructose, respectively. Preparation and activation treatments of Ni/Cu/Al hydrotalcite precursors had a significant impact on glucose hydrogenation;[242] high temperature reduction increased activity and selectivity toward sorbitol over a $Ni_{1.85}Cu_1Al_{1.15}$ catalyst (entry 7, Table 3)[243] independent of pH, and also increased the activity of a $Ni_{4.63}Cu_1Al_{1.82}Fe_{0.79}$ HT for fructose hydrogenation (Figure 33).

3.3.3. Ru. Ruthenium catalysts are more extensively investigated than Ni analogues for the hydrogenation of sugars,

DOI: 10.1021/acs.chemrev.6b00311
Chem. Rev. 2016, 116, 12328−12368

Table 3. Metal Catalysts for Xylose Hydrogenation to Xylitol and Glucose/Fructose Hydrogenation to Sorbitol/Mannitol

entry	catalyst	conv./%	sele./%	yield/%	initial rate/ mmol g_{metal}^{-1} h^{-1}	TOF/h^{-1}	reaction order, g = glucose	reaction conditions	ref
1	RaneyNiFe$_3$ (Fe/Ni × 10^3 = 186)				575			6.7 wt % glucose, 1.6 g of catalyst, 130 °C, 50 bar, 1400 rpm, 175 mL	233
2	Raney Ni−P, $Ni_{68}Al_{25}P_7$	56	100	56		1440		50 wt % glucose, 1 g of catalyst, 120 °C, 40 bar, 6 h, 1200 rpm, 50 mL	234
3	Ni−B/SiO_2 (fresh)	30				86	0, 10% < [g] < 50% 1, 0 < pH_2 < 40 bar	50 wt % glucose, 3 g of catalyst, 100 °C, 40 bar, 6 h, 1200 rpm, 50 mL	235
4	20.9%Ni/SiO_2 (calcined and reduced)	45	92	42	144	22		20 wt % glucose, 0.4 g of catalyst, 120 °C, 120 bar, 5 h, 850 rpm, 120 mL	241
5	$Co_{75.4}B_{24.6}$	89				319	0, 10% < [g] < 50% 1, 0 < pH_2 < 40 bar	50 wt % glucose, 1 g of catalyst, 120 °C, 40 bar, 6 h, 1200 rpm, 50 mL	237
6	Ni/Al_2O_3 C-en	33	88	28				40 wt % glucose, 0.5 g of catalyst, 120 °C, 120 bar, 5 h, 850 rpm, 120 mL	124
7	$Ni_{1.78}Cu_1Al_{1.11}Mg_{1.29}$	78	93	73				5 wt % glucose, 0.4 g of catalyst, 125 °C, 30 bar, 3 h, 600 rpm, 40 mL	242
8	$Ru_{86.7}Cr_{3.0}B_{10.3}$	100	100	100				50 wt % glucose, 0.3 g of catalyst, 80 °C, 40 bar, 2 h, 1800 rpm, 50 mL	240
9	Ru(5%)/NiO(5%)−TiO_2	100	100	100				20 wt % xylose, 120 °C, 55 bar, 2 h, 1200 rpm, 200 mL	253
10	Ru/CMFN (pyridine as the C source)				8554			40 wt % glucose, 0.05 g of catalyst, 100 °C, 80 bar, 3 h, 1000 rpm, 30 mL	247
11	Ru/MCM-41	91	90	82				10 wt % glucose, 0.25 g of catalyst, 120 °C, 30 bar, 3 h, 500 rpm, 25 mL	254
12	Ru/polystyrene	41	99	40	2101	212.4		29 wt % glucose, 0.4 g of catalyst, 100 °C, 40 bar, 1.33 h, 50 mL	255
13	1%Ru/HY (zeolites)	19	98	19	13 321	1306	0, 10% < [g] < 40% 1, 0 < pH_2 < 100 bar	25 wt % glucose, 1 g of catalyst, 120 °C, 55 bar, 0.33 h, 1200 rpm, 160 mL	256
14	Ru/ZSM-5-TF (template-free)	100	100	99		32		25 wt % glucose, 0.5 g of catalyst, 120 °C, 40 bar, 2 h, 500 rpm, 50 mL	257
15	Ru(1%)/NiO(5%)-TiO_2 (passivated and reduced)	95	98	93				20 wt % glucose, 120 °C, 55 bar, 2 h, 1200 rpm	258
16	1%Pt/AC reduced by $NaBH_4$	98	92	90		53.1		2.8 wt % glucose, 0.06 g of catalyst, 180 °C, 16 bar, 3 h, 1100 rpm, 5 mL	125
17	Pt/activated carbon cloths	100	100	100	1800			40 wt % glucose, 100 °C, 80 bar	259
18	Pt/γ-Al_2O_3 + 0.075 g of hydrotalcite	92	59	54		612.6		0.4 wt % glucose, 0.075 g of catalyst, 90 °C, 60 bar, 4 h, 700 rpm, 35 mL	260
19	Cu/ZnO/Al_2O_3	22	66	15				30 wt % fructose, 0.075 g of catalyst, 110 °C, 50 bar, 0.33 h, 1800 rpm	261
20	CuO−ZnO (61 wt % CuO, 39 wt % ZnO)	76	68	52			1, 30 < pH_2 < 45 bar	30 wt % fructose, 130 °C, 65 bar, 1 h, 1800 rpm, 150 mL	262
21	Ni/Cu/Al/Fe hydrotalcite-like compound	100	43	43				5 wt % fructose, 0.4 g of catalyst, 110 °C, 30 bar, 2 h, 600 rpm, 40 mL	243

being more efficient for aqueous phase carbonyl hydrogenation.[244,245] Ru supported on activated charcoal via cation or anion exchange was tested in a continuous trickle-bed reactor for glucose hydrogenation at 100 °C and 80 bar H_2 as a function of residence time,[241] with activity inversely proportional to Ru loading, and sorbitol selectivity inversely proportional to residence time, longer reaction leading to sorbitol epimerization to mannitol. Continuous-flow operation hence offered improved selectivity over batch. This catalyst was stable over several weeks' operation without Ru leaching. Overall Ru/C catalysts were comparable to, or more active, selective, and stable than, Raney Ni catalysts, which suffered from leaching of both Ni and promoters.[246]

Ru nanoparticles have been dispersed on mesoporous carbon (Ru/C-NFs) microfibers, using Al_2O_3 microfibers as templates by a chemical vapor deposition route.[247] Ru nanoparticles appear embedded within the mesoporous carbon matrix (Figure 34). Such Ru catalysts exhibited significantly enhanced activity and stability for glucose hydrogenation (entry 10, Table 3) due to the open mesoporous structure of the support, the unique microfiber morphology, and hydrogen spillover at the interface between the embedded Ru nanoparticles and carbon support. N-doping of the carbon also enhanced catalytic performance, attributed to stronger hydrogen adsorption, and better Ru wettability and electronic properties.

In fructose hydrogenation, Ru/C was compared to Pt/C and Pd/C catalysts. Heinen et al. found the furanose form of fructose reacted over Ru/C, whereas the pyranose form was inert under the same conditions (1 bar H_2, 72 °C),[248] despite these anomers adsorbing with comparable strength. It is interesting to note that the selectivity to mannitol for Pd/C and Pt/C could be improved by tin promotion. Structure−reactivity

DOI: 10.1021/acs.chemrev.6b00311
Chem. Rev. 2016, 116, 12328−12368

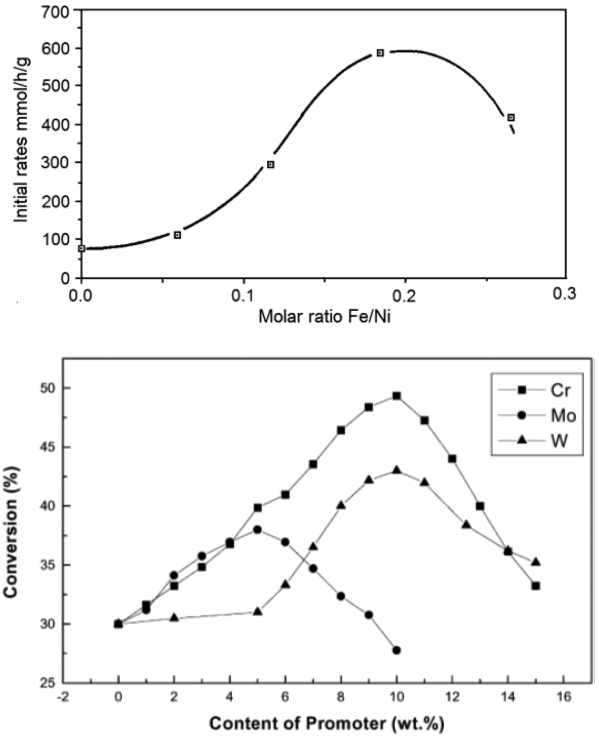

Figure 31. (top) Initial rate of glucose hydrogenation over fresh Raney $Ni_{40-x}Al_{60}Fe_x$ catalyst as a function of Fe:Ni ratio. Reproduced with permission from ref 233. Copyright 1994 Elsevier. (bottom) Glucose conversion over doped Ni−B/SiO_2 as a function of promoter concentration during hydrogenation. Adapted with permission from ref 235. Copyright 2002 Elsevier.

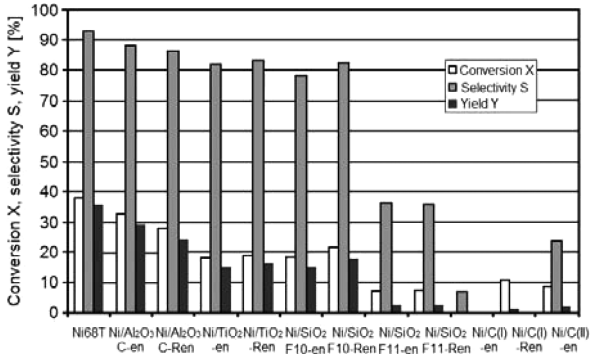

Figure 32. Catalytic performance of Ni systems in glucose hydrogenation: "en" = impregnation; "Ren" = incipient wetness. Reproduced with permission from ref 124. Copyright 2003 John Wiley & Sons.

relations in glucose hydrogenation to sorbitol[249] (and galactose/arabinose hydrogenation[250]) were explored by Murzin et al. over Ru/C catalysts with particle sizes spanning 1.2−10 nm. Hydrogenation of all three substrates was structure-sensitive with the highest TOFs observed for ∼3 nm Ru particles. Sorbitol selectivity peaked at 96% for nanoparticles <3 nm, with dehydration to glycerol favored over ≥10 nm Ru particles. The kinetics of D-glucose hydrogenation to D-sorbitol have also been investigated over a 5 wt % Ru/C catalyst in a semibatch slurry autoclave under high pressure (40−75 bar H_2) in the absence of mass transport limitations.[251] Hydrogenation was first order with respect to hydrogen, and also first order with respect to D-glucose for

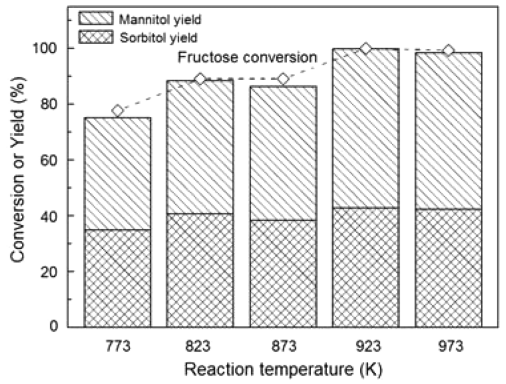

Figure 33. Catalytic performance of $Ni_{4.63}Cu_1Al_{1.82}Fe_{0.79}$ precursor after different reduction temperatures for fructose hydrogenation. Reaction conditions: 2 g of fructose, 40 mL of water, 0.4 g of catalyst, 110 °C, 2 h; 30 bar H_2; 600 rpm. Reproduced with permission from ref 243. Copyright 2013 Elsevier.

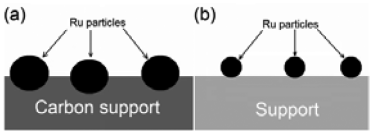

Figure 34. Schematic of Ru nanoparticles (a) embedded in porous carbon supports and (b) on the surface of a general support. Reproduced with permission from ref 247. Copyright 2011 The Royal Society of Chemistry.

concentrations <0.3 M (but zero order at high concentration). Modeling implicated Langmuir−Hinshelwood−Hougen−Watson (LHHW) kinetics wherein the surface reaction was rate-determining, but was unable to distinguish between (i) noncompetitive (molecular or dissociative) adsorption of H_2 and D-glucose; (ii) competitive adsorption of molecular H_2 and D-glucose; or (iii) competitive adsorption of dissociatively chemisorbed hydrogen and D-glucose.

In contrast to carbon supported Ru, glucose hydrogenation over silica analogues revealed growth/aggregation of Ru nanoparticles. In situ X-ray absorption spectroscopy and electron microscopy showed that SiO_2 supported Ru was in an oxidized state when air-exposed, undergoing reduction and concomitant sintering upon exposure to 40 bar H_2 at 100 °C in aqueous solution. However, the authors proposed that glucose acts to stabilize Ru against sintering (Figure 35),[252] preventing migration of Ru species during hydrolysis of the SiO_2 surface. This Ru/SiO_2 catalyst was entirely selective to sorbitol.

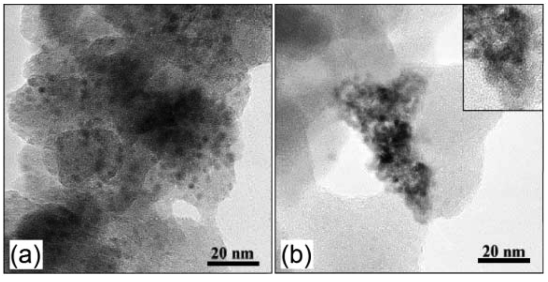

Figure 35. High-magnification TEM images of (a) as-prepared and (b) postreaction Ru/SiO_2 evidencing some in situ restructuring albeit with a common mean particle size. Reproduced with permission from ref 252. Copyright 2006 American Chemical Society.

DOI: 10.1021/acs.chemrev.6b00311
Chem. Rev. 2016, 116, 12328−12368

Ru/HYZ (H-formed zeolite Y) has also been investigated in the selective hydrogenations of xylose to xylitol and glucose to sorbitol,[123,256] as a function of reaction temperature, reaction time, catalyst loading, Si:Al ratio, and Ru concentration. Ru/HYZ exhibited exceptional TOFs in glucose hydrogenation, exceeding Ru/TiO_2 and Ru/NiO-TiO_2 (entry 13, Table 3), with >97% sorbitol selectivity. Reuse tests also found that Ru/HYZ had good stability, although some Ru nanoparticle aggregation was observed after four runs (Figure 36).[256]

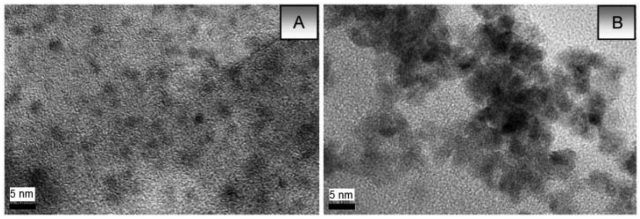

Figure 36. TEM images of (A) fresh and (B) spent Ru/HYZ after four glucose hydrogenation reactions. Adapted with permission from ref 256. Copyright 2014 Elsevier.

The influence of preparation method used to introduce Ru into ZSM-5 was investigated for glucose hydrogenation.[257] Ru-/ZSM-5 was obtained either by adding a Ru precursor to the parent ZSM-5 synthetic mixture (Ru/ZSM-5-TF), or through loading Ru nanoparticles on a commercial microporous ZSM-5 (Ru/ZSM-5-MS) or an alkali-treated mesoporous ZSM-5 (Ru/ZSM-5-AT) by incipient wetness impregnation. All of the Ru/ZSM-5 catalysts outperformed Ru/C (entry 14, Table 3), notably Ru/ZSM-5-TF, which offered the highest conversion and sorbitol selectivity. Ru incorporated in the Ru/ZSM-5-TF catalyst exhibited a uniform size and homogeneous distribution of nanoparticles throughout ZSM-5 (Figure 37).

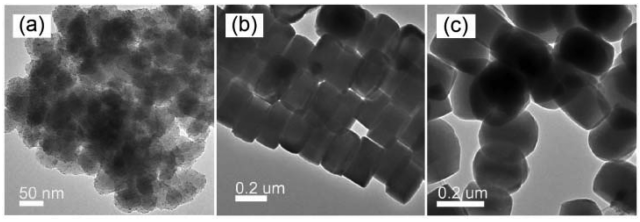

Figure 37. TEM images of (a) Ru/ZSM-5-TF, (b) Ru/ZSM-5-AT, and (c) Ru/ZSM-5-MS. Adapted with permission from ref 257. Copyright 2014 Elsevier.

Ru has also been explored over mesoporous MCM-41 silica (3.8 wt % Ru/MCM-41), prepared by impregnation and reduction with formaldehyde. This exhibited higher activity and sorbitol selectivity than a range of other transition metal catalysts for glucose hydrogenation (Figure 38).[254] Ru/MCM-41 has twice the metal surface area of Ru/C, suggesting the excellent performance is simply due to greater active site dispersion. Although the Ru/MCM-41 catalyst could be reused, the metal surface area decreased from 4.5 to 0.78 $m^2\ g^{-1}$, and hence stability is an issue.

Metal oxides are also popular supported for Ru, with Mishra et al. reporting Ru/NiO−TiO_2 for xylose and glucose hydrogenation.[253,258] The TiO_2 support was first modified by nickel chloride impregnation and subsequent oxidation.

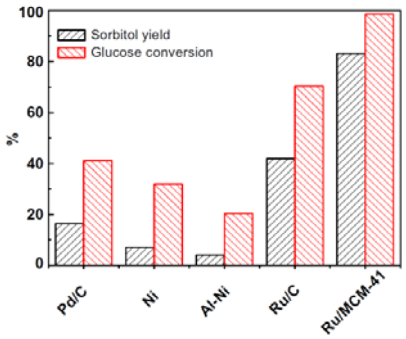

Figure 38. Glucose hydrogenation over Ru/MCM-41 and comparator catalysts. Reaction conditions: 2.5 g of glucose, 10 wt % catalyst, 25 mL of water, 120 °C, 2 h, 30 bar H_2. Reproduced with permission from ref 254. Copyright 2011 Elsevier.

Catalytic performance in xylose hydrogenation to xylitol was comparable to Raney Ni, Ru/C, and Ru/TiO_2 under identical reaction conditions; however, NiO addition enhanced conversion, yield, and selectivity toward xylitol. Considering glucose hydrogenation, the NiO-modified TiO_2 catalyst improved sorbitol selectivity by lowering fructose production and its subsequent hydrogenation to mannitol (entry 15, Table 3). Ru on poly(styrene-*co*-divinylbenzene) amine-functionalized polymers (Ru/PSN) was studied recently for xylose hydrogenation to xylitol.[263] In addition to facile Ru/PSN recovery and reuse, its selectivity to xylitol exceeded 90%. In a related study, Ru nanoparticles embedded within a mesoporous hyper-cross-linked polystyrene were investigated for glucose hydrogenation (entry 12, Table 3).[255] Two reaction mechanisms were considered: the interaction of glucose with hydrogen spilled-over from Ru to the support; and the direct reaction of adsorbed glucose with molecular hydrogen from the reaction medium. Catalyst deactivation was attributed to the complete consumption of "stored hydrogen" from spillover of the as-prepared catalyst following the initial stage of reaction.

Mechanistic aspects of Ru-catalyzed hydrogenation of bioderived carbonyl compounds (albeit not the C_5−C_6 parent sugars) offer some insight into the active species.[244] Jae et al. studied 5-HMF hydrogenation to 2,5-DMF by XPS, XAS, and HRTEM, noting that fresh Ru nanoparticles were dominated by surface RuO_x, which underwent in situ reduction to metallic Ru resulting in deactivation.[264] They proposed that RuO_x behaved akin to a Lewis acid, promoting an MPV pathway via interhydride transfer from 2-propanol to 5-HMF to form 2,5-bis(hydroxymethyl)furan. Prereduced Ru/C exhibited only moderate hydrogenolysis activity toward 5-HMF, with ∼30% selectivity to 2,5-DMF. A synergy between physically mixed (partially) oxidized and metal phases increased 2,5-DMF selectivity to 70%. DFT calculations and experimental studies of Ru-catalyzed levulinic acid,[245,265] furfural,[266] L-arabinose,[267] and 2-butanone[268] hydrogenation have highlighted a crucial role for surface H_2O in regulating substrate activity, Ru surface oxidation state, and intermediate reactivity, although the nature of the participating water species has yet to be fully elucidated. Cooperative interactions between C═O functions in reactive intermediates adsorbed over Ru with coadsorbed, neighboring water molecules are proposed to decrease the barriers toward levulinic acid hydrogenation to γ-valerolactone; higher experimental rates were observed as the hydrogen-bond donor capability of the solvent increased.[265] However, computational studies suggest that water undergoes dissociative

DOI: 10.1021/acs.chemrev.6b00311
Chem. Rev. 2016, 116, 12328−12368

adsorption over Ru metal to produce ionic surface species and atomic hydrogen,[269,270] which may participate in hydrogenation.

3.3.4. Pt. Pt (and bimetallic derivative) catalysts are the subject of many theoretical, experimental, and industrial hydrogenation studies.[271−273] However, in the context of xylose/glucose hydrogenation to xylitol/sorbitol, Pt has proven less popular than Ni or Ru catalysts.

Pt on activated carbon cloth (ACC), see Figure 39a−c, was investigated for glucose hydrogenation.[259] As compared to traditional powder or granular carbon supports, ACC displayed a high surface area and narrow micropore size distribution, which favored efficient liquid phase mass transport. Pt was introduced by cation exchange after oxidation of the ACC support, with TEM (Figure 39d) confirming a homogeneous dispersion of Pt in the carbon fibers (2−3 nm diameter nanoparticles). Pt/ACC catalysts were highly active for glucose hydrogenation, giving a sorbitol yield >99.5%, superior to conventional Pt/C catalysts. ACC was inexpensive and resistant to acidic and basic conditions. Activated charcoal is also a good support for Pt-catalyzed glucose hydrogenation,[274] and fructose hydrogenation to mannitol.[275] However, in common with many studies utilizing carbon supports, the chemical composition and distribution of surface functions on the carbon were poorly characterized, limiting their reproducibility. Kanie et al. studied glucose and fructose hydrogenation at 130−270 °C in subcritical water under 50 bar H_2 over Pt nanoparticles protected by polyethylenimine (Pt-PEI).[276] Unfortunately, these catalysts were unselective, converting glucose to 1,2-propanediol, 1,2-hexanediol, and ethylene glycol, and fructose to 1,2-propanediol, 1,2-hexanediol, and glycerol.

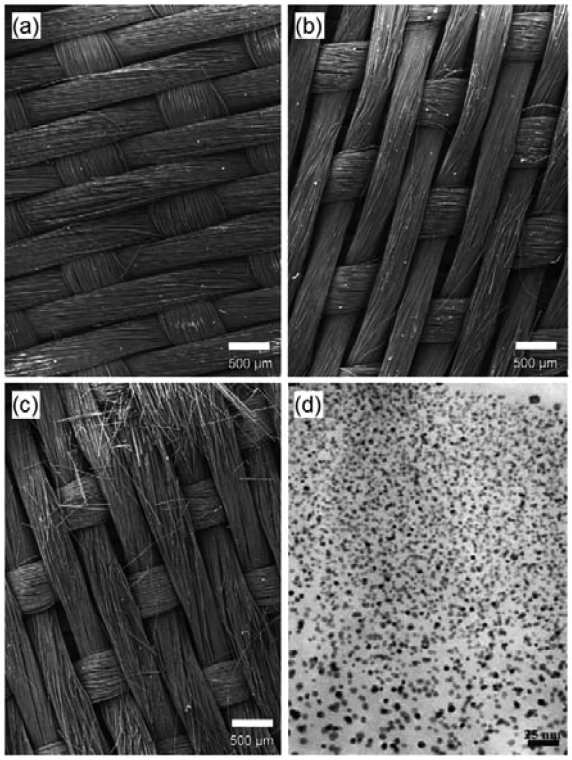

Figure 39. Scanning electron micrographs of activated carbon cloth at different preparation stages: (a) parent carbon, (b) after NaClO oxidation, (c) 10 wt % Pt/ACC, and (d) TEM image of 10 wt % Pt/ACC catalyst (25 nm scale bar). Adapted with permission from ref 259. Copyright 2007 Elsevier.

Bifunctional Pt catalysts employing acidic γ-Al_2O_3 and basic hydrotalcite supports have been examined for xylose and glucose hydrogenation (entry 18, Table 3 for glucose hydrogenation).[260] A combined sorbitol and mannitol yield of 68% was obtained from glucose over Pt/γ-Al_2O_3 in combination with hydrotalcite, with an alkaline medium increasing the concentration of open-form glucose, which is more readily hydrogenated. The same combination achieved 99% xylose conversion and 82% xylitol yield. However, these catalysts lost significant activity after only two runs at 90 °C.

3.3.5. Other Hydrogenation Catalysts. Copper catalysts popular in redox and photocatalysis,[277−281] and Cu/SiO_2 and Cu/ZnO/Al_2O_3, have also been studied in fructose hydrogenation to mannitol.[261] Ultrasonication enhanced the activity of Cu/SiO_2 (and a Raney Ni comparator), but did not improve selectivity (Figure 40), whereas it deactivated a Cu/ZnO/Al_2O_3 catalyst. A commercial methanol synthesis, CuO−ZnO (61 wt % CuO and 39 wt % ZnO) catalyst was also active for fructose hydrogenation.[262] In both cases, mannitol was the major hydrogenation product with some sorbitol formed through fructose isomerization to glucose. The best mannitol selectivity was around 70% for any Cu catalysts.

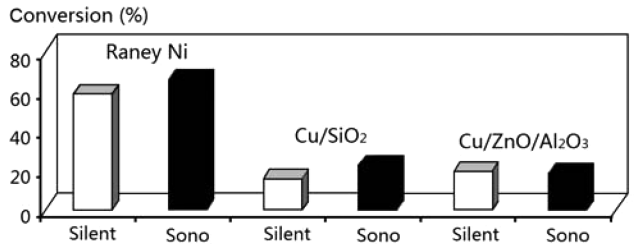

Figure 40. Influence of sonication in fructose conversion over Cu and Ni catalysts. Reaction conditions: 110 °C and 50 bar of H_2. Adapted with permission from ref 261. Copyright 2011 American Chemical Society.

3.3.6. Process Considerations. Catalytic hydrogenation of aqueous solutions of glucose to sorbitol has been explored in a high pressure, trickle-bed reactor over supported Ni[282] and Ru catalysts.[283] Selectivity toward sorbitol was improved over charcoal supported Ru catalysts at short residence times;[283] long residence times favored sorbitol epimerization to mannitol. Ru/C catalysts with 1−2 wt % metal prepared by anionic or cationic adsorption afforded 100% glucose and selectivities of 99% to sorbitol under 80 bar H_2 and 100 °C. However, scale-up of trickle-bed reactors is hindered by multiple hydrodynamic states, nonuniform temperature distributions, large pressure drops, and liquid holdup.[284,285] The wetting efficiency of solid catalysts, and gas−liquid−solid mass transfer limitations, also present barriers to continuous high pressure heterogeneous hydrogenations.[286,287] In stirred tank reactors, hydrogen is often sparged and mixed using hollow impellers to improve gas solubility; however, hydrogen dissolution in aqueous sugar solutions and uniform radial and axial transport is a challenge in trickle-bed reactors, even in counter-current flow operation.[288] Airlift loop reactors enhance the contact area between gas and liquid phases, and provide more favorable flow patterns for catalytic hydrogenation. Wen and co-workers reported the batch-wise catalytic hydrogenation of glucose to sorbitol in an airlift reactor.[289] Here, gas in the

DOI: 10.1021/acs.chemrev.6b00311
Chem. Rev. 2016, 116, 12328−12368

storage tank passed through a buffer tank prior to injection at pressure into the reactor in which 1.5 m^3 of 50 wt % glucose solution and 37.5 kg of Ni catalyst were added and mixed by continuous hydrogen addition. The sorbitol yield in the airlift loop reactor (98.6%) was higher than that in a stirred tank reactor under the same reaction conditions of 140 °C and 70 bar. In a separate study, Ru/γ-Al_2O_3 monoliths were assessed using an external airlift loop tubular reactor with independent recycle of gas and liquid, and compared to powder analogues using an integrated stirred tank reactor.[290] External mass transfer limitations were observed for the powder catalyst, whereas the monolithic catalyst exhibited internal mass transfer resistance. Catalyst performance was sensitive to reaction temperature and configuration (Figure 41).

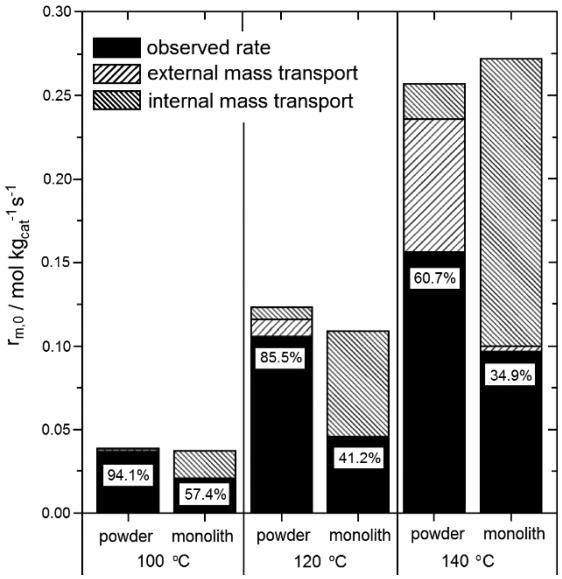

Figure 41. Initial rates of glucose hydrogenation, and potential improvements through overcoming external and internal mass transfer resistance. Reproduced with permission from ref 290. Copyright 2009 Elsevier.

Membrane trickle-bed reactors, which may offer integrated reaction and product separation, have also been studied for glucose hydrogenation to sorbitol,[291] and are compared against a conventional trickle-bed reactor in Figure 42a. In the membrane reactor, gas is uniformly distributed along the reactor bed through the membrane, with liquid reactant flowed over the catalyst bed (Figure 42b) delivering superior conversion due to the distributed addition of H_2. While membrane reactors are finding growing application,[292] their use in sugar transformations remains limited due to the lack of available membranes stable under reaction conditions, and the added challenge of incorporating on-stream product separation.

Solvent selection may also enhance catalytic hydrogenation of sugars through improved gas solubility. Use of CO_2 as a cosolvent for the catalytic conversion of biomass was recently reviewed,[49] wherein the aqueous phase catalytic hydrogenation of 5-HMF to DMF over Pd/C was promoted in CO_2/H_2O mixtures,[293] with poor DMF selectivity obtained in pure water or supercritical CO_2. Multiphase systems based on water, i-octane, and IL mixtures have also been reported for the Ru/C-catalyzed hydrogenation of levulinic acid to γ-valerolactone, in which substrate and product partition in the aqueous phase,

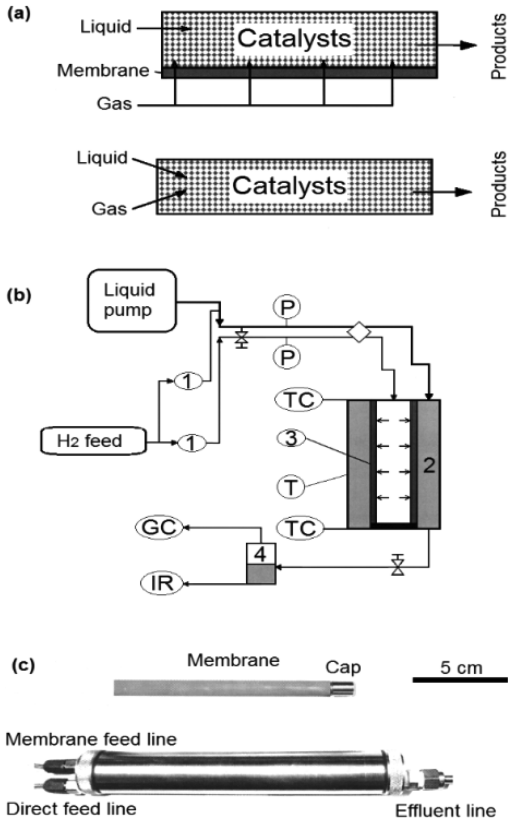

Figure 42. (a) Illustration of the membrane trickle-bed reactor and the conventional trickle-bed reactor; (b) experimental setup incorporating the membrane trickle-bed reactor; and (c) membrane trickle-bed reactor. Adapted with permission from ref 291. Copyright 2003 American Chemical Society.

with the metal catalyst residing in the IL, and *i*-octane aids phase separation for product recovery and catalyst reuse.[60]

Transfer hydrogenation has also been recently explored for the one-pot hydrogenation of cellulose and hemicellulose (xylan) to sugar alcohols, as a means to obviate the requirement for renewable H_2 and associated high pressures and expensive reactors. In both cases, Ru/C catalysts are efficacious in conjunction with *i*-propanol as a hydrogen source, with Ru/C-Q10 delivering 37% sorbitol and 9% mannitol from milled cellulose at 190 °C,[294] and 5 wt % Ru/C affording an 80% xylitol yield from xylan at 140 °C (albeit only with trace H_2SO_4 to initiate hemicellulose hydrolysis to xylose)[295] and a similar performance from sugar cane bagasse. In the former case, highly dispersed cationic Ru is proposed as the active site responsible for transfer hydrogenation, with metallic Ru nanoparticles on alumina inert. Recycling of residual *i*-propanol, and its regeneration from the reactively formed acetone byproduct, will be essential for large-scale processing.

3.3.7. Summary of Hydrogenation Catalysts. Ni, Ru, and Pt catalysts have been most extensively explored for xylose and glucose hydrogenation (Table 3). Quantitative catalyst comparison is, however, hampered by a lack of kinetic analyses in most studies regarding external and internal mass transfer limitations, which are problematic in such three-phase hydrogenations, and reporting of carbon mass balances. A wide range of hydrogen pressures (30−160 bar) have been employed to date, without adequate precautions to ensure that reactions are first order in catalyst and that reactions are not controlled by slow hydrogen transport at either the gas−liquid or the liquid−

DOI: 10.1021/acs.chemrev.6b00311
Chem. Rev. 2016, 116, 12328−12368

solid interfaces. Typical reaction temperatures span 80−120 °C, comparable to those under which glucose and xylose isomerization occur; however, most hydrogenation studies report very high selectivity to the direct sugar alcohol hydrogenation product. This surprising observation may reflect the difficulty in distinguishing sorbitol and mannitol by HPLC, which coelute over most columns, and hence questions remain as to whether high reported xylitol and sorbitol selectivity are reliable. Ru/ZSM-5 and Pt/activated carbon appear the best catalysts for glucose and xylose hydrogenation; however, there are wide variations in the sugar concentrations that hamper direct comparisons, and mass balances are again rarely reported, which is concerning giving the potential for competing isomerization and dehydration pathways (particularly where acidic, basic, or carbon supports with ill-defined surface properties are employed), that may promote humin or coke formation.

Few efforts have been made to determine the hydrogenation mechanism. About one-third of studies suggest that glucose hydrogenation is zero order in glucose for sugar concentrations >10 wt %, switching from first order at lower glucose concentration due to saturation of the catalyst surface by the sugar. Surprisingly, hydrogenation is also reported first order in H_2 pressure (rather than one-half order as for typical olefin hydrogenation). Deactivation is principally attributed to leaching of metals (especially Ni), and poisoning or site-blocking of active sites. Catalyst development should target more efficient desorption of reactive intermediates, and improved mass transfer through the use of high area and/or porous supports. Loss of precious metal by leaching may require encapsulated nanoparticles,[296] such as those developed by Joo et al. in which Pt nanoparticles were enclosed within porous silica to form a Pt core/porous silica-shell structure.[297] Such core−shell motifs have shown high thermal stability in CO oxidation and ethene hydrogenation, preventing metal sintering or loss, and are amenable to metal-catalyzed C_5−C_6 sugar hydrogenation.

3.4. Selective Oxidation

3.4.1. Pd. Metal catalysts are widely reported for the selective oxidation of glucose.[121] Early studies of Pt catalysts suggested they deactivated rapidly, and were strongly dependent on alkaline reaction media.[298] Pd has subsequently attracted significant interest due to its ability to selectively oxidize primary and secondary alcohols.[299,300] Pd/C,[301] Pd/Al_2O_3,[302] Pd−Bi/C,[303] and Pd−Bi/SiO_2[304] have been studied for glucose selox to gluconic acid, with alkaline conditions and Bi promoters originally believed to enhance activity and selectivity and/or prevent overoxidation of Pd surfaces and hence their deactivation (the latter hypothesis has been since discredited[305−308]). Promoter leaching in situ and on-stream deactivation have hampered industrial take-up of such catalyst systems.

Efforts to improve the performance of Pd catalysts have used new supports such as polymers and zeolites, and promoters.[309] For instance, Witońska et al. studied tellurium-modified Pd (5% Pd−x%Te/support, in which x = 0.5−1 wt % and the support = SiO_2 or Al_2O_3) in comparison with Bi-promoted analogues.[310] Supported Pd−Te catalysts were more active, selective [entry 14, Table 4], and stable, with no Te leaching for loading $x \leq 1$ wt %. This Te promotion was ascribed to the formation of interfacial Pd−Te compounds.

3.4.2. Nanoporous/Colloidal Au. Gold catalysis is now highly topical in large part due to the work of Haruta[311] and Hutchings,[312] and has been heavily investigated for selox,[313−315] notably the aerobic oxidation of alcohols to aldehydes and aldehydes to carboxylic acids.[300,316,317] Selox of sugars has also been examined using Au catalysts in the aqueous phase,[318−321] particularly over titania supports, which interestingly can themselves perform photocatalytic glucose oxidation.[322] The effect of catalyst preparation on glucose selox over Au bimetallic and trimetallic nanoparticles has highlighted the continued efforts to improve gold selox catalysts.[121] Here, we focus attention on recyclable catalyst systems.

Porous Au represents a new class of heterogeneous catalyst suitable for surface functionalization,[323] and unsupported nanoporous Au appears as an effective catalyst for glucose selox to gluconic acid with >99% selectivity under mild conditions.[134,318] Yin et al. prepared nanoporous Au by dealloying Ag/Au alloys (Figure 37), noting that activity was dependent on reaction temperature, pH of the reaction solution, and particle size (Figures 43 and 44). Active sites for glucose oxidation were low-coordinate surface Au atoms at corners and step edges (entry 2, Table 4). Such nanoporous Au catalysts were less active than Au nanoparticles due to their lower density of the under-coordinated active sites. Nonetheless, such porous Au catalysts are amenable to modification to form nanocomposites or direct incorporation into microreactors.

Colloidal Au nanoparticles have also been studied in selox and compared to monometallic Pt, Pd, and Rh colloids and bimetallic Au−Pt, Au−Pt, and Au−Rh colloids for glucose oxidation.[324] Under acidic conditions, activity was low for Au and Pt (TOF = 51−60 h^{-1}) and worse for Rh and Pd (TOF < 2 h^{-1}), whereas bimetallic colloids were far superior (Au−Pt TOF = 295 h^{-1} and Au−Pd TOF = 92 h^{-1}), highlighting strong synergies. Mirescu et al. compared Au/TiO_2 to Au colloids,[325] showing that both catalysts exhibited >99% selectivity toward gluconic acid (entry 3, Table 4). Direct use of unsupported colloids is problematic due to the difficulty in their recovery from the reaction media, although stabilizing polymers, such as naturally occurring chitosan, can overcome this. Supported Au catalysts are however preferable if commercial glucose oxidation is to be realized.

3.4.3. Au. Au/C catalysts have been investigated under pH control (7−9.5) and uncontrolled pH in aqueous glucose selox with O_2 under mild conditions (50−100 °C, pO_2 = 1−3 bar).[326] Au/C offered total conversion and high selectivity at all pH values, and was more active at low pH than supported Bi-promoted Pd and Pt catalysts. Au was also less sensitive to poisoning than the group VIII metals, but still underwent leaching and gradual deactivation over four runs.

The impact of mass-transport,[327] employing high glucose concentrations and O_2 partial pressures,[328] and the preparation method have been examined for Au/Al_2O_3,[329] and its performance has been compared to Au/TiO_2 and Au/C to determine their long-term stability,[330] and the role of particle size effects relative to Au/ZrO_2, Au/TiO_2, and Au/CeO_2 for glucose oxidation.[321,331] Au on silica and mesoporous SBA-15 (Figure 45)[332] were also compared to Au/TiO_2 and Au/Al_2O_3. Highest productivity (48 mol g_{Au}^{-1} h^{-1}) was obtained for Au supported on Al_2O_3-modified SBA-15 (entry 11, Table 4), attributed to gold stabilization by surface aminopropyl groups. All catalysts were selective to gluconic acid. Au nanoparticle

DOI: 10.1021/acs.chemrev.6b00311
Chem. Rev. 2016, 116, 12328−12368

Table 4. Metal Catalysts for Glucose Oxidation to Gluconic Acid or Gluconate[a]

entry	catalysts	conv.	sele.	yield	initial rate	TOF	reaction order	typical reaction conditions	ref
1	4.6%Pd/H-MORD-20	80	99.8	79.8	0.46	46.8		7–9 wt % glucose, 0.011 g of Pd, 95 °C, 1 bar, 2 h, 300 rpm, 20 mL, pH 7.2	309
2	nanoporous gold			48				25 °C, 1 bar, 40–60 h, pH 10	134
3	colloidal gold		99.8		810			1.8 wt % glucose, 0.002 g of Au, 40 °C, 1 bar, 40–60 h, 500 mL, pH 9	325
4	1%Au/TiO_2	100	98	98	14 160			1.8 wt % glucose, 0.5 g of catalyst, 40 °C, 1 bar, 2 h, 500 mL, pH 11	330
5	0.05%Au/cellulose					32 760	1.5 for [glucose], 2.5–10%	5 wt % glucose, 60 °C, 1 bar, 84 mL, pH 9.5	319
6	Au/Resin(HPA25)	60				28 000		5 wt % glucose, 60 °C, 1 bar, 1 h, 84 mL, pH 9.5	333
7	0.86%Au/Al_2O_3 solid grounding	83	>98	81.3		147 600	0.4 for glucose	5 wt % glucose, 0.03 g of Au, 50 °C, 1 bar, 0.5 h, 175 mL, pH 9	321
8	1.7%Au/SiO_2-PVA				4	5210		1.8 wt % glucose, 0.03 g of catalyst, 35 °C, 1 bar, 1000 rpm, 30 mL, pH 9.5	331
9	0.3%Au/Al_2O_3	100	>99	99	312		0.71 1.5 < pO_2 < 9 bar	20 wt % glucose, 0.1 g of catalyst, 40 °C, 9 bar, 1000 rpm, pH 9	328
10	2%Au/Al_2O_3 (Au: 1.9 nm)	97	96	93.1		12.9		10.8 wt % glucose, 60 °C, 1 bar, 7 h, 900 rpm, 25 mL, pH 9	327
11	Au/$NH_2$1AlSBA15 direct reduction	94	96	90.2	37.8			18 wt % glucose, 0.384 g of catalyst, 60 °C, 1 bar, 1 h, 1000 rpm, 120 mL, pH 7.5–8.5	332
12	0.5%Au–Pd/MgO_2 heated in N_2 or air	62	100	62				9 wt % glucose, 0.06 g of catalyst, 60 °C, 1 bar, 24 h, 5 mL, base-free	320
13	Au/mesoporous carbon	92.4	87.5	80.8		17 712		1.8 wt % glucose, 0.0396 g of catalyst, 110 °C, 3 bar, 2 h, 20 mL, base-free	365
14	5%Pd–5%Te/SiO_2	76.1	97.4	74.1		48.1		18 wt % glucose, 1 g of catalyst, 60 °C, 1 bar, 2 h, 1300 rpm, 250 mL, pH 9	310
15	$HAuCl_4$–$Pd(OAc)_2$/C (one-pot synthesis)	71	>96	68				18 wt % glucose, 0.1 g of catalyst, 50 °C, 1 bar, 10 h, 1000 rpm, 400 mL, pH 9.25	366
16	5%Pd–8%Bi/SiO_2	60	97	58.2				18 wt % glucose, 60 °C, 1 bar, 1 h, 1300 rpm, pH 9	304
17	[5%($Pd_{0.88}Pt_{0.12}$) + 5%Bi]/C	94	98	92.1	10.3	1547		15.8 wt % glucose, 0.24 g of catalyst, 50 °C, 1 bar, 20/60 h, 1800 rpm, 100 mL, pH 9.5	335
18	$Au_{90}Ag_{10}/SiO_2$ (calcined at 400 °C)					192		1.8 wt % glucose, 35 °C, 1 bar, 40/60 h, 1000 rpm, 30 mL, pH 9.5	339
19	$Au_{80}Ag_{20}$ (shell–core)					16 200		4.8 wt % glucose, 0.002 g of catalyst, 60 °C, 1 bar, 2 h, 30 mL, pH 9.5	76
20	$Au_{60}Pt_{30}Ag_{10}$ (addition of $NaBH_4$)					22 500		4.8 wt % glucose, 0.002 g of catalyst, 60 °C, 1 bar, 2 h, 30 mL, pH 9.4	336
21	Au/Pt/Rh (60/30/10) molar					23 000		4.8 wt % glucose, 0.002 g of catalyst, 60 °C, 1 bar, 2 h, 30 mL, pH 9.4	367
22	0.74%Ru/polystyrene	99.4	99.8	99.2	6.2	4.1		7.9 wt % glucose, 0.024 g of catalyst, 60 °C, 1 bar, 2 h, 1000 rpm, 20 mL, pH 6–7.5	368

[a]Units: Conv, %; Sele, %; Yield, %; Initial rate, mol g_{metal}^{-1} h^{-1}; TOF, h^{-1}.

DOI: 10.1021/acs.chemrev.6b00311
Chem. Rev. 2016, 116, 12328–12368

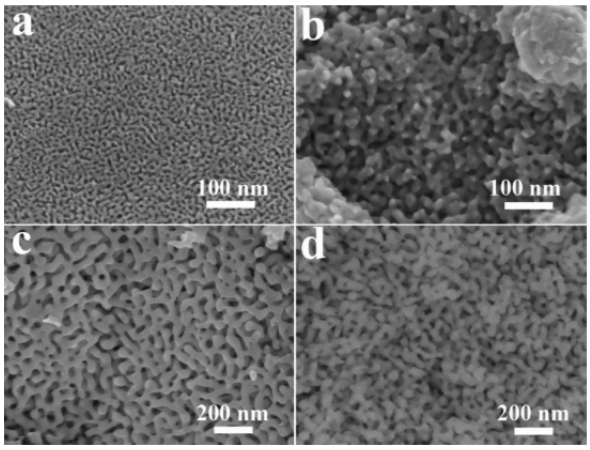

Figure 43. SEM images of nanoporous Au: (a,c) before reaction, and (b,d) after use. Note that nanopores in (a) and (b) are 6 nm in diameter and 30 nm in (c) and (d). Reproduced with permission from ref 318. Copyright 2011 American Chemical Society.

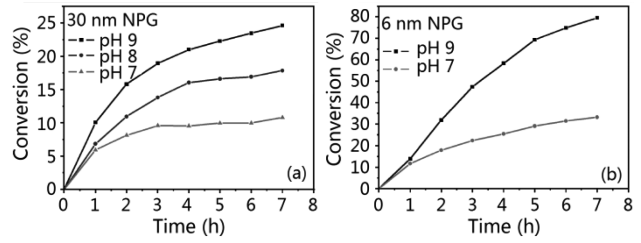

Figure 44. Catalytic activity of (a) 30 nm nanoporous Au catalysts (NPG), and (b) 6 nm NPG at different pH values. Reproduced with permission from ref 318. Copyright 2011 American Chemical Society.

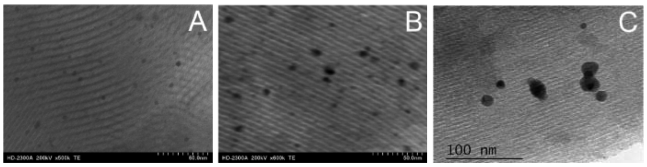

Figure 45. STEM images of (A) Au(DR)$NH_2$1%AlS, (B) Au(DR)-NH_2S, and (C) Au(DR)10%AlS. Note that S refers to SBA-15, AlS refers to alumina-functionalized SBA-15 (AlSBA-15, with different loadings of Al in wt %), NH_2S refers to aminopropyl-functionalized SBA-15, AlS refers to aminopropyl-functionalized AlSBA-15, and DR refers to direct reduction from $HAuCl_4$. Adapted with permission from ref 332. Copyright 2014 Elsevier.

synthesis by direct reduction was more effective than deposition of colloidal Au sols.

Au/resins have also been tested for glucose selox[333] using ion-exchanged resins to obtain acid or base sites, and modified by, for example, amines to serve as stabilizers and reductants to create well-dispersed Au (Figure 46a). Catalytic performances decreased with decreasing basicity of anion-exchanged resins, while resin hydrophilicity enhanced activity (entry 6, Table 4). Operation under neutral conditions offers a more environmentally benign process, but catalyst stability was problematic. The same researchers investigated Au/cellulose for glucose selox (entry 5, Table 4),[319] with the biopolymer support stabilizing 2 nm Au nanoparticles (Figure 46b), through direct deposition by solid grinding with a volatile dimethyl Au(III) acetylacetonate precursor and subsequent H_2 reduction. These catalysts exhibited a high TOF of 11 s^{-1} in the production of

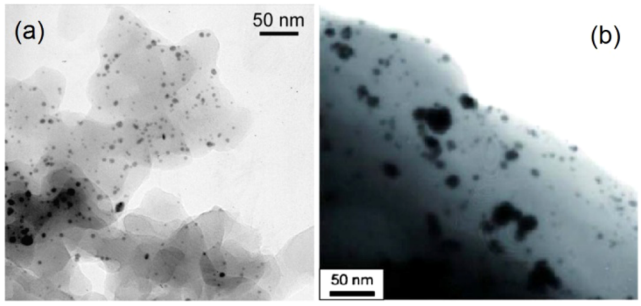

Figure 46. TEM image of (a) Au/resin (IRA96SB). Adapted with permission from ref 333. Copyright 2009 Elsevier. (b) Au/cellulose prepared by DR (the deposition-reduction method). Adapted with permission from ref 319. Copyright 2010 Elsevier.

sodium gluconate at 60 °C and pH 9.5 (gluconic acid exists as the gluconate ion in aqueous solution at neutral pH). This activity is comparable to Au/C for similar size Au nanoparticles, which are easier to obtain with a cellulose support due to surface OH groups; however, the Au loading over cellulose was limited to 0.23 wt % due to the low cellulose surface area. As for carbon, the performance of cellulose supported Au nanoparticles was improved under basic conditions.

Base-free glucose selox has been a recent focus of attention by Hutchings and co-workers, with 1 wt % Au nanoparticles supported over P25 titania by sol-immobilization or deposition-precipitation offering good conversion and excellent selectivity toward the aerobic selox of glucose to gluconic acid at 160 °C and 3 bar oxygen.[334] Gluconic acid yields of 67% were obtained following mild calcination of the sol-immobilized Au/TiO_2, attributed to removal of the PVA stabilizer ligands improving access to active sites without compromising particle size (optimum ∼2.5 nm), with negligible glucaric or glycolic acid observed. However, the role (if any) of the titania support remains unclear, and no kinetics were reported; hence the high selectivity to the single carboxylic acid product remains unclear.

3.4.4. Supported Alloys. A bimetallic Pd−Pt/charcoal catalyst, prepared from Pd−Pt colloids using a tetra-*n*-octylammonium chloride ($NOct_4Cl$) stabilizer, has been reported for glucose selox.[335] A synergy was found for $Pd_{88}Pt_{12}$/C impregnated with Bi, although it was also claimed that the surfactant stabilizer acted to modify catalytic reactivity, rendering it difficult to distinguish the roles of metal and organic components. Ag−Au bimetallic nanoparticles with a Au shell,[76] Ag−Au bimetallics formed from a physical mixture of monometallic nanoparticles,[121] Au−Pt bimetallics with a Pt-rich shell,[243] and Au/Pt/Ag trimetallic nanoparticles have all been explored for glucose selox.[336,337] Trimetallic systems were an order of magnitude more active than pure Au counterparts of the same particle size, and exhibited excellent stability. Comotti et al. also compared Au−Pt, Au−Pd, and Au−Rh free and supported colloids[324] Enhanced TOFs were obtained for the bimetallic catalysts, although similar performance was observed for mono- and bimetallic catalysts under alkaline conditions. Au−Pt bimetal nanoparticles with a Pt-rich shell were reported recently for glucose aerobic selox,[243] delivering 10-fold rate enhancements over similar size pure gold nanoparticles. Bimetallic Au−Pt catalysts prepared by the rapid injection of excess $NaBH_4$ into $AuCl_4^-$/$PtCl_6^{2-}$/PVP outperformed pure Au nanoparticles. High activity was attributed to the small particle diameter (∼1.5 nm) and the presence of negatively charged Au and Pt atoms due to electron donation from the

DOI: 10.1021/acs.chemrev.6b00311
Chem. Rev. 2016, 116, 12328−12368

PVP, as shown in Figure 47a. In contrast, Au−Pt prepared by dropwise addition of $NaBH_4$ or alcohol reduction exhibited

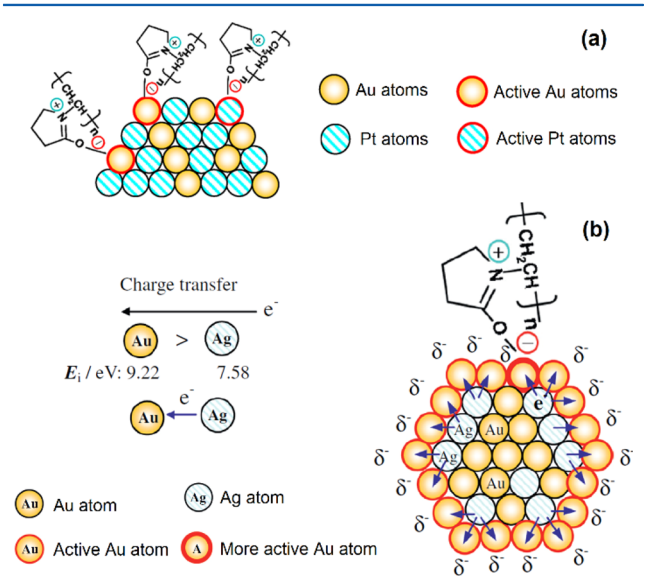

Figure 47. (a) Proposed PVP-mediated charge transfer to Au/Pt bimetallic nanoparticles. Adapted with permission from ref 243. Copyright 2013 Elsevier. (b) Possible electronic charge transfer in the Ag/Au bimetallic nanoparticles. Adapted with permission from ref 338. Copyright 2014 Elsevier.

poor activity. Zhang et al. also reported that PVP-stabilized Ag_{core}/Au_{shell} bimetallic particles (1.4 nm) exhibited higher activity in glucose selox than Au−Ag particles prepared by dropwise addition of $NaBH_4$ (which had a larger mean size, entry 19, Table 4).[76,338] They proposed that charge transfer from Ag to Au neighbors was responsible for the improved selox (Figure 47b), although there was no spectroscopic evidence (e.g., XPS or valence band measurements) to support their hypothesis. Benkó and co-workers also studied Au−Ag alloys, in this case supported on SiO_2, for glucose selox,[339] finding similar results, that is, that activity was dependent on particle size and the Au:Ag ratio, with Au−Ag alloys more active than pure Au nanoparticles (Ag nanoparticles being inactive). The alloy enhancement was however assigned to Ag active sites and associated increased O_2 activation, although excess Ag blocked surface Au sites, suggesting both elements are required to form the requisite surface active ensemble. Base-free glucose aerobic selox under extremely mild conditions (1 bar O_2 and 60 °C) has also been demonstrated over bimetallic Au−Pd nanoparticles supported by sol-immobilization on calcined MgO. Pd strongly promotes gold, affording 62% conversion and 100% selectivity to gluconic acid following mild alloying treatment, although the composition of the alloy and surface termination were not reported.[320]

Au/Pt/Ag trimetallic nanoparticles (TNPs) prepared by dropwise $NaBH_4$ addition (D)[337] were compared for aerobic glucose selox against other Au mono- and bimetallic catalysts (entry 20, Table 4). Bimetallic Au/Pt(7/3)(D) with a TOF of 4290 h^{-1} was twice as active as pure Au(D) (TOF = 2170 h^{-1}), while $Au_{70}Pt_{20}Ag_{10}$(D) (T-1 in Figure 48(left)) gave the highest TOF; activity was dependent on particle size and more importantly alloy composition (Figure 48(right)) with XPS and quantum-chemical DFT calculations implicating negatively charged Au; the latter differs from results obtained for $Ag_{core}/$

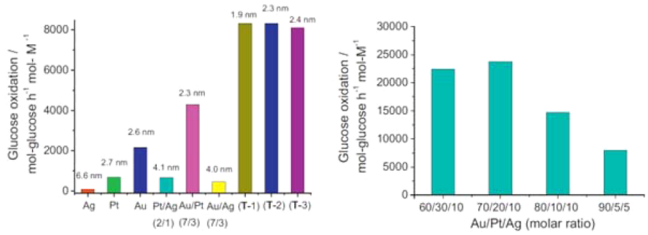

Figure 48. (left) Catalytic activities of monometallic Ag(D), Pt(D), Au(D), bimetallic Pt/Ag(2/1)(D), Au/Pt(7/3)(D), Au/Ag(7/3)(D), and trimetallic Au/Pt/AgD) nanoparticles with (T-1) = $Au_{70}Pt_{20}Ag_{10}$, (T-2) = $Au_{36}Pt_9Ag_4$, and (T-3) = $Au_{80}Pt_{10}Ag_{10}$. "D" refers to catalysts prepared by dropwise $NaBH_4$ addition. (right) Glucose selox oxidation activity of Au/Pt/Ag TNPs. Adapted with permission from ref 336. Copyright 2011 Elsevier.

Au_{shell} bimetallics[76] in which particle size effects were believed to be the dominant factor.

3.4.5. Process Considerations. The continuous selective oxidation of glucose to gluconic acid has been reported over 0.25 wt % Au/Al_2O_3 using a continuous stirred tank reactor (CSTR) reactor shown in Figure 49 for 70 days operation at 40

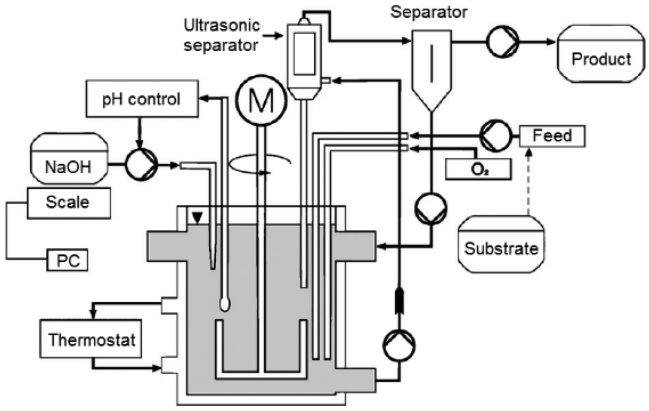

Figure 49. Continuous stirred tank reactor for the catalytic oxidation of glucose to gluconic acid over Au/Al_2O_3. Reproduced with permission from ref 340. Copyright 2007 Elsevier.

°C, pH 9, and 1 bar O_2 to study long-term catalyst stability,[340] with unreacted glucose recirculated into the reactor. After 5 days operation, the reaction attained a steady-state specific activity of 150−200 mmol min^{-1} g_{Au}^{-1}. Reversible catalyst deactivation occurred using high glucose feed concentrations, with activity recovered upon lowering the glucose concentration, indicating the excellent stability and robust nature of this catalyst for industrial application.

Pelleted or formed catalysts with large particle sizes are necessary for continuous reactors to facilitate their separation and/or entrainment, for example, within a basket.[341] In such cases, support textural and mechanical properties are critical to maximize intraparticle diffusion and minimize catalyst friability.[342] Pelleted catalysts often employ eggshell-type catalysts to improve active site accessibility. Particle morphology was explored using slurry, pellet, and rotating foam catalysts for Pt−Bi/Al_2O_3-catalyzed oxidation of glucose to gluconic acid.[343] The rotating foam block exhibited superior gas−liquid and liquid−solid mass transfer coefficients, which increased the surface oxygen concentration and afforded higher glucose conversion at lower catalyst loadings than the slurry or pellet

DOI: 10.1021/acs.chemrev.6b00311
Chem. Rev. 2016, 116, 12328−12368

catalysts. Further enhancements were obtained using wash-coated versus sol gel prepared foam blocks; the former comprised sintered micrometer sized particles exhibiting both macro- and mesoporosity, allowing rapid oxygen diffusion and a high dispersion of the bimetal active phase.

3.4.6. Summary of Glucose Oxidation Catalysts. Glucose selective oxidation to gluconic acid (or gluconate) is generally conducted under ambient oxygen, which hinders the extent of metal nanoparticle surface oxidation. While the latter is of benefit for gold catalysts, wherein anionic gold is believed the active site in selox, the converse applies to Pt and Pd systems in which electron-deficient (PdO[308,344] and PtO_2[345]) are strongly implicated by ex situ and operando X-ray spectroscopy. Unlike sugar isomerization, dehydration, and hydrogenation, selox occurs at lower temperature (35−60 °C) and hence affords high selectivity to the desired gluconic acid in most catalyst systems, although almost all studies show that glucose selox is very pH-sensitive. For instances, Au on activated carbon is far more active under basic conditions, with TOFs reaching 1.5×10^5 h^{-1} (42 s^{-1}) per surface Au atom for glucose selox at 50 °C and pH 9.5.[346] This need for a strong alkaline medium makes reactor design and handling of the reaction media more hazardous. Solid base metal oxide supports such as MgO or hydrotalcites may thus be advantageous over, for example, carbons (see entry 12, Table 4), potentially obviating the need for additional pH control, although support stability is contentious with Mg^{2+} leaching into the reaction media, opening routes to competing homogeneous sugar catalysis.[320,347] The importance of employing alkali-free routes to hydrotalcites was recently highlighted in Au-catalyzed 5-HMF selox over Mg−Al supports.[348]

Au/cellulose, Au/resin, and Au/ZrO_2 also show remarkable TOFs (entries 5, 6, and 7, Table 4), as do Au-derived bimetallic Au/Ag or trimetallic Au/Pt/Ag and Au/Pt/Rh catalysts (entries 19, 20, and 21, Table 4). TOFs vary hugely across supported and colloidal catalysts, from <1 to 1.5×10^5 h^{-1}, although little information is provided on either mass balance or product selectivity in some cases (entries 18, 19, 20, and 21, Table 4), and the assumption is that only gluconic acid is formed. Kinetic studies are also limited, with an order of 1.5 in glucose concentration for Au/cellulose for concentrations between 2.5 and 10 wt %, whereas Au/Al_2O_3 exhibited a reaction order of only 0.4 with respect to glucose concentration. Detailed kinetic and mechanistic investigations are still required to understand the respective roles of metal, support, and solution pH, and identify the optimum reaction conditions in terms of temperature and oxygen pressure. Recycle tests reveal that 0.45 wt % Au/TiO_2 (entry 4, Table 4) was the most stable glucose selox catalyst, with complete conversion and high selectivity observed for 17 consecutive runs. In contrast, Au/MgO lost 70% activity after only three runs (entry 12, Table 4), and there is a notable dearth of reusability studies for colloidal catalysts.

3.4.7. Nonglucose Monosaccharide Oxidations. The selective oxidation of less common C_5 (arabinose, ribose, xylose, lyxose) and C_6 (mannose, rhamnose, and galactose) monosaccharides is also of interest for applications in the food, pharmaceutical, and cosmetic industries. L-Arabinose and D-galactose are readily obtained from water-soluble arabinogalactans within woody biomass.[349] Selective aerobic oxidation of these monosaccharides catalyzed by supported Pd, Au, Pt, and bimetallic Pd−Au catalysts to the valuable arabinonic acid and galactonic acid products was comprehensively reviewed by Kusema and Murzin.[350] In brief, the relative oxidation reactivity of sugar isomers depends on the accessibility of the oxidizable carbonyl group. Saccharides can be classified as unprotected aldoses or (1-*O*)-protected aldoses, such as glucose or (1-*O*)-glucose methyl-glucose, respectively, or ketoses such as fructose, sorbose, and sucrose.

Pentose and hexose oxidation to their aldonic acids is reported over Pd/Al_2O_3, Pt/Al_2O_3, and Au/TiO_2, revealing striking (and unexplained) differences between the metals.[351] Au proved most active and selective for both pentose (arabinose > xylose > ribose > lyxose) and hexose (D-glucose, D-galactose, and D-mannose) oxidation, achieving >99.5% selectivity to the aldonic acids in every case. In general, Pd was less selective to the oxidation of C_5 than C_6 sugars, with the exception of xylose oxidation to xylose acid, which occurred with 99% selectivity (as was also observed over Pd/C[352]), whereas Pt exhibited the reverse behavior.

Selective oxidation of the disaccharide D-lactose (comprising glucose and galactose units joined by a β-1,4-glycosidic linker) to lactobionic acid, an important antioxidant in food and medicine, has also been reviewed, highlighting the importance of tuning support porosity and acidity, and metal loading in Pd-catalyzed oxidation.[100] Au/TiO_2[353] and bimetallic Cu−Au/TiO_2[354] are reported excellent catalysts for cellobiose oxidation to gluconic acid with 100% conversion and 89% selectivity at 145 °C and 10 bar O_2. Au/C is also active for cellobiose oxidation to gluconic acid under base-free conditions at 145 °C and 5 bar O_2, with surface phenolic functions on the carbon support providing acidity to hydrolyze the glycosidic bond while metallic Au catalyzing oxidation of the resulting glucose.[355] Excellent gluconic acid selectivity (approaching 80%) was observed, with the support pore diameter influencing activity likely through modifying the adsorption mode of cellobiose, glycosidic bonds being more readily activated in larger pores. Bifunctional strategies also employ Au supported on acidic multiwall carbon nanotubes,[356] polyoxometalates,[357,358] and Pt on sulfonated carbon.[359]

4. FUTURE PERSPECTIVES

Catalytic routes for biomass conversion to renewable fuels and chemicals will underpin the valorization of bioderived feedstocks this century. The development of new heterogeneous catalysts tailored for biorefinery applications represents a grand challenge that requires collaboration across the bio-chemo-engineering interfaces. The complex nature of biomass means that no single conversion technology based on thermocatalytic or biocatalytic processing alone will likely prove successful, with a shift toward toolkits based around (tandem) biochemo catalytic routes arising from collaborations between biochemists, catalytic and materials chemists, chemical engineers, and experts in molecular and process simulation to exploit innovative reactor designs and integrated process optimization and intensification.

Mechanistic studies will continue to be of growing importance in elucidating new reaction pathways and developing associated kinetic models to guide the design process. Insight into catalyst deactivation will derive from a broader application of operando spectroscopies of liquid-phase transformations, underpinned by in-silico insight into molecular adsorption and surface dynamics. Practical implementation of new catalytic processes will be supported by advanced online monitoring and control systems for faster reaction optimization to maintain catalyst performance. Many C_5−C_6 sugar trans-

DOI: 10.1021/acs.chemrev.6b00311
Chem. Rev. 2016, 116, 12328−12368

formations involve multiphase systems (e.g., gas−solid−liquid with cosolvents and pH regulation); hence multiscale modeling will become increasingly important. Process intensification[157] will also have a significant role in improving the energy efficiency of conversion and separation unit operations, for example, through the use of spinning-disc,[360] oscillatory-baffled,[361] or microfluidic[362] reactors. Catalytic hydrogenation and oxidation of sugars is still effected by noble metals, and hence strategies to reduce precious metal usage (e.g., by substitution with base metals or the use of single atom alloys[363]) will likely come to the fore. However, early/mid transition metals are often more susceptible to deactivation than noble metals, and will require efficient reactivation/recycling protocols to minimize waste. Improved and more user-friendly decision support systems for risk management of biorefineries, coupled with more extensive life cycle analysis tools, will also prove invaluable to ensure process economic viability and sustainability.

4.1. Process and Economic Considerations

While there are significant advances in catalytic technology for biomass conversion, widespread uptake and the development of next-generation biofuels and chemical feedstocks is ultimately hampered by uncertainty of industry over investment strategy. Progressive government policies and incentive schemes are essential to place biomass-derived chemicals on a comparable footing with heavily subsidized fossil fuel-derived resources. In the short- to medium-term, it is likely that so-called drop-in replacements of crude oil-derived chemicals, or methods to coprocess biomass in conventional oil refineries, will be most cost-effective to circumvent high capital costs of new processing facilities. Targeting processes that require drop-in chemical feedstocks to replace existing fossil-derived chemicals has the advantage of providing raw materials to mature markets wherein necessary infrastructure and technology exists, thereby maximizing the impact of value added chemicals. In parallel, bioderived chemicals such as lactic acid offer a new value chain of products that may offer enhanced performance and potential for business opportunities.

Techno-economic analysis of biomass conversion processes will be essential to guide industry as to the most efficient processing conditions to employ. Biomass pretreatments employed to isolate sugars are among the most wasteful steps in a biorefinery, and hence an area where improvements in the atom and energy efficiency of lignocellulose processing are needed, such that preliminary acid hydrolysis/extraction of sugars from lignocellulose occurs under mild conditions with minimal waste generation. To overcome some of the infrastructure problems for biomass processing, economic models for biorefineries have proposed enhanced revenue that could be achieved by making more use of underutilized infrastructure in corn wet and dry mills, or pulp and paper operations.

To reduce dependency on fossil fuels, it is essential that the conversion processes used to produce fuels, chemicals, and materials from biomass are economically viable. The market for bioderived fuels and chemicals is linked to crude oil prices, which for biofuels only becomes competitive when oil prices are >$50−75 per barrel.[364] Techno-economic evaluation is critical when applying newly developed technologies, particularly when precious noble metal catalysts are involved. Insight into the challenges facing a heterogeneously catalyzed process utilizing bioderived sugars can be gained from related renewable technologies for producing methanol, dimethyl ether, or hydrogen, and fast pyrolysis bio-oil from biomass conversion.[24,369] These analogues highlight that biomass costs and capital costs are the two major factors that determine plant running costs for methanol synthesis (Figure 50a) and miscanthus pyrolysis (Figure 50b).[24] Plant running costs are also influenced by opportunities for the local sale of district heat to generate revenue, which is more significant for H_2 production due to the high levels of heat generated.[369]

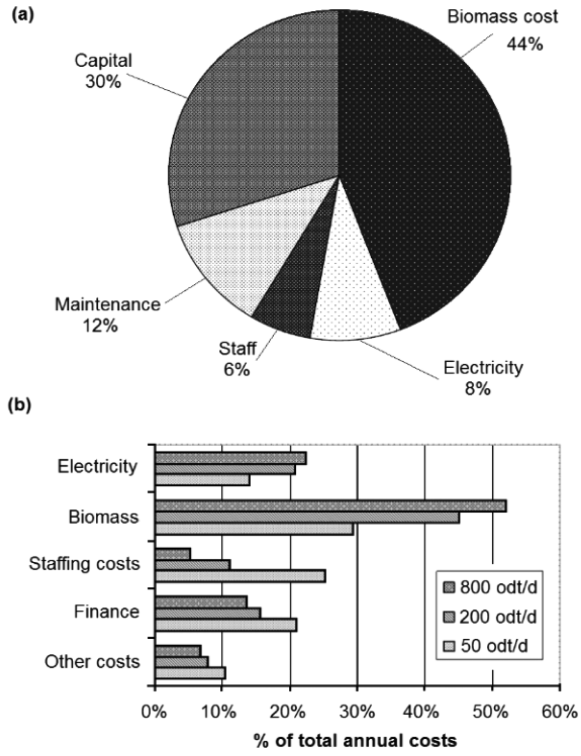

Figure 50. (a) Breakdown of yearly running costs for a present-day design methanol plant. Adapted with permission from ref 369. Copyright 2011 Elsevier. (b) Cost fractions for Miscanthus fired plants. Adapted with permission from ref 24. Copyright 2012 Elsevier.

Oil pricing, and the availability of cheap H_2 from fracking, are a major barrier to biomass-derived routes to commodity chemicals such as methanol, DME, and H_2, in the absence of green subsidies. Production costs of sugar-derived chemicals such as sorbitol and gluconic acid will be affected by similar factors, in addition to feedstock availability, number of operating units (e.g., catalysts, reactors, separators, and maintenance), energy consumption, waste treatment, staffing, and location proximate to infrastructure, but may be counterbalanced by the higher value of final product. Below, we estimate the cost of four metal catalysts used for the hydrogenation of glucose to sorbitol (Pt and Ru) or the oxidation of glucose to gluconic acid (Au and Pd). We adopt the method of Thielecke and co-workers, for continuous-flow glucose oxidation over 70 days,[340] to extrapolate the 70 day productivity employing 1 g of metal catalysts to the five examples and hence calculate the final cost of either sorbitol or gluconic acid (Table 5). For glucose hydrogenation to sorbitol, Ru catalysts (entry 2) are cheaper than Pt catalysts (entry 1), and there is no significant difference between batch (entry 2) versus continuous mode (entry 3) operation over Ru. For glucose oxidation, gold is more efficient than Pd in terms of

DOI: 10.1021/acs.chemrev.6b00311
Chem. Rev. 2016, 116, 12328−12368

Table 5. Cost Analysis and Comparison between Metal Catalysts for Glucose Hydrogenation/Oxidation and Production Modes

entry	catalyst and quantity	productivity/g_{metal} h^{-1}	extrapolated productivity/kg[a]	cost of 1 g of metal/€[b]	cost of product/€ kg^{-1}	mode	ref
1[c]	10%Pt/activated C	sorbitol	547.6	26.6	0.049	batch	259
	1000 mg of Pt	325.9					
2[d]	5%Ru/ZSM-TF	sorbitol	419.6	1.25	0.0029	batch	257
	25 mg of Ru	6.2					
3[e]	1.6%Ru/C	sorbitol	181.8	1.25	0.0069	continuous	283
	132 mg of Ru	14.3					
4[f]	0.86%Au/Al_2O_3	gluconic acid	705.2	32.1	0.0455	batch	321
	30 mg of Au	12.6					
5[g]	0.25%Au/Al_2O_3	gluconate	4171	32.1	0.00769	continuous	340
	3.75 mg of Au	9.3					
6[h]	4.6%Pd/H-MORD-20	gluconic acid	96.9	17.2	0.177	batch	309
	11 mg of Pd	0.63					

[a]70 days operation. [b]Metal prices taken from http://www.hardassetsalliance.com/charts/platinum-price/eur/kg (accessed December 15 2015); support prices not included. [c]40 wt % glucose, 100 °C, 80 bar. [d]25 wt % glucose, 120 °C, 40 bar. [e]40 wt % glucose, 36 mL h^{-1}, 100 °C, 80 bar (100 L h^{-1}). [f]5 wt % glucose, 50 °C, 1 bar, pH 9. [g]400 mL min^{-1} glucose, 40 °C, pH 9. [h]7.9 wt % glucose, 95 °C, 1 bar, pH 7.2.

both productivity and product cost, reflecting the current intensive focus on gold-catalyzed biomass transformations; continuous gluconate production over Au/Al_2O_3 is much more cost-effective than batch production of the acid.

Reactor design and in particular process intensification will also enhance the commercial viability of biomass conversion technologies,[370] permitting more compact, cost-effective, and safer biorefineries.[371] Process designs wherein heat recovery and utilization are coupled will help to mitigate energy losses.[221] Because many of the reactions in this Review may be biphasic, reactor design will also need to account for the thermodynamics of phase separation and partitioning, which are significant technological challenges. Process design will require multiscale modeling for complex multiphase systems to include interactions at interfaces, solvent, and pH effects, along with new instrumental technologies and designs of new reactors.[361] Innovative separation processes will also be important for on-stream feedstock purification and product recovery, recycling of unreacted components, and the treatment of effluent streams in bio/chemical processes to meet product standards and environmental regulations.[372−374] Adsorption, ion-exchange, chromatography, solvent extraction or leaching, evaporation or distillation, crystallization or precipitation, and membrane separation are all expected to be featured in biorefinery plant designs.[292,375] The choice of separation technology will depend on intrinsic chemical properties and on economical flexibility.[376] Reactive distillation, combining chemical conversion and separation steps in a single unit, is a promising technology to reduce operating complexity and expense,[377] but necessitates a reaction media compatible with the temperature/pressure to effect distillation of the product (byproduct) of interest. Separation of thermally sensitive compounds, or macromolecules that have very low volatility, requires further advances in membrane separation and membrane reactors to become an attractive technology.[292,375]

Hydrogen is critical to many of the steps in transforming C_5−C_6 sugars into platform chemicals (and their products) and drop-in biofuels, and hence increasing demand is anticipated for renewable sources of hydrogen such as from water electrolysis (using renewable energy) or biomass gasification/reforming.[378] Use of molecular hydrogen is also predominantly accompanied by a requirement for noble metal catalysts and high pressure operation (>30 bar), together negatively impacting on the economics of hydrogenation.[379] Transfer hydrogenation offers an alternative, attractive route to in situ hydrogen generation,[380,381] permitting mild reaction conditions and obviating the need for pressurized reactor systems, such as in the cascade production of the renewable solvent γ-valerolactone via stepwise fructose dehydration to levulinic acid and subsequent transfer hydrogenation.[382,383] Formic acid is a particularly attractive hydrogen donor in this application[384,385] as a byproduct of levulinic acid production, and has been successfully applied in the one-pot cascade conversion of fructose to γ-valerolactone over Ru catalysts in the presence of mineral acids,[386] although the requirement for noble metal catalysts and corrosive nature of formic acid remains a challenge to catalyst stability/lifetime. Catalytic transfer hydrogenation employing an alcohol as both solvent and H-donor via the MPV mechanism is hence more favorable, being catalyzed by non-noble metal oxide Lewis acid/bases such as ZrO_2.[387] Secondary alcohols are generally more efficient H-donors as compared to primary alcohols, but tertiary alcohols cannot serve as H donors due to the lack of an α-H.[380] Lewis acidic catalysts such as zeolites with tetravalent metal dopants, for example, Ti, Sn, Zr, and Hf,[379,388] and amorphous ZrO_2 or highly dispersed ZrO_2 on SBA-15[387,389−391] have shown remarkable activity in MPV reduction of levulinic acid. Moderate strength solid base catalysts are also reported as efficient catalysts for this reaction.[392] Direct γ-valerolactone production from C_5−C_6 sugars would require coupling of a MPV process with an upstream Brønsted acid-catalyzed step for sugar dehydration.[393−395] It must be recognized that any transfer hydrogenation process requires either a low-cost, abundant bioderived source of sacrificial hydrogen donor, or routes to reuse any unreacted donor and regenerate the hydrogen donor from, for example, the reactively formed ketone byproduct.

4.2. Future Catalyst Development

Biomass pretreatments such as steam explosion[45] or enzymatic[61] and chemical (acid or base)[62,63] routes to fractionate and hydrolyze cellulose will ultimately produce aqueous sugar streams. From a practical and environmental perspective, the development of stable catalysts able to operate in the aqueous phase is hence critical. One of the most important challenges in the development of new catalytic materials is the design of catalysts with controllable active sites and strong stability that are robust under hydrothermal conditions. Support materials based upon niobia, titania,

DOI: 10.1021/acs.chemrev.6b00311
Chem. Rev. 2016, 116, 12328−12368

zirconia, or tungstates exhibit excellent stability under hydrothermal conditions, and catalysts based on such oxide supports will be of growing importance for high temperature sugar transformations. Templated porous carbons with controlled surface functionality will also likely come to the fore in aqueous phase sugar conversion due to their stability under acidic and alkaline environments.[396]

A major influence on the selectivity of catalytic sugar transformations is the prevalence of simultaneous side reactions (e.g., isomerization accompanying dehydration or hydrogenation at high reaction temperatures) and attendant deactivation of active sites and accumulation of insoluble side products (e.g., solid humins and residual organic species). Several strategies may offer improved selectivity: (i) passivation of catalyst supports for hydrogenation and oxidation to minimize the contribution of supports in reactions;[258,397,398] (ii) development of materials exposing preferred crystal facets, which have different adsorptive or catalytic capacities;[398−400] (iii) development of catalysts with tunable hydrophobicity to minimize water inhibition and favor interaction with organic reactants in water;[401,402] and (iv) control over acid site distributions to tune Brønsted:Lewis acid ratio and strength.[403,404]

Advanced nanomaterials with hierarchical macro-mesoporous or meso-microporous architectures offer a means to improve mass transport as compared to microporous materials through superior in-pore accessibility.[405] Besides improved diffusion, hierarchical porous materials are also effective in stabilizing highly dispersed active species. A recent study reports a new concept of catalyst design by spatially orthogonal chemical functionalization of the macroporous−mesoporous hierarchical pore network of silica, which offers new possibilities for cascade reactions.[406]

Atomic layer deposition (ALD) is becoming a more mature technology for catalyst preparation that is underpinning breakthroughs in catalyst development.[407] ALD employs self-limiting chemical reactions between gaseous precursors and a solid surface to deposit thin films of single or bimetallic metals[408] or oxides. Precursors can infiltrate mesoporous materials, producing highly uniform, conformal thin films coatings on surfaces with atomic scale precision.[409,410] The development of a diverse range of coated support materials with desirable properties such as improved hydrothermal stability and/or acid:base properties for hydrothermal sugar conversion should be possible by the application of ALD to coating tailored porous architectures generated by dual templating methods.

To bridge the gap between homogeneous and heterogeneous catalysis and improve precious metal usage, single atom (site) catalysts offer exciting opportunities for application in sugar transformations.[411] While the concept of single site catalysts is common in framework solids or immobilized organometallic complexes,[412] single site catalysts based around atoms anchored to graphene are attracting significant attention.[413,414] The application of N-doped graphene encapsulated nanoparticles generated via pyrolysis of well-defined amine-ligated metal complexes[415] offers an interesting route to prepare nonprecious metal-based chemo-selective hydrogenation catalysts, with the selection of nitrogen ligands hoped to tuned catalyst performance. Such iron-based catalysts are active for transfer hydrogenation using formic acid,[416] and while not explored in sugar conversion would appear to be attractive materials to explore.

In catalytic C_5−C_6 sugar reforming, many cascade reactions exist, for example, glucose isomerization to fructose over solid base or Lewis acid sites followed by fructose dehydration to 5-HMF over Brønsted acid sites,[154] and the stepwise hydrogenation of glucose to sorbitol over metal (Ni, Pt, or Ru) sites and subsequent hydrogenolysis to polyols over metal-acid bifunctional catalysts.[127] Isosorbide, an important intermediate for the synthesis of a wide range of pharmaceuticals, chemicals, and polymers, is another promising target for cascade synthesis directly from cellulose or sugars wherein metal-promoted solid acids show promise.[417−420] Such cascade reactions have great advantages with respect to atom economy, reducing time, labor and resource management, and waste generation.[421] One-pot catalytic synthetic processes are highly desirable in industry and necessitate the use of multifunctional catalysts.[422]

5. CONCLUSIONS

Significant progress has been made in the development of heterogeneous catalysts and associated processes for the transformation of C_5 and C_6 sugars related to biorefinery applications. Waste-derived sugars are a promising feedstock for the production of renewable chemicals and advanced transportation fuels through low temperature, predominantly hydrothermal routes, which exploit advances in materials and surface chemistry to engineer tailored inorganic and hybrid inorganic−organic solid catalysts with tunable acid/base character and/or electronic/geometric properties. However, as with all areas of catalysis, efforts are required to standardize reaction conditions, reactor designs, and performance indicators to permit quantitative comparisons of disparate catalytic systems.

Aqueous phase sugar processing presents new challenges for heterogeneous catalysis related to the variable nature of the feed stream (in terms of component composition and concentration), solubility of sugars and reaction products, and the dissolution of reactive gases.[211,423,424] Biphasic media and cosolvents may serve to overcome some of these issues, and facilitate continuous processing and integrated product separation, although solvent selection must adhere to general green chemistry and sustainable technology principles,[425−428] being nontoxic, safe to handle, inflammable, and noncorrosive. Such aspects are particularly important when water itself is considered a finite resource, whose use in product isolation and purification must be minimized.

AUTHOR INFORMATION

Corresponding Author

*Tel.: +44-121-2044036. E-mail: a.f.lee@aston.ac.uk.

Notes

The authors declare no competing financial interest.

Biographies

Xingguang Zhang received his Bachelor of Engineering in Chemical Engineering and Technology from Guizhou University (Guiyang, China) in 2007, Master of Engineering in Industrial Catalysis under the supervison of Professor Jun Wang in Nanjing Tech University (Nanjing, China) in 2010, and Ph.D. under the supervision of Dr. Xuebin Ke and Professor Huaiyong Zhu at Queensland University of Technology (Brisbane, Australia) in 2014. He subsequently undertook postdoctoral research with Professor Adam Lee and Professor Karen Wilson to develop supported metal catalysts and solid acid catalysts for clean chemicals synthesis within Aston University (Birmingham, UK).

DOI: 10.1021/acs.chemrev.6b00311
Chem. Rev. 2016, 116, 12328−12368

Karen Wilson is Professor of Catalysis and Research Director of the European Bioenergy Research Institute at Aston University, where she holds a Royal Society Industry Fellowship. Her research interests lie in the design of heterogeneous catalysts for clean chemical synthesis, particularly the design of tunable porous materials for sustainable biofuels and chemicals production from renewable resources. She was educated at the Universities of Cambridge and Liverpool, and following postdoctoral research at Cambridge and the University of York, was appointed a Lecturer and subsequently Senior Lecturer at York, prior to appointment as a Reader in Physical Chemistry at Cardiff University.

Adam Lee is Professor of Sustainable Chemistry and an EPSRC Leadership Fellow in the European Bioenergy Research Institute, Aston University. He holds a B.A. (Natural Sciences) and Ph.D. from the University of Cambridge, and following postdoctoral research at Cambridge and Lecturer/Senior Lecturer roles at the Universities of Hull and York, respectively, held Chair appointments at Cardiff, Warwick, and Monash universities. His research addresses the rational design of nanoengineered materials for clean catalytic technologies, with particular focus on sustainable chemical processes and energy production, and the development of in situ methods to provide molecular insight into surface reactions, for which he was awarded the 2012 Beilby Medal and Prize by the Royal Society of Chemistry.

ACKNOWLEDGMENTS

X.Z. thanks the Engineering and Physical Sciences Council (EPSRC) for a postdoctoral fellowship under award EP/K014706/1. A.F.L. and K.W. were supported in part by the EPSRC (EP/G007594/4, EP/K000616/2, EP/K014676/1, and EP/K014749/1), the Royal Society, and British Council GB3-Net. We thank Dr. Lee Durndell and Dr. Amin Osatiashtiani (Aston University) for valuable discussions.

REFERENCES

(1) Li, X.; Luque-Moreno, L. C.; Oudenhoven, S. R. G.; Rehmann, L.; Kersten, S. R. A.; Schuur, B. Aromatics Extraction From Pyrolytic Sugars Using Ionic Liquid to Enhance Sugar Fermentability. *Bioresour. Technol.* **2016**, *216*, 12−18.
(2) Rogelj, J.; Nabel, J.; Chen, C.; Hare, W.; Markmann, K.; Meinshausen, M.; Schaeffer, M.; Macey, K.; Höhne, N. Copenhagen Accord Pledges are Paltry. *Nature* **2010**, *464*, 1126−1128.
(3) Gerrard, E.; Mansour, A. COP21 and the Paris Agreement. *Aust. Environ. Law Digest* **2015**, *2*, 3.
(4) Jacobson, M. Z.; Delucchi, M. A. Providing all Global Energy With Wind, Water, and Solar Power, Part I: Technologies, Energy Resources, Quantities and Areas of Infrastructure, and Materials. *Energy Policy* **2011**, *39*, 1154−1169.
(5) Melero, J. A.; Iglesias, J.; Garcia, A. Biomass as Renewable Feedstock in Standard Refinery Units. Feasibility, Opportunities and Challenges. *Energy Environ. Sci.* **2012**, *5*, 7393−7420.
(6) Lanzafame, P.; Centi, G.; Perathoner, S. Catalysis for Biomass and CO_2 Use Through Solar Energy: Opening New Scenarios for a Sustainable and Low-Carbon Chemical Production. *Chem. Soc. Rev.* **2014**, *43*, 7562−7580.
(7) Lee, A. F.; Bennett, J. A.; Manayil, J. C.; Wilson, K. Heterogeneous Catalysis for Sustainable Biodiesel Production Via Esterification and Transesterification. *Chem. Soc. Rev.* **2014**, *43*, 7887−7916.
(8) Azadi, P.; Inderwildi, O. R.; Farnood, R.; King, D. A. Liquid Fuels, Hydrogen and Chemicals From Lignin: a Critical Review. *Renewable Sustainable Energy Rev.* **2013**, *21*, 506−523.
(9) Zhou, C.-H.; Xia, X.; Lin, C.-X.; Tong, D.-S.; Beltramini, J. Catalytic Conversion of Lignocellulosic Biomass to Fine Chemicals and Fuels. *Chem. Soc. Rev.* **2011**, *40*, 5588−5617.
(10) Möller, M.; Schroder, U. Hydrothermal Production of Furfural From Xylose and Xylan as Model Compounds for Hemicelluloses. *RSC Adv.* **2013**, *3*, 22253−22260.
(11) Zakzeski, J.; Bruijnincx, P. C. A.; Jongerius, A. L.; Weckhuysen, B. M. The Catalytic Valorization of Lignin for the Production of Renewable Chemicals. *Chem. Rev.* **2010**, *110*, 3552−3599.
(12) Alonso, D. M.; Wettstein, S. G.; Dumesic, J. A. Bimetallic Catalysts for Upgrading of Biomass to Fuels and Chemicals. *Chem. Soc. Rev.* **2012**, *41*, 8075−8098.
(13) Kobayashi, H.; Ohta, H.; Fukuoka, A. Conversion of Lignocellulose Into Renewable Chemicals by Heterogeneous Catalysis. *Catal. Sci. Technol.* **2012**, *2*, 869−883.
(14) Ahrenfeldt, J.; Thomsen, T. P.; Henriksen, U.; Clausen, L. R. Biomass Gasification Cogeneration − a Review of State of the Art Technology and Near Future Perspectives. *Appl. Therm. Eng.* **2013**, *50*, 1407−1417.
(15) Göransson, K.; Söderlind, U.; He, J.; Zhang, W. Review of Syngas Production Via Biomass DFBGS. *Renewable Sustainable Energy Rev.* **2011**, *15*, 482−492.
(16) Richardson, Y.; Blin, J.; Julbe, A. A Short Overview on Purification and Conditioning of Syngas Produced by Biomass Gasification: Catalytic Strategies, Process Intensification and New Concepts. *Prog. Energy Combust. Sci.* **2012**, *38*, 765−781.
(17) Kirkels, A. F.; Verbong, G. P. J. Biomass Gasification: Still Promising? A 30-Year Global Overview. *Renewable Sustainable Energy Rev.* **2011**, *15*, 471−481.
(18) He, C.; Chen, C.-L.; Giannis, A.; Yang, Y.; Wang, J.-Y. Hydrothermal Gasification of Sewage Sludge and Model Compounds for Renewable Hydrogen Production: a Review. *Renewable Sustainable Energy Rev.* **2014**, *39*, 1127−1142.
(19) Reddy, S. N.; Nanda, S.; Dalai, A. K.; Kozinski, J. A. Supercritical Water Gasification of Biomass for Hydrogen Production. *Int. J. Hydrogen Energy* **2014**, *39*, 6912−6926.
(20) Czernik, S.; Bridgwater, A. V. Overview of Applications of Biomass Fast Pyrolysis Oil. *Energy Fuels* **2004**, *18*, 590−598.
(21) Venderbosch, R. H.; Prins, W. Fast Pyrolysis Technology Development. *Biofuels, Bioprod. Biorefin.* **2010**, *4*, 178−208.
(22) Meier, D.; Van De Beld, B.; Bridgwater, A. V.; Elliott, D. C.; Oasmaa, A.; Preto, F. State-Of-The-Art of Fast Pyrolysis in IEA Bioenergy Member Countries. *Renewable Sustainable Energy Rev.* **2013**, *20*, 619−641.
(23) Vispute, T. P.; Zhang, H.; Sanna, A.; Xiao, R.; Huber, G. W. Renewable Chemical Commodity Feedstocks From Integrated Catalytic Processing of Pyrolysis Oils. *Science* **2010**, *330*, 1222−1227.
(24) Rogers, J. G.; Brammer, J. G. Estimation of the Production Cost of Fast Pyrolysis Bio-Oil. *Biomass Bioenergy* **2012**, *36*, 208−217.
(25) Elliott, D. C.; Biller, P.; Ross, A. B.; Schmidt, A. J.; Jones, S. B. Hydrothermal Liquefaction of Biomass: Developments From Batch to Continuous Process. *Bioresour. Technol.* **2015**, *178*, 147−156.
(26) Akhtar, J.; Amin, N. A. S. a Review on Process Conditions for Optimum Bio-Oil Yield in Hydrothermal Liquefaction of Biomass. *Renewable Sustainable Energy Rev.* **2011**, *15*, 1615−1624.
(27) Tekin, K.; Karagöz, S.; Bektaş, S. A Review of Hydrothermal Biomass Processing. *Renewable Sustainable Energy Rev.* **2014**, *40*, 673−687.
(28) Sun, Y.; Cheng, J. Hydrolysis of Lignocellulosic Materials for Ethanol Production: A Review. *Bioresour. Technol.* **2002**, *83*, 1−11.
(29) Jørgensen, H.; Kristensen, J. B.; Felby, C. Enzymatic Conversion of Lignocellulose Into Fermentable Sugars: Challenges and Opportunities. *Biofuels, Bioprod. Biorefin.* **2007**, *1*, 119−134.
(30) Galbe, M.; Zacchi, G. A Review of the Production of Ethanol From Softwood. *Appl. Microbiol. Biotechnol.* **2002**, *59*, 618−628.
(31) Singh, R.; Shukla, A.; Tiwari, S.; Srivastava, M. A Review on Delignification of Lignocellulosic Biomass for Enhancement of Ethanol Production Potential. *Renewable Sustainable Energy Rev.* **2014**, *32*, 713−728.
(32) Laluce, C.; Schenberg, A. C. G.; Gallardo, J. C. M.; Coradello, L. F. C.; Pombeiro-Sponchiado, S. R. Advances and Developments in Strategies to Improve Strains of Saccharomyces Cerevisiae and

DOI: 10.1021/acs.chemrev.6b00311
Chem. Rev. 2016, 116, 12328−12368

Processes to Obtain the Lignocellulosic Ethanol—A Review. *Appl. Biochem. Biotechnol.* **2012**, *166*, 1908−1926.
(33) García, V.; Päkkilä, J.; Ojamo, H.; Muurinen, E.; Keiski, R. L. Challenges in Biobutanol Production: How to Improve the Efficiency? *Renewable Sustainable Energy Rev.* **2011**, *15*, 964−980.
(34) Weber, C.; Farwick, A.; Benisch, F.; Brat, D.; Dietz, H.; Subtil, T.; Boles, E. Trends and Challenges in the Microbial Production of Lignocellulosic Bioalcohol Fuels. *Appl. Microbiol. Biotechnol.* **2010**, *87*, 1303−1315.
(35) Jurgens, G.; Survase, S.; Berezina, O.; Sklavounos, E.; Linnekoski, J.; Kurkijärvi, A.; Väkevä, M.; Van Heiningen, A.; Granström, T. Butanol Production From Lignocellulosics. *Biotechnol. Lett.* **2012**, *34*, 1415−1434.
(36) Adsul, M. G.; Singhvi, M. S.; Gaikaiwari, S. A.; Gokhale, D. V. Development of Biocatalysts for Production of Commodity Chemicals From Lignocellulosic Biomass. *Bioresour. Technol.* **2011**, *102*, 4304−4312.
(37) Hasunuma, T.; Okazaki, F.; Okai, N.; Hara, K. Y.; Ishii, J.; Kondo, A. A Review of Enzymes and Microbes for Lignocellulosic Biorefinery and the Possibility of Their Application to Consolidated Bioprocessing Technology. *Bioresour. Technol.* **2013**, *135*, 513−522.
(38) Jäger, G.; Büchs, J. Biocatalytic Conversion of Lignocellulose to Platform Chemicals. *Biotechnol. J.* **2012**, *7*, 1122−1136.
(39) Chiaramonti, D.; Prussi, M.; Buffi, M.; Rizzo, A. M.; Pari, L. Review and Experimental Study on Pyrolysis and Hydrothermal Liquefaction of Microalgae for Biofuel Production. *Appl. Energy* **2016**, DOI: 10.1016/j.apenergy.2015.12.001.
(40) Ou, L.; Thilakaratne, R.; Brown, R. C.; Wright, M. M. Techno-Economic Analysis of Transportation Fuels From Defatted Microalgae Via Hydrothermal Liquefaction and Hydroprocessing. *Biomass Bioenergy* **2015**, *72*, 45−54.
(41) Heux, S.; Meynial-Salles, I.; O'Donohue, M. J.; Dumon, C. White Biotechnology: State of the Art Strategies for the Development of Biocatalysts for Biorefining. *Biotechnol. Adv.* **2015**, *33*, 1653−1670.
(42) Lee, S. K.; Chou, H.; Ham, T. S.; Lee, T. S.; Keasling, J. D. Metabolic Engineering of Microorganisms for Biofuels Production: From Bugs to Synthetic Biology to Fuels. *Curr. Opin. Biotechnol.* **2008**, *19*, 556−563.
(43) Tufvesson, P.; Fu, W.; Jensen, J. S.; Woodley, J. M. Process Considerations for the Scale-Up and Implementation of Biocatalysis. *Food Bioprod. Process.* **2010**, *88*, 3−11.
(44) Mosier, N.; Wyman, C.; Dale, B.; Elander, R.; Lee, Y. Y.; Holtzapple, M.; Ladisch, M. Features of Promising Technologies for Pretreatment of Lignocellulosic Biomass. *Bioresour. Technol.* **2005**, *96*, 673−686.
(45) Glasser, W. G.; Wright, R. S. Steam-Assisted Biomass Fractionation. II. Fractionation Behavior of Various Biomass Resources. *Biomass Bioenergy* **1998**, *14*, 219−235.
(46) Zhao, X.; Cheng, K.; Liu, D. Organosolv Pretreatment of Lignocellulosic Biomass for Enzymatic Hydrolysis. *Appl. Microbiol. Biotechnol.* **2009**, *82*, 815−827.
(47) Fatih Demirbas, M. Biorefineries for Biofuel Upgrading: A Critical Review. *Appl. Energy* **2009**, *86* (Supplement 1), S151−S161.
(48) María, P. D. D.; Grande, P. M.; Leitner, W. Current Trends in Pretreatment and Fractionation of Lignocellulose as Reflected in Industrial Patent Activities. *Chem. Ing. Tech.* **2015**, *87*, 1686−1695.
(49) Morais, A. R. C.; Da Costa Lopes, A. M.; Bogel-Łukasik, R. Carbon Dioxide in Biomass Processing: Contributions to the Green Biorefinery Concept. *Chem. Rev.* **2015**, *115*, 3−27.
(50) Schacht, C.; Zetzl, C.; Brunner, G. From Plant Materials to Ethanol by Means of Supercritical Fluid Technology. *J. Supercrit. Fluids* **2008**, *46*, 299−321.
(51) Mora-Pale, M.; Meli, L.; Doherty, T. V.; Linhardt, R. J.; Dordick, J. S. Room Temperature Ionic Liquids as Emerging Solvents for the Pretreatment of Lignocellulosic Biomass. *Biotechnol. Bioeng.* **2011**, *108*, 1229−1245.
(52) Da Costa Lopes, A. M.; João, K. G.; Morais, A. R. C.; Bogel-Łukasik, E.; Bogel-Łukasik, R. Ionic Liquids as a Tool for Lignocellulosic Biomass Fractionation. *Sustainable Chem. Processes* **2013**, *1*, 1−31.
(53) Brandt, A.; Gräsvik, J.; Hallett, J. P.; Welton, T. Deconstruction of Lignocellulosic Biomass With Ionic Liquids. *Green Chem.* **2013**, *15*, 550−583.
(54) Swatloski, R. P.; Spear, S. K.; Holbrey, J. D.; Rogers, R. D. Dissolution of Cellose With Ionic Liquids. *J. Am. Chem. Soc.* **2002**, *124*, 4974−4975.
(55) Brandt, A.; Grasvik, J.; Hallett, J. P.; Welton, T. Deconstruction of Lignocellulosic Biomass With Ionic Liquids. *Green Chem.* **2013**, *15*, 550−583.
(56) Brandt, A.; Hallett, J. P.; Leak, D. J.; Murphy, R. J.; Welton, T. The Effect of the Ionic Liquid Anion in the Pretreatment of Pine Wood Chips. *Green Chem.* **2010**, *12*, 672−679.
(57) Francisco, M.; Van Den Bruinhorst, A.; Kroon, M. C. Low-Transition-Temperature Mixtures (LTTMs): a New Generation of Designer Solvents. *Angew. Chem., Int. Ed.* **2013**, *52*, 3074−3085.
(58) Xia, S.; Baker, G. A.; Li, H.; Ravula, S.; Zhao, H. Aqueous Ionic Liquids and Deep Eutectic Solvents for Cellulosic Biomass Pretreatment and Saccharification. *RSC Adv.* **2014**, *4*, 10586−10596.
(59) Chheda, J. N.; Roman-Leshkov, Y.; Dumesic, J. A. Production of 5-Hydroxymethylfurfural and Furfural by Dehydration of Biomass-Derived Mono- and Poly-Saccharides. *Green Chem.* **2007**, *9*, 342−350.
(60) Selva, M.; Gottardo, M.; Perosa, A. Upgrade of Biomass-Derived Levulinic Acid Via Ru/C-Catalyzed Hydrogenation to γ-Valerolactone in Aqueous−Organic−Ionic Liquids Multiphase Systems. *ACS Sustain. Chem. Eng.* **2013**, *1*, 180−189.
(61) Alvira, P.; Tomás-Pejó, E.; Ballesteros, M.; Negro, M. J. Pretreatment Technologies for an Efficient Bioethanol Production Process Based on Enzymatic Hydrolysis: a Review. *Bioresour. Technol.* **2010**, *101*, 4851−4861.
(62) Mok, W. S.; Antal, M. J.; Varhegyi, G. Productive and Parasitic Pathways in Dilute Acid-Catalyzed Hydrolysis of Cellulose. *Ind. Eng. Chem. Res.* **1992**, *31*, 94−100.
(63) Rinaldi, R.; Schüth, F. Acid Hydrolysis of Cellulose as the Entry Point Into Biorefinery Schemes. *ChemSusChem* **2009**, *2*, 1096−1107.
(64) Sasaki, M.; Kabyemela, B.; Malaluan, R.; Hirose, S.; Takeda, N.; Adschiri, T.; Arai, K. Cellulose Hydrolysis in Subcritical and Supercritical Water. *J. Supercrit. Fluids* **1998**, *13*, 261−268.
(65) Binder, J. B.; Raines, R. T. Fermentable Sugars by Chemical Hydrolysis of Biomass. *Proc. Natl. Acad. Sci. U. S. A.* **2010**, *107*, 4516−4521.
(66) Da Costa Lopes, A. M.; Brenner, M.; Falé, P.; Roseiro, L. B.; Bogel-Łukasik, R. Extraction and Purification of Phenolic Compounds From Lignocellulosic Biomass Assisted by Ionic Liquid, Polymeric Resins, and Supercritical CO_2. *ACS Sustainable Chem. Eng.* **2016**, *4*, 3357−3367.
(67) Dee, S. J.; Bell, A. T. A Study of the Acid-Catalyzed Hydrolysis of Cellulose Dissolved in Ionic Liquids and the Factors Influencing the Dehydration of Glucose and the Formation of Humins. *ChemSusChem* **2011**, *4*, 1166−1173.
(68) Jablonský, M.; Škulcová, A.; Kamenská, L.; Vrška, M.; Šíma, J. Deep Eutectic Solvents: Fractionation of Wheat Straw. *BioResources* **2015**, *10*, 8039−8047.
(69) Abbott, A. P.; Capper, G.; Davies, D. L.; Rasheed, R. K.; Tambyrajah, V. Novel Solvent Properties of Choline Chloride/Urea Mixtures. *Chem. Commun.* **2003**, 70−71.
(70) Thuy Pham, T. P.; Cho, C.-W.; Yun, Y.-S. Environmental Fate and Toxicity of Ionic Liquids: a Review. *Water Res.* **2010**, *44*, 352−372.
(71) Amde, M.; Liu, J.-F.; Pang, L. Environmental Application, Fate, Effects, and Concerns of Ionic Liquids: a Review. *Environ. Sci. Technol.* **2015**, *49*, 12611−12627.
(72) Kevin, R. F.; Margaret, S. T.; Michael, H. O. H.; Daniel, M. K. Accounting for the Water Impacts of Ethanol Production. *Environ. Res. Lett.* **2010**, *5*, 014020.
(73) Gerbens-Leenes, W.; Hoekstra, A. Y.; Van Der Meer, T. H. The Water Footprint of Bioenergy. *Proc. Natl. Acad. Sci. U. S. A.* **2009**, *106*, 10219−10223.

DOI: 10.1021/acs.chemrev.6b00311
Chem. Rev. 2016, 116, 12328−12368

(74) Simon, M.-O.; Li, C.-J. Green Chemistry Oriented Organic Synthesis in Water. *Chem. Soc. Rev.* **2012**, *41*, 1415−1427.
(75) Peleteiro, S.; Rivas, S.; Alonso, J. L.; Santos, V.; Parajó, J. C. Utilization of Ionic Liquids in Lignocellulose Biorefineries as Agents for Separation, Derivatization, Fractionation, or Pretreatment. *J. Agric. Food Chem.* **2015**, *63*, 8093−8102.
(76) Zhang, H.; Okuni, J.; Toshima, N. One-Pot Synthesis of Ag−Au Bimetallic Nanoparticles With Au Shell and Their High Catalytic Activity for Aerobic Glucose Oxidation. *J. Colloid Interface Sci.* **2011**, *354*, 131−138.
(77) Passos, H.; Freire, M. G.; Coutinho, J. A. P. Ionic Liquid Solutions as Extractive Solvents for Value-Added Compounds From Biomass. *Green Chem.* **2014**, *16*, 4786−4815.
(78) Freudenmann, D.; Wolf, S.; Wolff, M.; Feldmann, C. Ionic Liquids: New Perspectives for Inorganic Synthesis? *Angew. Chem., Int. Ed.* **2011**, *50*, 11050−11060.
(79) Gericke, M.; Fardim, P.; Heinze, T. Ionic Liquids — Promising But Challenging Solvents for Homogeneous Derivatization of Cellulose. *Molecules* **2012**, *17*, 7458.
(80) Meindersma, G. W.; Quijada-Maldonado, E.; Aelmans, T. A. M.; Hernandez, J. P. G.; De Haan, A. B. *Ionic Liquids: Science and Applications*; American Chemical Society: Washington, DC, 2012; Vol. *1117*.
(81) Kluson, D. P.; Figueroa, J. J.; Lunelli, B. H.; Filho, R. M.; Maciel, M. R. W. Improvements on Anhydrous Ethanol Production by Extractive Distillation Using Ionic Liquid as Solvent. *Procedia Eng.* **2012**, *42*, 1016−1026.
(82) Zakrzewska, M. E.; Bogel-Łukasik, E.; Bogel-Łukasik, R. Ionic Liquid-Mediated Formation of 5-Hydroxymethylfurfural—A Promising Biomass-Derived Building Block. *Chem. Rev.* **2011**, *111*, 397−417.
(83) Wu, L.; Song, J.; Zhang, B.; Zhou, B.; Zhou, H.; Fan, H.; Yang, Y.; Han, B. Very Efficient Conversion of Glucose to 5-Hydroxymethylfurfural in DBU-Based Ionic Liquids With Benzenesulfonate Anion. *Green Chem.* **2014**, *16*, 3935−3941.
(84) Hu, S.; Zhang, Z.; Song, J.; Zhou, Y.; Han, B. Efficient Conversion of Glucose Into 5-Hydroxymethylfurfural Catalyzed by a Common Lewis Acid $SnCl_4$ in an Ionic Liquid. *Green Chem.* **2009**, *11*, 1746−1749.
(85) Zhang, Z.; Wang, Q.; Xie, H.; Liu, W.; Zhao, Z. Catalytic Conversion of Carbohydrates Into 5-Hydroxymethylfurfural by Germanium(IV) Chloride in Ionic Liquids. *ChemSusChem* **2011**, *4*, 131−138.
(86) Carrasquillo-Flores, R.; Kaeldstroem, M.; Schueth, F.; Dumesic, J. A.; Rinaldi, R. Mechanocatalytic Depolymerization of Dry (Ligno)Cellulose as an Entry Process for High-Yield Production of Furfurals. *ACS Catal.* **2013**, *3*, 993−997.
(87) Hick, S. M.; Griebel, C.; Restrepo, D. T.; Truitt, J. H.; Buker, E. J.; Bylda, C.; Blair, R. G. Mechanocatalysis for Biomass-Derived Chemicals and Fuels. *Green Chem.* **2010**, *12*, 468−474.
(88) Kaufman Rechulski, M. D.; Käldström, M.; Richter, U.; Schüth, F.; Rinaldi, R. Mechanocatalytic Depolymerization of Lignocellulose Performed on Hectogram and Kilogram Scales. *Ind. Eng. Chem. Res.* **2015**, *54*, 4581−4592.
(89) Serrano-Ruiz, J. C.; Dumesic, J. A. Catalytic Routes for the Conversion of Biomass Into Liquid Hydrocarbon Transportation Fuels. *Energy Environ. Sci.* **2011**, *4*, 83−99.
(90) Albuquerque, T. L. D.; Da Silva, I. J., Jr; De Macedo, G. R.; Rocha, M. V. P. Biotechnological Production of Xylitol From Lignocellulosic Wastes: A Review. *Process Biochem.* **2014**, *49*, 1779−1789.
(91) Schnyder, B. J. Continuous Isomerization of Glucose to Fructose on a Commercial Basis. *Starch/Stärke* **1974**, *26*, 409−412.
(92) Erickson, B.; Nelson, J. E.; Winters, P. Perspective on Opportunities in Industrial Biotechnology in Renewable Chemicals. *Biotechnol. J.* **2012**, *7*, 176−185.
(93) De Jong, E.; Jungmeier, G. Chapter 1 − Biorefinery Concepts in Comparison to Petrochemical Refineries. *Industrial Biorefineries & White Biotechnology* **2015**, 3−33.
(94) Wang, T.; Nolte, M. W.; Shanks, B. H. Catalytic Dehydration of C_6 Carbohydrates for the Production of Hydroxymethylfurfural (HMF) as a Versatile Platform Chemical. *Green Chem.* **2014**, *16*, 548−572.
(95) Grande, P. M.; Bergs, C.; Domínguez De María, P. Chemo-Enzymatic Conversion of Glucose Into 5-Hydroxymethylfurfural in Seawater. *ChemSusChem* **2012**, *5*, 1203−1206.
(96) Sweeney, M. D.; Xu, F. Biomass Converting Enzymes as Industrial Biocatalysts for Fuels and Chemicals: Recent Developments. *Catalysts* **2012**, *2*, 244−263.
(97) Hood, E. E.; Nelson, P.; Powell, R. *Plant Biomass Conversion*; Wiley: New York, 2011.
(98) Wilson, K.; Lee, A. F. Catalyst Design for Biorefining. *Philos. Trans. R. Soc., A* **2016**, *374*, 20150081.
(99) Kobayashi, H.; Fukuoka, A. Synthesis and Utilisation of Sugar Compounds Derived From Lignocellulosic Biomass. *Green Chem.* **2013**, *15*, 1740−1763.
(100) Climent, M. J.; Corma, A.; Iborra, S. Converting Carbohydrates to Bulk Chemicals and Fine Chemicals Over Heterogeneous Catalysts. *Green Chem.* **2011**, *13*, 520−540.
(101) Ruppert, A. M.; Weinberg, K.; Palkovits, R. Hydrogenolysis Goes Bio: From Carbohydrates and Sugar Alcohols to Platform Chemicals. *Angew. Chem., Int. Ed.* **2012**, *51*, 2564−2601.
(102) Yang, B. Y.; Montgomery, R. Alkaline Degradation of Glucose: Effect of Initial Concentration of Reactants. *Carbohydr. Res.* **1996**, *280*, 27−45.
(103) De Wit, G.; Kieboom, A. P. G.; Van Bekkum, H. Enolisation and Isomerisation of Monosaccharides in Aqueous, Alkaline Solution. *Carbohydr. Res.* **1979**, *74*, 157−175.
(104) Kooyman, C.; Vellenga, K.; De Wilt, H. G. J. The Isomerization of D-Glucose Into D-Fructose in Aqueous Alkaline Solutions. *Carbohydr. Res.* **1977**, *54*, 33−44.
(105) Girisuta, B.; Janssen, L. P. B. M.; Heeres, H. J. Green Chemicals: a Kinetic Study on the Conversion of Glucose to Levulinic Acid. *Chem. Eng. Res. Des.* **2006**, *84*, 339−349.
(106) Ross, J. R. H. In *Heterogeneous Catalysis*; Ross, J. R. H., Ed.; Elsevier: Amsterdam, 2012.
(107) Hagen, J. *Industrial Catalysis*; Wiley-VCH Verlag Gmbh & Co. Kgaa: New York, 2006.
(108) Lin, Y.-C.; Huber, G. W. The Critical Role of Heterogeneous Catalysis in Lignocellulosic Biomass Conversion. *Energy Environ. Sci.* **2009**, *2*, 68−80.
(109) Choudhary, V.; Pinar, A. B.; Sandler, S. I.; Vlachos, D. G.; Lobo, R. F. Xylose Isomerization to Xylulose and Its Dehydration to Furfural in Aqueous Media. *ACS Catal.* **2011**, *1*, 1724−1728.
(110) Delidovich, I.; Palkovits, R. Catalytic Activity and Stability of Hydrophobic Mg-Al Hydrotalcites in the Continuous Aqueous-Phase Isomerization of Glucose Into Fructose. *Catal. Sci. Technol.* **2014**, *4*, 4322−4329.
(111) Bozell, J. J.; Petersen, G. R. Technology Development for the Production of Biobased Products From Biorefinery Carbohydrates-The US Department of Energy's "Top 10" Revisited. *Green Chem.* **2010**, *12*, 539−554.
(112) Ravenelle, R. M.; Schüβler, F.; D'Amico, A.; Danilina, N.; Van Bokhoven, J. A.; Lercher, J. A.; Jones, C. W.; Sievers, C. Stability of Zeolites in Hot Liquid Water. *J. Phys. Chem. C* **2010**, *114*, 19582−19595.
(113) Van Putten, R.-J.; Van Der Waal, J. C.; De Jong, E.; Rasrendra, C. B.; Heeres, H. J.; De Vries, J. G. Hydroxymethylfurfural, a Versatile Platform Chemical Made From Renewable Resources. *Chem. Rev.* **2013**, *113*, 1499−1597.
(114) Tong, X.; Ma, Y.; Li, Y. Biomass Into Chemicals: Conversion of Sugars to Furan Derivatives by Catalytic Processes. *Appl. Catal., A* **2010**, *385*, 1−13.
(115) Dornath, P.; Fan, W. Dehydration of Fructose Into Furans Over Zeolite Catalyst Using Carbon Black as Adsorbent. *Microporous Mesoporous Mater.* **2014**, *191*, 10−17.
(116) Jeong, G. H.; Kim, E. G.; Kim, S. B.; Park, E. D.; Kim, S. W. Fabrication of Sulfonic Acid Modified Mesoporous Silica Shells and

DOI: 10.1021/acs.chemrev.6b00311
Chem. Rev. 2016, 116, 12328−12368

Their Catalytic Performance With Dehydration Reaction of D-Xylose Into Furfural. *Microporous Mesoporous Mater.* **2011**, *144*, 134−139.
(117) Sairanen, E.; Vilonen, K.; Karinen, R.; Lehtonen, J. Functionalized Activated Carbon Catalysts in Xylose Dehydration. *Top. Catal.* **2013**, *56*, 512−521.
(118) Chen, X.; Jiang, Z.-H.; Chen, S.; Qin, W. Microbial and Bioconversion Production of D-Xylitol and Its Detection and Application. *Int. J. Biol. Sci.* **2010**, *6*, 834−844.
(119) Wisniak, J.; Hershkowitz, M.; Stein, S. Hydrogenation of Xylose Over Platinum Group Catalysts. *Ind. Eng. Chem. Prod. Res. Dev.* **1974**, *13*, 232−236.
(120) Da Silva, S. S.; Chandel, A. K. *D-Xylitol: Fermentative Production, Application and Commercialization*; Springer Group: Berlin; New York, 2012.
(121) Zhang, H.; Haba, M.; Okumura, M.; Akita, T.; Hashimoto, S.; Toshima, N. Novel Formation of Ag/Au Bimetallic Nanoparticles by Physical Mixture of Monometallic Nanoparticles in Dispersions and Their Application to Catalysts for Aerobic Glucose Oxidation. *Langmuir* **2013**, *29*, 10330−10339.
(122) Vilcocq, L.; Cabiac, A.; Especel, C.; Guillon, E.; Duprez, D. Transformation of Sorbitol to Biofuels by Heterogeneous Catalysis: Chemical and Industrial Considerations. *Oil Gas Sci. Technol.* **2013**, *68*, 841−860.
(123) Mishra, D. K.; Dabbawala, A. A.; Hwang, J.-S. Ruthenium Nanoparticles Supported on Zeolite Y as an Efficient Catalyst for Selective Hydrogenation of Xylose to Xylitol. *J. Mol. Catal. A: Chem.* **2013**, *376*, 63−70.
(124) Kusserow, B.; Schimpf, S.; Claus, P. Hydrogenation of Glucose to Sorbitol Over Nickel and Ruthenium Catalysts. *Adv. Synth. Catal.* **2003**, *345*, 289−299.
(125) Lazaridis, P. A.; Karakoulia, S.; Delimitis, A.; Coman, S. M.; Parvulescu, V. I.; Triantafyllidis, K. S. D-Glucose Hydrogenation/Hydrogenolysis Reactions on Noble Metal (Ru, Pt)/Activated Carbon Supported Catalysts. *Catal. Today* **2015**, *257*, 281−290.
(126) Liu, C.; Zhang, C.; Hao, S.; Sun, S.; Liu, K.; Xu, J.; Zhu, Y.; Li, Y. WO_x Modified Cu/Al_2O_3 as a High-Performance Catalyst for the Hydrogenolysis of Glucose to 1,2-Propanediol. *Catal. Today* **2016**, *261*, 116−127.
(127) Vilcocq, L.; Cabiac, A.; Especel, C.; Lacombe, S.; Duprez, D. New Insights Into the Mechanism of Sorbitol Transformation Over an Original Bifunctional Catalytic System. *J. Catal.* **2014**, *320*, 16−25.
(128) Liu, C.; Zhang, C.; Liu, K.; Wang, Y.; Fan, G.; Sun, S.; Xu, J.; Zhu, Y.; Li, Y. Aqueous-Phase Hydrogenolysis of Glucose to Value-Added Chemicals and Biofuels: a Comparative Study of Active Metals. *Biomass Bioenergy* **2015**, *72*, 189−199.
(129) Matsumoto, T.; Shimada, S.; Yamamoto, K.; Tanaka, T.; Kondo, A. Two-Stage Oxidation of Glucose by an Enzymatic Bioanode. *Fuel Cells* **2013**, *13*, 960−964.
(130) Ribeiro, M. L.; Schuchardt, U. Cooperative Effect of Cobalt Acetylacetonate and Silica in the Catalytic Cyclization and Oxidation of Fructose to 2,5-Furandicarboxylic Acid. *Catal. Commun.* **2003**, *4*, 83−86.
(131) Zhang, H.; Toshima, N. Glucose Oxidation Using Au-Containing Bimetallic and Trimetallic Nanoparticles. *Catal. Sci. Technol.* **2013**, *3*, 268−278.
(132) Hermans, S.; Devillers, M. On the Role of Ruthenium Associated With Pd and/or Bi in Carbon-Supported Catalysts for the Partial Oxidation of Glucose. *Appl. Catal., A* **2002**, *235*, 253−264.
(133) Clark, J. H. Solid Acids for Green Chemistry. *Acc. Chem. Res.* **2002**, *35*, 791−797.
(134) Basheer, C.; Swaminathan, S.; Lee, H. K.; Valiyaveettil, S. Development and Application of a Simple Capillary-Microreactor for Oxidation of Glucose With a Porous Gold Catalyst. *Chem. Commun.* **2005**, 409−410.
(135) De Bruyn, C. A. L.; Van Ekenstein, W. A. Action Des Alcalis Sur Les Sucres, II. Transformation Réciproque Des Uns Dans Les Autres Des Sucres Glucose, Fructose Et Mannose. *Recl. Trav. Chim. Pays-Bas* **1895**, *14*, 203−216.
(136) Bermejo-Deval, R.; Orazov, M.; Gounder, R.; Hwang, S.-J.; Davis, M. E. Active Sites in Sn-Beta for Glucose Isomerization to Fructose and Epimerization to Mannose. *ACS Catal.* **2014**, *4*, 2288−2297.
(137) Li, Y.-P.; Head-Gordon, M.; Bell, A. T. Analysis of the Reaction Mechanism and Catalytic Activity of Metal-Substituted Beta Zeolite for the Isomerization of Glucose to Fructose. *ACS Catal.* **2014**, *4*, 1537−1545.
(138) Moreau, C.; Durand, R.; Roux, A.; Tichit, D. Isomerization of Glucose Into Fructose in the Presence of Cation-Exchanged Zeolites and Hydrotalcites. *Appl. Catal., A* **2000**, *193*, 257−264.
(139) Yu, S.; Kim, E.; Park, S.; Song, I. K.; Jung, J. C. Isomerization of Glucose Into Fructose Over Mg−Al Hydrotalcite Catalysts. *Catal. Commun.* **2012**, *29*, 63−67.
(140) Lima, S.; Dias, A. S.; Lin, Z.; Brandão, P.; Ferreira, P.; Pillinger, M.; Rocha, J.; Calvino-Casilda, V.; Valente, A. A. Isomerization of D-Glucose to D-Fructose Over Metallosilicate Solid Bases. *Appl. Catal., A* **2008**, *339*, 21−27.
(141) Smit, B.; Maesen, T. L. M. Towards a Molecular Understanding of Shape Selectivity. *Nature* **2008**, *451*, 671−678.
(142) Weitkamp, J. Zeolites and Catalysis. *Solid State Ionics* **2000**, *131*, 175−188.
(143) Gu, J.; Jin, Y.; Zhou, Y.; Zhang, M.; Wu, Y.; Wang, J. Unseeded Organotemplate-Free Hydrothermal Synthesis of Heteroatomic MFI Zeolite Poly-Nanocrystallites. *J. Mater. Chem. A* **2013**, *1*, 2453−2460.
(144) Corma, A.; Domine, M. E.; Nemeth, L.; Valencia, S. Al-Free Sn-Beta Zeolite as a Catalyst for the Selective Reduction of Carbonyl Compounds (Meerwein−Ponndorf−Verley Reaction). *J. Am. Chem. Soc.* **2002**, *124*, 3194−3195.
(145) Moliner, M.; Román-Leshkov, Y.; Davis, M. E. Tin-Containing Zeolites are Highly Active Catalysts for the Isomerization of Glucose in Water. *Proc. Natl. Acad. Sci. U. S. A.* **2010**, *107*, 6164−6168.
(146) Bermejo-Deval, R.; Gounder, R.; Davis, M. E. Framework and Extraframework Tin Sites in Zeolite Beta React Glucose Differently. *ACS Catal.* **2012**, *2*, 2705−2713.
(147) Gounder, R.; Davis, M. E. Titanium-Beta Zeolites Catalyze the Stereospecific Isomerization of D-Glucose to L-Sorbose Via Intramolecular C_5−C_1 Hydride Shift. *ACS Catal.* **2013**, *3*, 1469−1476.
(148) Román-Leshkov, Y.; Moliner, M.; Labinger, J. A.; Davis, M. E. Mechanism of Glucose Isomerization Using a Solid Lewis Acid Catalyst in Water. *Angew. Chem., Int. Ed.* **2010**, *49*, 8954−8957.
(149) Cantrell, D. G.; Gillie, L. J.; Lee, A. F.; Wilson, K. Structure-Reactivity Correlations in Mgal Hydrotalcite Catalysts for Biodiesel Synthesis. *Appl. Catal., A* **2005**, *287*, 183−190.
(150) Di Serio, M.; Ledda, M.; Cozzolino, M.; Minutillo, G.; Tesser, R.; Santacesaria, E. Transesterification of Soybean Oil to Biodiesel by Using Heterogeneous Basic Catalysts. *Ind. Eng. Chem. Res.* **2006**, *45*, 3009−3014.
(151) Lecomte, J.; Finiels, A.; Moreau, C. Kinetic Study of the Isomerization of Glucose Into Fructose in the Presence of Anion-Modified Hydrotalcites. *Starch/Stärke* **2002**, *54*, 75−79.
(152) Delidovich, I.; Palkovits, R. Structure−Performance Correlations of Mg−Al Hydrotalcite Catalysts for the Isomerization of Glucose Into Fructose. *J. Catal.* **2015**, *327*, 1−9.
(153) Tichit, D.; Coq, B. Catalysis by Hydrotalcites and Related Materials. *CATTECH* **2003**, *7*, 206−217.
(154) Osatiashtiani, A.; Lee, A. F.; Brown, D. R.; Melero, J. A.; Morales, G.; Wilson, K. Bifunctional SO_4/ZrO_2 Catalysts for 5-Hydroxymethylfufural (5-HMF) Production From Glucose. *Catal. Sci. Technol.* **2014**, *4*, 333−342.
(155) Osatiashtiani, A.; Lee, A. F.; Granollers, M.; Brown, D. R.; Olivi, L.; Morales, G.; Melero, J. A.; Wilson, K. Hydrothermally Stable, Conformal, Sulfated Zirconia Monolayer Catalysts for Glucose Conversion to 5-HMF. *ACS Catal.* **2015**, *5*, 4345−4352.
(156) Toumi, A.; Engell, S. Optimization-Based Control of a Reactive Simulated Moving Bed Process for Glucose Isomerization. *Chem. Eng. Sci.* **2004**, *59*, 3777−3792.
(157) Stankiewicz, A. Reactive Separations for Process Intensification: An Industrial Perspective. *Chem. Eng. Process.* **2003**, *42*, 137−144.

DOI: 10.1021/acs.chemrev.6b00311
Chem. Rev. 2016, 116, 12328−12368

(158) Saravanamurugan, S.; Paniagua, M.; Melero, J. A.; Riisager, A. Efficient Isomerization of Glucose to Fructose Over Zeolites in Consecutive Reactions in Alcohol and Aqueous Media. *J. Am. Chem. Soc.* **2013**, *135*, 5246−5249.
(159) Christianson, J. R.; Caratzoulas, S.; Vlachos, D. G. Computational Insight Into the Effect of Sn-Beta Na Exchange and Solvent on Glucose Isomerization and Epimerization. *ACS Catal.* **2015**, *5*, 5256−5263.
(160) Liu, M.; Jia, S.; Li, C.; Zhang, A.; Song, C.; Guo, X. Facile Preparation of Sn-B Zeolites by Post-Synthesis (Isomorphous Substitution) Method for Isomerization of Glucose to Fructose. *Chin. J. Catal.* **2014**, *35*, 723−732.
(161) Lee, G.; Jeong, Y.; Takagaki, A.; Jung, J. C. Sonication Assisted Rehydration of Hydrotalcite Catalyst for Isomerization of Glucose to Fructose. *J. Mol. Catal. A: Chem.* **2014**, *393*, 289−295.
(162) Son, P.; Nishimura, S.; Ebitani, K. Preparation of Zirconium Carbonate as Water-Tolerant Solid Base Catalyst for Glucose Isomerization and One-Pot Synthesis of Levulinic Acid With Solid Acid Catalyst. *React. Kinet., Mech. Catal.* **2014**, *111*, 183−197.
(163) Watanabe, M.; Aizawa, Y.; Iida, T.; Nishimura, R.; Inomata, H. Catalytic Glucose and Fructose Conversions With TiO_2 and ZrO_2 in Water at 473 K: Relationship Between Reactivity and Acid−Base Property Determined by TPD Measurement. *Appl. Catal., A* **2005**, *295*, 150−156.
(164) Salak Asghari, F.; Yoshida, H. Acid-Catalyzed Production of 5-Hydroxymethyl Furfural From D-Fructose in Subcritical Water. *Ind. Eng. Chem. Res.* **2006**, *45*, 2163−2173.
(165) Hansen, T. S.; Woodley, J. M.; Riisager, A. Efficient Microwave-Assisted Synthesis of 5-Hydroxymethylfurfural From Concentrated Aqueous Fructose. *Carbohydr. Res.* **2009**, *344*, 2568−2572.
(166) Choudhary, V.; Sandler, S. I.; Vlachos, D. G. Conversion of Xylose to Furfural Using Lewis and Brønsted Acid Catalysts in Aqueous Media. *ACS Catal.* **2012**, *2*, 2022−2028.
(167) Choudhary, V.; Mushrif, S. H.; Ho, C.; Anderko, A.; Nikolakis, V.; Marinkovic, N. S.; Frenkel, A. I.; Sandler, S. I.; Vlachos, D. G. Insights Into the Interplay of Lewis and Brønsted Acid Catalysts in Glucose and Fructose Conversion to 5-(Hydroxymethyl)Furfural and Levulinic Acid in Aqueous Media. *J. Am. Chem. Soc.* **2013**, *135*, 3997−4006.
(168) Lourvanij, K.; Rorrer, G. L. Reactions of Aqueous Glucose Solutions Over Solid-Acid Y-Zeolite Catalyst at 110−160.Degree.C. *Ind. Eng. Chem. Res.* **1993**, *32*, 11−19.
(169) You, S. J.; Park, E. D. Effects of Dealumination and Desilication of H-ZSM-5 on Xylose Dehydration. *Microporous Mesoporous Mater.* **2014**, *186*, 121−129.
(170) Antunes, M. M.; Lima, S.; Fernandes, A.; Pillinger, M.; Ribeiro, M. F.; Valente, A. A. Aqueous-Phase Dehydration of Xylose to Furfural in the Presence of MCM-22 and ITQ-2 Solid Acid Catalysts. *Appl. Catal., A* **2012**, *417*−*418*, 243−252.
(171) Rac, V.; Rakić, V.; Stošić, D.; Otman, O.; Auroux, A. Hierarchical ZSM-5, Beta and USY Zeolites: Acidity Assessment by Gas and Aqueous Phase Calorimetry and Catalytic Activity in Fructose Dehydration Reaction. *Microporous Mesoporous Mater.* **2014**, *194*, 126−134.
(172) Kruger, J. S.; Nikolakis, V.; Vlachos, D. G. Aqueous-Phase Fructose Dehydration Using Brønsted Acid Zeolites: Catalytic Activity of Dissolved Aluminosilicate Species. *Appl. Catal., A* **2014**, *469*, 116−123.
(173) Kruger, J. S.; Choudhary, V.; Nikolakis, V.; Vlachos, D. G. Elucidating the Roles of Zeolite H-BEA in Aqueous-Phase Fructose Dehydration and HMF Rehydration. *ACS Catal.* **2013**, *3*, 1279−1291.
(174) Zhou, Y.; Huang, R.; Ding, F.; Brittain, A. D.; Liu, J.; Zhang, M.; Xiao, M.; Meng, Y.; Sun, L. Sulfonic Acid-Functionalized α-Zirconium Phosphate Single-Layer Nanosheets as a Strong Solid Acid for Heterogeneous Catalysis Applications. *ACS Appl. Mater. Interfaces* **2014**, *6*, 7417−7425.
(175) Nabae, Y.; Liang, J.; Huang, X.; Hayakawa, T.; Kakimoto, M.-A. Sulfonic Acid Functionalized Hyperbranched Poly(Ether Sulfone) as a Solid Acid Catalyst. *Green Chem.* **2014**, *16*, 3596−3602.
(176) Russo, P. A.; Antunes, M. M.; Neves, P.; Wiper, P. V.; Fazio, E.; Neri, F.; Barreca, F.; Mafra, L.; Pillinger, M.; Pinna, N.; Valente, A. A. Solid Acids With SO_3H Groups and Tunable Surface Properties: Versatile Catalysts for Biomass Conversion. *J. Mater. Chem. A* **2014**, *2*, 11813−11824.
(177) Toda, M.; Takagaki, A.; Okamura, M.; Kondo, J. N.; Hayashi, S.; Domen, K.; Hara, M. Green Chemistry: Biodiesel Made With Sugar Catalyst. *Nature* **2005**, *438*, 178−178.
(178) Hara, M.; Yoshida, T.; Takagaki, A.; Takata, T.; Kondo, J. N.; Hayashi, S.; Domen, K. A Carbon Material as a Strong Protonic Acid. *Angew. Chem., Int. Ed.* **2004**, *43*, 2955−2958.
(179) Chung, P.-W.; Charmot, A.; Olatunji-Ojo, O. A.; Durkin, K. A.; Katz, A. Hydrolysis Catalysis of Miscanthus Xylan to Xylose Using Weak-Acid Surface Sites. *ACS Catal.* **2014**, *4*, 302−310.
(180) Lansalot-Matras, C.; Moreau, C. Dehydration of Fructose Into 5-Hydroxymethylfurfural in the Presence of Ionic Liquids. *Catal. Commun.* **2003**, *4*, 517−520.
(181) Dias, A. S.; Pillinger, M.; Valente, A. A. Dehydration of Xylose Into Furfural Over Micro-Mesoporous Sulfonic Acid Catalysts. *J. Catal.* **2005**, *229*, 414−423.
(182) Tian, C.; Bao, C.; Binder, A.; Zhu, Z.; Hu, B.; Guo, Y.; Zhao, B.; Dai, S. An Efficient and Reusable "Hairy" Particle Acid Catalyst for the Synthesis of 5-Hydroxymethylfurfural From Dehydration of Fructose in Water. *Chem. Commun.* **2013**, *49*, 8668−8670.
(183) Lam, E.; Chong, J. H.; Majid, E.; Liu, Y.; Hrapovic, S.; Leung, A. C. W.; Luong, J. H. T. Carbocatalytic Dehydration of Xylose to Furfural in Water. *Carbon* **2012**, *50*, 1033−1043.
(184) Liu, D.; Nimlos, M. R.; Johnson, D. K.; Himmel, M. E.; Qian, X. Free Energy Landscape for Glucose Condensation Reactions. *J. Phys. Chem. A* **2010**, *114*, 12936−12944.
(185) Qian, X.; Wei, X. Glucose Isomerization to Fructose From Ab Initio Molecular Dynamics Simulations. *J. Phys. Chem. B* **2012**, *116*, 10898−10904.
(186) Zhao, H.; Holladay, J. E.; Brown, H.; Zhang, Z. C. Metal Chlorides in Ionic Liquid Solvents Convert Sugars to 5-Hydroxymethylfurfural. *Science* **2007**, *316*, 1597−1600.
(187) Li, G.; Pidko, E. A.; Hensen, E. J. M. Synergy Between Lewis Acid Sites and Hydroxyl Groups for the Isomerization of Glucose to Fructose Over Sn-Containing Zeolites: a Theoretical Perspective. *Catal. Sci. Technol.* **2014**, *4*, 2241−2250.
(188) Qian, X.; Johnson, D. K.; Himmel, M. E.; Nimlos, M. R. The Role of Hydrogen-Bonding Interactions in Acidic Sugar Reaction Pathways. *Carbohydr. Res.* **2010**, *345*, 1945−1951.
(189) Morales, G.; Osatiashtiani, A.; Hernandez, B.; Iglesias, J.; Melero, J. A.; Paniagua, M.; Robert Brown, D.; Granollers, M.; Lee, A. F.; Wilson, K. Conformal Sulfated Zirconia Monolayer Catalysts for the One-Pot Synthesis of Ethyl Levulinate From Glucose. *Chem. Commun.* **2014**, *50*, 11742−11745.
(190) Armaroli, T.; Busca, G.; Carlini, C.; Giuttari, M.; Raspolli Galletti, A. M.; Sbrana, G. Acid Sites Characterization of Niobium Phosphate Catalysts and Their Activity in Fructose Dehydration to 5-Hydroxymethyl-2-Furaldehyde. *J. Mol. Catal. A: Chem.* **2000**, *151*, 233−243.
(191) Lin, R.; Ding, Y. A Review on the Synthesis and Applications of Mesostructured Transition Metal Phosphates. *Materials* **2013**, *6*, 217−243.
(192) Carlini, C.; Patrono, P.; Galletti, A. M. R.; Sbrana, G. Heterogeneous Catalysts Based on Vanadyl Phosphate for Fructose Dehydration to 5-Hydroxymethyl-2-Furaldehyde. *Appl. Catal., A* **2004**, *275*, 111−118.
(193) Khemthong, P.; Daorattanachai, P.; Laosiripojana, N.; Faungnawakij, K. Copper Phosphate Nanostructures Catalyze Dehydration of Fructose to 5-Hydroxymethylfufural. *Catal. Commun.* **2012**, *29*, 96−100.
(194) Daorattanachai, P.; Khemthong, P.; Viriya-Empikul, N.; Laosiripojana, N.; Faungnawakij, K. Conversion of Fructose, Glucose,

DOI: 10.1021/acs.chemrev.6b00311
Chem. Rev. 2016, 116, 12328−12368

and Cellulose to 5-Hydroxymethylfurfural by Alkaline Earth Phosphate Catalysts in Hot Compressed Water. *Carbohydr. Res.* **2012**, *363*, 58−61.
(195) Asghari, F. S.; Yoshida, H. Dehydration of Fructose to 5-Hydroxymethylfurfural in Sub-Critical Water Over Heterogeneous Zirconium Phosphate Catalysts. *Carbohydr. Res.* **2006**, *341*, 2379−2387.
(196) Ordomsky, V. V.; Sushkevich, V. L.; Schouten, J. C.; Van Der Schaaf, J.; Nijhuis, T. A. Glucose Dehydration to 5-Hydroxymethylfurfural Over Phosphate Catalysts. *J. Catal.* **2013**, *300*, 37−46.
(197) Cheng, L.; Guo, X.; Song, C.; Yu, G.; Cui, Y.; Xue, N.; Peng, L.; Guo, X.; Ding, W. High Performance Mesoporous Zirconium Phosphate for Dehydration of Xylose to Furfural in Aqueous-Phase. *RSC Adv.* **2013**, *3*, 23228−23235.
(198) Sanz, F.; Parada, C.; Rojo, J. M.; Ruiz-Valero, C. Crystal Structure, Magnetic Properties, and Ionic Conductivity of a New Mixed-Anion Phosphate $Na_4Ni_5(PO_4)_2(P_2O_7)_2$. *Chem. Mater.* **1999**, *11*, 2673−2679.
(199) Luo, Q.; Shen, S.; Lu, G.; Xiao, X.; Mao, D.; Wang, Y. Synthesis of Cubic Ordered Mesoporous YPO_4:Ln^{3+} and Their Photoluminescence Properties. *J. Mater. Chem.* **2009**, *19*, 8079−8085.
(200) Jiménez-Jiménez, J.; Maireles-Torres, P.; Olivera-Pastor, P.; Rodríguez-Castellón, E.; Jiménez-López, A.; Jones, D. J.; Rozière, J. Surfactant-Assisted Synthesis of a Mesoporous Form of Zirconium Phosphate With Acidic Properties. *Adv. Mater.* **1998**, *10*, 812−815.
(201) Qi, X.; Watanabe, M.; Aida, T. M.; Smith, R. L., Jr Catalytical Conversion of Fructose and Glucose Into 5-Hydroxymethylfurfural in Hot Compressed Water by Microwave Heating. *Catal. Commun.* **2008**, *9*, 2244−2249.
(202) Russo, P. A.; Lima, S.; Rebuttini, V.; Pillinger, M.; Willinger, M.-G.; Pinna, N.; Valente, A. A. Microwave-Assisted Coating of Carbon Nanostructures With Titanium Dioxide for the Catalytic Dehydration of D-Xylose Into Furfural. *RSC Adv.* **2013**, *3*, 2595−2603.
(203) Stošić, D.; Bennici, S.; Rakić, V.; Auroux, A. CeO_2−Nb_2O_5 Mixed Oxide Catalysts: Preparation, Characterization and Catalytic Activity in Fructose Dehydration Reaction. *Catal. Today* **2012**, *192*, 160−168.
(204) Fan, C.; Guan, H.; Zhang, H.; Wang, J.; Wang, S.; Wang, X. Conversion of Fructose and Glucose Into 5-Hydroxymethylfurfural Catalyzed by a Solid Heteropolyacid Salt. *Biomass Bioenergy* **2011**, *35*, 2659−2665.
(205) Jadhav, A. H.; Kim, H.; Hwang, I. T. An Efficient and Heterogeneous Recyclable Silicotungstic Acid With Modified Acid Sites as a Catalyst for Conversion of Fructose and Sucrose Into 5-Hydroxymethylfurfural in Superheated Water. *Bioresour. Technol.* **2013**, *132*, 342−350.
(206) Yi, X.; Delidovich, I.; Sun, Z.; Wang, S.; Wang, X.; Palkovits, R. A Heteropoly Acid Ionic Crystal Containing Cr as an Active Catalyst for Dehydration of Monosaccharides to Produce 5-HMF in Water. *Catal. Sci. Technol.* **2015**, *5*, 2496−2502.
(207) O'Neill, R.; Ahmad, M. N.; Vanoye, L.; Aiouache, F. Kinetics of Aqueous Phase Dehydration of Xylose Into Furfural Catalyzed by ZSM-5 Zeolite. *Ind. Eng. Chem. Res.* **2009**, *48*, 4300−4306.
(208) Weingarten, R.; Tompsett, G. A.; Conner, W. C., Jr; Huber, G. W. Design of Solid Acid Catalysts for Aqueous-Phase Dehydration of Carbohydrates: the Role of Lewis and Brønsted Acid Sites. *J. Catal.* **2011**, *279*, 174−182.
(209) Carniti, P.; Gervasini, A.; Biella, S.; Auroux, A. Niobic Acid and Niobium Phosphate as Highly Acidic Viable Catalysts in Aqueous Medium: Fructose Dehydration Reaction. *Catal. Today* **2006**, *118*, 373−378.
(210) Gomes, F. N. D. C.; Pereira, L. R.; Ribeiro, N. F. P.; Souza, M. M. V. M Production of 5-Hydroxymethylfurfural (HMF) Via Fructose Dehydration: Effect of Solvent and Salting-Out. *Braz. J. Chem. Eng.* **2015**, *32* (32), 119−126.
(211) Román-Leshkov, Y.; Chheda, J. N.; Dumesic, J. A. Phase Modifiers Promote Efficient Production of Hydroxymethylfurfural From Fructose. *Science* **2006**, *312*, 1933−1937.
(212) Gürbüz, E. I.; Wettstein, S. G.; Dumesic, J. A. Conversion of Hemicellulose to Furfural and Levulinic Acid Using Biphasic Reactors With Alkylphenol Solvents. *ChemSusChem* **2012**, *5*, 383−387.
(213) Xu, H.; Miao, Z.; Zhao, H.; Yang, J.; Zhao, J.; Song, H.; Liang, N.; Chou, L. Dehydration of Fructose Into 5-Hydroxymethylfurfural by High Stable Ordered Mesoporous Zirconium Phosphate. *Fuel* **2015**, *145*, 234−240.
(214) Saha, B.; Abu-Omar, M. M. Advances in 5-Hydroxymethylfurfural Production From Biomass in Biphasic Solvents. *Green Chem.* **2014**, *16*, 24−38.
(215) Gao, J.; Chen, L.; Xin, Y.; Yan, Z. Ionic Liquid-Based Aqueous Biphasic Systems With Controlled Hydrophobicity: the Polar Solvent Effect. *J. Chem. Eng. Data* **2014**, *59*, 2150−2158.
(216) Aellig, C.; Scholz, D.; Dapsens, P. Y.; Mondelli, C.; Perez-Ramirez, J. When Catalyst Meets Reactor: Continuous Biphasic Processing of Xylan to Furfural Over Gausy/Amberlyst-36. *Catal. Sci. Technol.* **2015**, *5*, 142−149.
(217) Dias, A. S.; Pillinger, M.; Valente, A. A. Mesoporous Silica-Supported 12-Tungstophosphoric Acid Catalysts for the Liquid Phase Dehydration of D-Xylose. *Microporous Mesoporous Mater.* **2006**, *94*, 214−225.
(218) Qian, X.; Liu, D. Free Energy Landscape for Glucose Condensation and Dehydration Reactions in Dimethyl Sulfoxide and the Effects of Solvent. *Carbohydr. Res.* **2014**, *388*, 50−60.
(219) Lai, L.; Zhang, Y. The Production of 5-Hydroxymethylfurfural From Fructose in Isopropyl Alcohol: a Green and Efficient System. *ChemSusChem* **2011**, *4*, 1745−1748.
(220) Román-Leshkov, Y.; Dumesic, J. Solvent Effects on Fructose Dehydration to 5-Hydroxymethylfurfural in Biphasic Systems Saturated With Inorganic Salts. *Top. Catal.* **2009**, *52*, 297−303.
(221) Vlachos, D. G.; Caratzoulas, S. The Roles of Catalysis and Reaction Engineering in Overcoming the Energy and the Environment Crisis. *Chem. Eng. Sci.* **2010**, *65*, 18−29.
(222) Azadi, P.; Carrasquillo-Flores, R.; Pagan-Torres, Y. J.; Gurbuz, E. I.; Farnood, R.; Dumesic, J. A. Catalytic Conversion of Biomass Using Solvents Derived From Lignin. *Green Chem.* **2012**, *14*, 1573−1576.
(223) Faria, J.; Ruiz, M. P.; Resasco, D. E. Phase-Selective Catalysis in Emulsions Stabilized by Janus Silica-Nanoparticles. *Adv. Synth. Catal.* **2010**, *352*, 2359−2364.
(224) Gounder, R.; Davis, M. E. Beyond Shape Selective Catalysis With Zeolites: Hydrophobic Void Spaces in Zeolites Enable Catalysis in Liquid Water. *AIChE J.* **2013**, *59*, 3349−3358.
(225) Song, J.; Fan, H.; Ma, J.; Han, B. Conversion of Glucose and Cellulose Into Value-Added Products in Water and Ionic Liquids. *Green Chem.* **2013**, *15*, 2619−2635.
(226) Qi, X.; Watanabe, M.; Aida, T. M.; Smith, R. L. Synergistic Conversion of Glucose Into 5-Hydroxymethylfurfural in Ionic Liquid−Water Mixtures. *Bioresour. Technol.* **2012**, *109*, 224−228.
(227) Brown, G. E.; Henrich, V. E.; Casey, W. H.; Clark, D. L.; Eggleston, C.; Felmy, A.; Goodman, D. W.; Grätzel, M.; Maciel, G.; Mccarthy, M. I.; Nealson, K. H.; Sverjensky, D. A.; Toney, M. F.; Zachara, J. M. Metal Oxide Surfaces and Their Interactions With Aqueous Solutions and Microbial Organisms. *Chem. Rev.* **1999**, *99*, 77−174.
(228) Morales, G.; Athens, G.; Chmelka, B. F.; Van Grieken, R.; Melero, J. A. Aqueous-Sensitive Reaction Sites in Sulfonic Acid-Functionalized Mesoporous Silicas. *J. Catal.* **2008**, *254*, 205−217.
(229) Okuhara, T. Water-Tolerant Solid Acid Catalysts. *Chem. Rev.* **2002**, *102*, 3641−3666.
(230) Mikkola, J.-P.; Salmi, T.; Sjöholm, R. Modelling of Kinetics and Mass Transfer in the Hydrogenation of Xylose Over Raney Nickel Catalyst. *J. Chem. Technol. Biotechnol.* **1999**, *74*, 655−662.
(231) Raney, M. U.S. Patent 1,563,787, 1925.
(232) Wisnlak, J.; Simon, R. Hydrogenation of Glucose, Fructose, and Their Mixtures. *Ind. Eng. Chem. Prod. Res. Dev.* **1979**, *18*, 50−57.
(233) Gallezot, P.; Cerino, P. J.; Blanc, B.; Flèche, G.; Fuertes, P. Glucose Hydrogenation on Promoted Raney-Nickel Catalysts. *J. Catal.* **1994**, *146*, 93−102.

DOI: 10.1021/acs.chemrev.6b00311
Chem. Rev. 2016, 116, 12328−12368

(234) Li, H.; Wang, W.; Fa Deng, J. Glucose Hydrogenation to Sorbitol Over a Skeletal Ni-P Amorphous Alloy Catalyst (Raney Ni-P). *J. Catal.* **2000**, *191*, 257−260.
(235) Li, H.; Li, H.; Deng, J.-F. Glucose Hydrogenation Over Ni−B/SiO_2 Amorphous Alloy Catalyst and the Promoting Effect of Metal Dopants. *Catal. Today* **2002**, *74*, 53−63.
(236) Nguyen, H.; Nikolakis, V.; Vlachos, D. G. Mechanistic Insights Into Lewis Acid Metal Salt-Catalyzed Glucose Chemistry in Aqueous Solution. *ACS Catal.* **2016**, *6*, 1497−1504.
(237) Li, H.; Deng, J.-F. Glucose Hydrogenation on Co−B Amorphous Alloy Catalysts and the Promoting Effect of Metal Additives. *J. Chem. Technol. Biotechnol.* **2001**, *76*, 985−990.
(238) Li, H.; Li, H.; Wang, M. Glucose Hydrogenation Over Promoted Co−B Amorphous Alloy Catalysts. *Appl. Catal., A* **2001**, *207*, 129−137.
(239) Guo, H.; Li, H.; Zhu, J.; Ye, W.; Qiao, M.; Dai, W. Liquid Phase Glucose Hydrogenation to D-Glucitol Over an Ultrafine Ru-B Amorphous Alloy Catalyst. *J. Mol. Catal. A: Chem.* **2003**, *200*, 213−221.
(240) Guo, H.; Li, H.; Xu, Y.; Wang, M. Liquid Phase Glucose Hydrogenation Over Cr-Promoted Ru−B Amorphous Alloy Catalysts. *Mater. Lett.* **2002**, *57*, 392−398.
(241) Schimpf, S.; Louis, C.; Claus, P. Ni/SiO_2 Catalysts Prepared With Ethylenediamine Nickel Precursors: Influence of the Pretreatment on the Catalytic Properties in Glucose Hydrogenation. *Appl. Catal., A* **2007**, *318*, 45−53.
(242) Zhang, J.; Wu, S.; Liu, Y.; Li, B. Hydrogenation of Glucose Over Reduced Ni/Cu/Al Hydrotalcite Precursors. *Catal. Commun.* **2013**, *35*, 23−26.
(243) Zhang, J.; Xu, S.; Wu, S.; Liu, Y. Hydrogenation of Fructose Over Magnetic Catalyst Derived From Hydrotalcite Precursor. *Chem. Eng. Sci.* **2013**, *99*, 171−176.
(244) Michel, C.; Gallezot, P. Why Is Ruthenium an Efficient Catalyst for the Aqueous-Phase Hydrogenation of Biosourced Carbonyl Compounds? *ACS Catal.* **2015**, *5*, 4130−4132.
(245) Tan, J.; Cui, J.; Deng, T.; Cui, X.; Ding, G.; Zhu, Y.; Li, Y. Water-Promoted Hydrogenation of Levulinic Acid to γ-Valerolactone on Supported Ruthenium Catalyst. *ChemCatChem* **2015**, *7*, 508−512.
(246) Hoffer, B. W.; Crezee, E.; Mooijman, P. R. M.; Van Langeveld, A. D.; Kapteijn, F.; Moulijn, J. A. Carbon Supported Ru Catalysts as Promising Alternative for Raney-Type Ni in the Selective Hydrogenation of D-Glucose. *Catal. Today* **2003**, *79*−*80*, 35−41.
(247) Liu, J.; Bai, P.; Zhao, X. S. Ruthenium Nanoparticles Embedded in Mesoporous Carbon Microfibers: Preparation, Characterization and Catalytic Properties in the Hydrogenation of D-Glucose. *Phys. Chem. Chem. Phys.* **2011**, *13*, 3758−3763.
(248) Heinen, A. W.; Peters, J. A.; Van Bekkum, H. Hydrogenation of Fructose on Ru/C Catalysts. *Carbohydr. Res.* **2000**, *328*, 449−457.
(249) Aho, A.; Roggan, S.; Simakova, O. A.; Salmi, T.; Murzin, D. Y. Structure Sensitivity in Catalytic Hydrogenation of Glucose Over Ruthenium. *Catal. Today* **2015**, *241* (Part B), 195−199.
(250) Simakova, I. L.; Demidova, Y. S.; Murzina, E. V.; Aho, A.; Murzin, D. Y. Structure Sensitivity in Catalytic Hydrogenation of Galactose and Arabinose Over Ru/C Catalysts. *Catal. Lett.* **2016**, *146*, 1291−1299.
(251) Crezee, E.; Hoffer, B. W.; Berger, R. J.; Makkee, M.; Kapteijn, F.; Moulijn, J. A. Three-Phase Hydrogenation of D-Glucose Over a Carbon Supported Ruthenium Catalyst—Mass Transfer and Kinetics. *Appl. Catal., A* **2003**, *251*, 1−17.
(252) Maris, E. P.; Ketchie, W. C.; Oleshko, V.; Davis, R. J. Metal Particle Growth During Glucose Hydrogenation Over Ru/SiO_2 Evaluated by X-Ray Absorption Spectroscopy and Electron Microscopy. *J. Phys. Chem. B* **2006**, *110*, 7869−7876.
(253) Yadav, M.; Mishra, D. K.; Hwang, J.-S. Catalytic Hydrogenation of Xylose to Xylitol Using Ruthenium Catalyst on NiO Modified TiO_2 Support. *Appl. Catal., A* **2012**, *425*−*426*, 110−116.
(254) Zhang, J.; Lin, L.; Zhang, J.; Shi, J. Efficient Conversion of D-Glucose Into D-Sorbitol Over MCM-41 Supported Ru Catalyst Prepared by a Formaldehyde Reduction Process. *Carbohydr. Res.* **2011**, *346*, 1327−1332.
(255) Sapunov, V. N.; Grigoryev, M. Y.; Sulman, E. M.; Konyaeva, M. B.; Matveeva, V. G. D-Glucose Hydrogenation Over Ru Nanoparticles Embedded in Mesoporous Hypercrosslinked Polystyrene. *J. Phys. Chem. A* **2013**, *117*, 4073−4083.
(256) Mishra, D. K.; Dabbawala, A. A.; Park, J. J.; Jhung, S. H.; Hwang, J.-S. Selective Hydrogenation of D-Glucose to D-Sorbitol Over HY Zeolite Supported Ruthenium Nanoparticles Catalysts. *Catal. Today* **2014**, *232*, 99−107.
(257) Guo, X.; Wang, X.; Guan, J.; Chen, X.; Qin, Z.; Mu, X.; Xian, M. Selective Hydrogenation of D-Glucose to D-Sorbitol Over Ru/ZSM-5 Catalysts. *Chin. J. Catal.* **2014**, *35*, 733−740.
(258) Mishra, D. K.; Lee, J.-M.; Chang, J.-S.; Hwang, J.-S. Liquid Phase Hydrogenation of D-Glucose to D-Sorbitol Over the Catalyst (Ru/NiO−TiO_2) of Ruthenium on a NiO-Modified TiO_2 Support. *Catal. Today* **2012**, *185*, 104−108.
(259) Perrard, A.; Gallezot, P.; Joly, J.-P.; Durand, R.; Baljou, C.; Coq, B.; Trens, P. Highly Efficient Metal Catalysts Supported on Activated Carbon Cloths: a Catalytic Application for the Hydrogenation of D-Glucose to D-Sorbitol. *Appl. Catal., A* **2007**, *331*, 100−104.
(260) Tathod, A.; Kane, T.; Sanil, E. S.; Dhepe, P. L. Solid Base Supported Metal Catalysts for the Oxidation and Hydrogenation of Sugars. *J. Mol. Catal. A: Chem.* **2014**, *388*−*389*, 90−99.
(261) Toukoniitty, B.; Kuusisto, J.; Mikkola, J.-P.; Salmi, T.; Murzin, D. Y. Effect of Ultrasound on Catalytic Hydrogenation of D-Fructose to D-Mannitol. *Ind. Eng. Chem. Res.* **2005**, *44*, 9370−9375.
(262) Kuusisto, J.; Mikkola, J.-P.; Casal, P. P.; Karhu, H.; Väyrynen, J.; Salmi, T. Kinetics of the Catalytic Hydrogenation of D-Fructose Over a CuO-ZnO Catalyst. *Chem. Eng. J.* **2005**, *115*, 93−102.
(263) Mishra, D. K.; Dabbawala, A. A.; Hwang, J.-S. Poly (Styrene-Co-Divinylbenzene) Amine Functionalized Polymer Supported Ruthenium Nanoparticles Catalyst Active in Hydrogenation of Xylose. *Catal. Commun.* **2013**, *41*, 52−55.
(264) Jae, J.; Zheng, W.; Karim, A. M.; Guo, W.; Lobo, R. F.; Vlachos, D. G. The Role of Ru and RuO_2 in the Catalytic Transfer Hydrogenation of 5-Hydroxymethylfurfural for the Production of 2,5-Dimethylfuran. *ChemCatChem* **2014**, *6*, 848−856.
(265) Michel, C.; Zaffran, J.; Ruppert, A. M.; Matras-Michalska, J.; Jedrzejczyk, M.; Grams, J.; Sautet, P. Role of Water in Metal Catalyst Performance for Ketone Hydrogenation: a Joint Experimental and Theoretical Study on Levulinic Acid Conversion Into γ-Valerolactone. *Chem. Commun.* **2014**, *50*, 12450−12453.
(266) Jenness, G. R.; Vlachos, D. G. DFT Study of the Conversion of Furfuryl Alcohol to 2-Methylfuran on RuO_2 (110). *J. Phys. Chem. C* **2015**, *119*, 5938−5945.
(267) Cortese, R.; Duca, D.; Sifontes Herrera, V. A.; Murzin, D. Y. L-Arabinose Conformers Adsorption on Ruthenium Surfaces: A DFT Study. *J. Phys. Chem. C* **2012**, *116*, 14908−14916.
(268) Wan, H.; Vitter, A.; Chaudhari, R. V.; Subramaniam, B. Kinetic Investigations of Unusual Solvent Effects During Ru/C Catalyzed Hydrogenation of Model Oxygenates. *J. Catal.* **2014**, *309*, 174−184.
(269) Feibelman, P. J. Partial Dissociation of Water on Ru(0001). *Science* **2002**, *295*, 99−102.
(270) Kim, Y.; Moon, E.-S.; Shin, S.; Kang, H. Acidic Water Monolayer on Ruthenium(0001). *Angew. Chem., Int. Ed.* **2012**, *51*, 12806−12809.
(271) Delbecq, F.; Sautet, P. Competitive C═C and C═O Adsorption of A-B-Unsaturated Aldehydes on Pt and Pd Surfaces in Relation With the Selectivity of Hydrogenation Reactions: A Theoretical Approach. *J. Catal.* **1995**, *152*, 217−236.
(272) Zheng, R.; Porosoff, M. D.; Weiner, J. L.; Lu, S.; Zhu, Y.; Chen, J. G. Controlling Hydrogenation of C═O and C═C Bonds in Cinnamaldehyde Using Silica Supported Co-Pt and Cu-Pt Bimetallic Catalysts. *Appl. Catal., A* **2012**, *419*−*420*, 126−132.
(273) Yu, W.; Porosoff, M. D.; Chen, J. G. Review of Pt-Based Bimetallic Catalysis: From Model Surfaces to Supported Catalysts. *Chem. Rev.* **2012**, *112*, 5780−5817.

DOI: 10.1021/acs.chemrev.6b00311
Chem. Rev. 2016, 116, 12328−12368

(274) Ahmed, M. Kinetics Studies of D-Glucose Hydrogenation Over Activated Charcoal Supported Platinum Catalyst. *Heat Mass Transfer* **2012**, *48*, 343−347.
(275) Ahmed, M. J.; Kadhum, A. A. H. Hydrogenation of D-Fructose Over Activated Charcoal Supported Platinum Catalyst. *J. Taiwan Inst. Chem. Eng.* **2011**, *42*, 114−119.
(276) Kanie, Y.; Akiyama, K.; Iwamoto, M. Reaction Pathways of Glucose and Fructose on Pt Nanoparticles in Subcritical Water Under a Hydrogen Atmosphere. *Catal. Today* **2011**, *178*, 58−63.
(277) Benyahya, S.; Monnier, F.; Wong Chi Man, M.; Bied, C.; Ouazzani, F.; Taillefer, M. Sol-Gel Immobilized and Reusable Copper-Catalyst for Arylation of Phenols From Aryl Bromides. *Green Chem.* **2009**, *11*, 1121−1123.
(278) Wang, J.; Lu, S.; Cao, X.; Gu, H. Common Metal of Copper(0) as an Efficient Catalyst for Preparation of Nitriles and Imines by Controlling Additives. *Chem. Commun.* **2014**, *50*, 5637−5640.
(279) Delannoy, L.; Thrimurthulu, G.; Reddy, P. S.; Methivier, C.; Nelayah, J.; Reddy, B. M.; Ricolleau, C.; Louis, C. Selective Hydrogenation of Butadiene Over TiO_2 Supported Copper, Gold and Gold-Copper Catalysts Prepared by Deposition-Precipitation. *Phys. Chem. Chem. Phys.* **2014**, *16*, 26514−26527.
(280) Shiraishi, Y.; Sakamoto, H.; Sugano, Y.; Ichikawa, S.; Hirai, T. Pt−Cu Bimetallic Alloy Nanoparticles Supported on Anatase TiO_2: Highly Active Catalysts for Aerobic Oxidation Driven by Visible Light. *ACS Nano* **2013**, *7*, 9287−9297.
(281) Ge, X.; Chen, L.; Kang, J.; Fujita, T.; Hirata, A.; Zhang, W.; Jiang, J.; Chen, M. A Core-Shell Nanoporous Pt-Cu Catalyst With Tunable Composition and High Catalytic Activity. *Adv. Funct. Mater.* **2013**, *23*, 4156−4162.
(282) Déchamp, N.; Gamez, A.; Perrard, A.; Gallezot, P. Kinetics of Glucose Hydrogenation in a Trickle-Bed Reactor. *Catal. Today* **1995**, *24*, 29−34.
(283) Gallezot, P.; Nicolaus, N.; Flèche, G.; Fuertes, P.; Perrard, A. Glucose Hydrogenation on Ruthenium Catalysts in a Trickle-Bed Reactor. *J. Catal.* **1998**, *180*, 51−55.
(284) Mederos, F. S.; Ancheyta, J.; Chen, J. Review on Criteria to Ensure Ideal Behaviors in Trickle-Bed Reactors. *Appl. Catal., A* **2009**, *355*, 1−19.
(285) Maiti, R.; Khanna, R.; Nigam, K. D. P. Hysteresis in Trickle-Bed Reactors: A Review. *Ind. Eng. Chem. Res.* **2006**, *45*, 5185−5198.
(286) Mocciaro, C.; Martínez, O. M.; Barreto, G. F. Assessment of Mass Transfer in the Stagnant Liquid Regions in Trickle-Bed Reactors. *Chem. Eng. J.* **2011**, *173*, 813−827.
(287) Maiti, R. N.; Nigam, K. D. P. Gas−Liquid Distributors for Trickle-Bed Reactors: A Review. *Ind. Eng. Chem. Res.* **2007**, *46*, 6164−6182.
(288) Saroha, A. K.; Nandi, I. Pressure Drop Hysteresis in Trickle Bed Reactors. *Chem. Eng. Sci.* **2008**, *63*, 3114−3119.
(289) Wen, J.-P.; Wang, C.-L.; Liu, Y.-X. Preparation of Sorbitol From D-Glucose Hydrogenation in Gas−Liquid−Solid Three-Phase Flow Airlift Loop Reactor. *J. Chem. Technol. Biotechnol.* **2004**, *79*, 403−406.
(290) Eisenbeis, C.; Guettel, R.; Kunz, U.; Turek, T. Monolith Loop Reactor for Hydrogenation of Glucose. *Catal. Today* **2009**, *147* (Supplement), S342−S346.
(291) Diakov, V.; Varma, A. Glucose Hydrogenation in a Membrane Trickle-Bed Reactor. *AIChE J.* **2003**, *49*, 2933−2936.
(292) Dong, X.; Jin, W.; Xu, N.; Li, K. Dense Ceramic Catalytic Membranes and Membrane Reactors for Energy and Environmental Applications. *Chem. Commun.* **2011**, *47*, 10886−10902.
(293) Chatterjee, M.; Ishizaka, T.; Kawanami, H. Hydrogenation of 5-Hydroxymethylfurfural in Supercritical Carbon Dioxide-Water: a Tunable Approach to Dimethylfuran Selectivity. *Green Chem.* **2014**, *16*, 1543−1551.
(294) Kobayashi, H.; Matsuhashi, H.; Komanoya, T.; Hara, K.; Fukuoka, A. Transfer Hydrogenation of Cellulose to Sugar Alcohols Over Supported Ruthenium Catalysts. *Chem. Commun.* **2011**, *47*, 2366−2368.
(295) Yi, G.; Zhang, Y. One-Pot Selective Conversion of Hemicellulose (Xylan) to Xylitol Under Mild Conditions. *ChemSusChem* **2012**, *5*, 1383−1387.
(296) Mao, H.; Peng, S.; Yu, H.; Chen, J.; Zhao, S.; Huo, F. Facile Synthesis of Highly Stable Heterogeneous Catalysts by Entrapping Metal Nanoparticles Within Mesoporous Carbon. *J. Mater. Chem. A* **2014**, *2*, 5847−5851.
(297) Joo, S. H.; Park, J. Y.; Tsung, C.-K.; Yamada, Y.; Yang, P.; Somorjai, G. A. Thermally Stable Pt/Mesoporous Silica Core-Shell Nanocatalysts for High-Temperature Reactions. *Nat. Mater.* **2009**, *8*, 126−131.
(298) Dirkx, J. M. H.; Van Der Baan, H. S. The Oxidation of Gluconic Acid With Platinum on Carbon as Catalyst. *J. Catal.* **1981**, *67*, 14−20.
(299) Muzart, J. Palladium-Catalysed Oxidation of Primary and Secondary Alcohols. *Tetrahedron* **2003**, *59*, 5789−5816.
(300) Mallat, T.; Baiker, A. Oxidation of Alcohols With Molecular Oxygen on Solid Catalysts. *Chem. Rev.* **2004**, *104*, 3037−3058.
(301) Abbadi, A.; Makkee, M.; Visscher, W.; Van Veen, J. A. R.; Bekkum, H. V. Effect of pH in the Pd-Catalyzed Oxidation of D-Glucose to D-Gluconic Acid. *J. Carbohydr. Chem.* **1993**, *12*, 573−587.
(302) Nikov, I.; Paev, K. Palladium on Alumina Catalyst for Glucose Oxidation: Reaction Kinetics and Catalyst Deactivation. *Catal. Today* **1995**, *24*, 41−47.
(303) Wenkin, M.; Renard, C.; Ruiz, P.; Delmon, B.; Devillers, M. In *Studies in Surface Science and Catalysis*; Oyama, S. T., Gaffney, A. M., Lyons, J. E., Grasselli, R. K., Eds.; Elsevier: New York, 1997; Vol. *110*.
(304) Karski, S.; Witońska, I. Bismuth as an Additive Modifying the Selectivity of Palladium Catalysts. *J. Mol. Catal. A: Chem.* **2003**, *191*, 87−92.
(305) Lee, A. F.; Wilson, K. Structure-Reactivity Correlations in the Selective Aerobic Oxidation of Cinnamyl Alcohol: in Situ XAFS. *Green Chem.* **2004**, *6*, 37−42.
(306) Lee, A. F.; Hackett, S. F. J.; Hargreaves, J. S. J.; Wilson, K. On the Active Site in Heterogeneous Palladium Selox Catalysts. *Green Chem.* **2006**, *8*, 549−555.
(307) Parlett, C. M. A.; Bruce, D. W.; Hondow, N. S.; Lee, A. F.; Wilson, K. Support-Enhanced Selective Aerobic Alcohol Oxidation Over Pd/Mesoporous Silicas. *ACS Catal.* **2011**, *1*, 636−640.
(308) Lee, A. F.; Ellis, C. V.; Naughton, J. N.; Newton, M. A.; Parlett, C. M. A.; Wilson, K. Reaction-Driven Surface Restructuring and Selectivity Control in Allylic Alcohol Catalytic Aerobic Oxidation Over Pd. *J. Am. Chem. Soc.* **2011**, *133*, 5724−5727.
(309) Matveeva, V.; Bykov, A.; Doluda, V.; Sulman, M.; Kumar, N.; Dzwigaj, S.; Marceau, E.; Kustov, L.; Tkachenko, O.; Sulman, E. Direct D-Glucose Oxidation Over Noble Metal Nanoparticles Introduced on Polymer and Inorganic Supports. *Top. Catal.* **2009**, *52*, 387−393.
(310) Witońska, I.; Frajtak, M.; Karski, S. Selective Oxidation of Glucose to Gluconic Acid Over Pd−Te Supported Catalysts. *Appl. Catal., A* **2011**, *401*, 73−82.
(311) Haruta, M.; Kobayashi, T.; Sano, H.; Yamada, N. Novel Gold Catalysts for the Oxidation of Carbon Monoxide at a Temperature Far Below 0 °C. *Chem. Lett.* **1987**, *16*, 405−408.
(312) Enache, D. I.; Edwards, J. K.; Landon, P.; Solsona-Espriu, B.; Carley, A. F.; Herzing, A. A.; Watanabe, M.; Kiely, C. J.; Knight, D. W.; Hutchings, G. J. Solvent-Free Oxidation of Primary Alcohols to Aldehydes Using Au-Pd/TiO_2 Catalysts. *Science* **2006**, *311*, 362−365.
(313) Wang, F.; Ueda, W.; Xu, J. Detection and Measurement of Surface Electron Transfer on Reduced Molybdenum Oxides (MoO_x) and Catalytic Activities of Au/MoO_x. *Angew. Chem., Int. Ed.* **2012**, *51*, 3883−3887.
(314) Stratakis, M.; Garcia, H. Catalysis by Supported Gold Nanoparticles: Beyond Aerobic Oxidative Processes. *Chem. Rev.* **2012**, *112*, 4469−4506.
(315) Min, B. K.; Friend, C. M. Heterogeneous Gold-Based Catalysis for Green Chemistry: Low-Temperature CO Oxidation and Propene Oxidation. *Chem. Rev.* **2007**, *107*, 2709−2724.
(316) Conte, M.; Miyamura, H.; Kobayashi, S.; Chechik, V. Spin Trapping of Au−H Intermediate in the Alcohol Oxidation by

DOI: 10.1021/acs.chemrev.6b00311
Chem. Rev. 2016, 116, 12328−12368

Supported and Unsupported Gold Catalysts. *J. Am. Chem. Soc.* **2009**, *131*, 7189−7196.
(317) Conte, M.; Miyamura, H.; Kobayashi, S.; Chechik, V. Enhanced Acyl Radical Formation in the Au Nanoparticle-Catalysed Aldehydeoxidation. *Chem. Commun.* **2010**, *46*, 145−147.
(318) Yin, H.; Zhou, C.; Xu, C.; Liu, P.; Xu, X.; Ding, Y. Aerobic Oxidation of D-Glucose on Support-Free Nanoporous Gold. *J. Phys. Chem. C* **2008**, *112*, 9673−9678.
(319) Ishida, T.; Watanabe, H.; Bebeko, T.; Akita, T.; Haruta, M. Aerobic Oxidation of Glucose Over Gold Nanoparticles Deposited on Cellulose. *Appl. Catal., A* **2010**, *377*, 42−46.
(320) Miedziak, P. J.; Alshammari, H.; Kondrat, S. A.; Clarke, T. J.; Davies, T. E.; Morad, M.; Morgan, D. J.; Willock, D. J.; Knight, D. W.; Taylor, S. H.; Hutchings, G. J. Base-Free Glucose Oxidation Using Air With Supported Gold Catalysts. *Green Chem.* **2014**, *16*, 3132−3141.
(321) Ishida, T.; Kinoshita, N.; Okatsu, H.; Akita, T.; Takei, T.; Haruta, M. Influence of the Support and the Size of Gold Clusters on Catalytic Activity for Glucose Oxidation. *Angew. Chem., Int. Ed.* **2008**, *47*, 9265−9268.
(322) Jiang, D.; Zhao, H.; Zhang, S.; John, R. Characterization of Photoelectrocatalytic Processes at Nanoporous TiO_2 Film Electrodes: Photocatalytic Oxidation of Glucose. *J. Phys. Chem. B* **2003**, *107*, 12774−12780.
(323) Wittstock, A.; Wichmann, A.; Bäumer, M. Nanoporous Gold as a Platform for a Building Block Catalyst. *ACS Catal.* **2012**, *2*, 2199−2215.
(324) Comotti, M.; Pina, C. D.; Rossi, M. Mono- and Bimetallic Catalysts for Glucose Oxidation. *J. Mol. Catal. A: Chem.* **2006**, *251*, 89−92.
(325) Mirescu, A.; Prüße, U. Selective Glucose Oxidation on Gold Colloids. *Catal. Commun.* **2006**, *7*, 11−17.
(326) Biella, S.; Prati, L.; Rossi, M. Selective Oxidation of D-Glucose on Gold Catalyst. *J. Catal.* **2002**, *206*, 242−247.
(327) Delidovich, I. V.; Moroz, B. L.; Taran, O. P.; Gromov, N. V.; Pyrjaev, P. A.; Prosvirin, I. P.; Bukhtiyarov, V. I.; Parmon, V. N. Aerobic Selective Oxidation of Glucose to Gluconate Catalyzed by Au/Al_2O_3 and Au/C: Impact of the Mass-Transfer Processes on the Overall Kinetics. *Chem. Eng. J.* **2013**, *223*, 921−931.
(328) Prüße, U.; Herrmann, M.; Baatz, C.; Decker, N. Gold-Catalyzed Selective Glucose Oxidation at High Glucose Concentrations and Oxygen Partial Pressures. *Appl. Catal., A* **2011**, *406*, 89−93.
(329) Prüße, U.; Jarzombek, P.; Vorlop, K.-D. Gold-Catalyzed Glucose Oxidation Using Novel Spherical Sol−Gel Derived Alumina Supports Produced Via the Jetcutter. *Top. Catal.* **2012**, *55*, 453−459.
(330) Mirescu, A.; Berndt, H.; Martin, A.; Prüße, U. Long-Term Stability of a 0.45% Au/TiO_2 Catalyst in the Selective Oxidation of Glucose At Optimised Reaction Conditions. *Appl. Catal., A* **2007**, *317*, 204−209.
(331) Benkó, T.; Beck, A.; Geszti, O.; Katona, R.; Tungler, A.; Frey, K.; Guczi, L.; Schay, Z. Selective Oxidation of Glucose Versus CO Oxidation Over Supported Gold Catalysts. *Appl. Catal., A* **2010**, *388*, 31−36.
(332) Odrozek, K.; Maresz, K.; Koreniuk, A.; Prusik, K.; Mrowiec-Białoń, J. Amine-Stabilized Small Gold Nanoparticles Supported on AlSBA-15 as Effective Catalysts for Aerobic Glucose Oxidation. *Appl. Catal., A* **2014**, *475*, 203−210.
(333) Ishida, T.; Okamoto, S.; Makiyama, R.; Haruta, M. Aerobic Oxidation of Glucose and 1-Phenylethanol Over Gold Nanoparticles Directly Deposited on Ion-Exchange Resins. *Appl. Catal., A* **2009**, *353*, 243−248.
(334) Cao, Y.; Liu, X.; Iqbal, S.; Miedziak, P. J.; Edwards, J. K.; Armstrong, R. D.; Morgan, D. J.; Wang, J.; Hutchings, G. J. Base-Free Oxidation of Glucose to Gluconic Acid Using Supported Gold Catalysts. *Catal. Sci. Technol.* **2016**, *6*, 107−117.
(335) Bönnemann, H.; Brijoux, W.; Brinkmann, R.; Schulze Tilling, A.; Schilling, T.; Tesche, B.; Seevogel, K.; Franke, R.; Hormes, J.; Köhl, G.; Pollmann, J.; Rothe, J.; Vogel, W. Selective Oxidation of Glucose on Bismuth-Promoted Pd-Pt/C Catalysts Prepared From $NOct_4Cl$-Stabilized Pd-Pt Colloids. *Inorg. Chim. Acta* **1998**, *270*, 95−110.
(336) Zhang, H.; Toshima, N. Preparation of Novel Au/Pt/Ag Trimetallic Nanoparticles and Their High Catalytic Activity for Aerobic Glucose Oxidation. *Appl. Catal., A* **2011**, *400*, 9−13.
(337) Zhang, H.; Okumura, M.; Toshima, N. Stable Dispersions of PVP-Protected Au/Pt/Ag Trimetallic Nanoparticles as Highly Active Colloidal Catalysts for Aerobic Glucose Oxidation. *J. Phys. Chem. C* **2011**, *115*, 14883−14891.
(338) Zhang, H.; Toshima, N.; Takasaki, K.; Okumura, M. Preparation of Agcore/Aushell Bimetallic Nanoparticles From Physical Mixtures of Au Clusters and Ag Ions Under Dark Conditions and Their Catalytic Activity for Aerobic Glucose Oxidation. *J. Alloys Compd.* **2014**, *586*, 462−468.
(339) Benkó, T.; Beck, A.; Frey, K.; Srankó, D. F.; Geszti, O.; Sáfrán, G.; Maróti, B.; Schay, Z. Bimetallic Ag−Au/SiO_2 Catalysts: Formation, Structure and Synergistic Activity in Glucose Oxidation. *Appl. Catal., A* **2014**, *479*, 103−111.
(340) Thielecke, N.; Aytemir, M.; Prüsse, U. Selective Oxidation of Carbohydrates With Gold Catalysts: Continuous-Flow Reactor System for Glucose Oxidation. *Catal. Today* **2007**, *121*, 115−120.
(341) Lallemand, M.; Finiels, A.; Fajula, F.; Hulea, V. Continuous Stirred Tank Reactor for Ethylene Oligomerization Catalyzed by NiMCM-41. *Chem. Eng. J.* **2011**, *172*, 1078−1082.
(342) Salehi, S.; Shahrokhi, M. Two Observer-Based Nonlinear Control Approaches for Temperature Control of a Class of Continuous Stirred Tank Reactors. *Chem. Eng. Sci.* **2008**, *63*, 395−403.
(343) Tschentscher, R.; Nijhuis, T. A.; Van Der Schaaf, J.; Schouten, J. C. Glucose Oxidation in Slurry Reactors and Rotating Foam Reactors. *Ind. Eng. Chem. Res.* **2012**, *51*, 1620−1634.
(344) Parlett, C. M. A.; Gaskell, C. V.; Naughton, J. N.; Newton, M. A.; Wilson, K.; Lee, A. F. Operando Synchronous DRIFTS/MS/XAS as a Powerful Tool for Guiding the Design of Pd Catalysts for the Selective Oxidation of Alcohols. *Catal. Today* **2013**, *205*, 76−85.
(345) Durndell, L. J.; Parlett, C. M. A.; Hondow, N. S.; Wilson, K.; Lee, A. F. Tunable Pt Nanocatalysts for the Aerobic Selox of Cinnamyl Alcohol. *Nanoscale* **2013**, *5*, 5412−5419.
(346) Comotti, M.; Della Pina, C.; Falletta, E.; Rossi, M. Is the Biochemical Route Always Advantageous? The Case of Glucose Oxidation. *J. Catal.* **2006**, *244*, 122−125.
(347) Abad, A.; Concepción, P.; Corma, A.; García, H. A Collaborative Effect Between Gold and a Support Induces the Selective Oxidation of Alcohols. *Angew. Chem., Int. Ed.* **2005**, *44*, 4066−4069.
(348) Ardemani, L.; Cibin, G.; Dent, A. J.; Isaacs, M. A.; Kyriakou, G.; Lee, A. F.; Parlett, C. M. A.; Parry, S. A.; Wilson, K. Solid Base Catalysed 5-HMF Oxidation to 2,5-FDCA Over Au/Hydrotalcites: Fact or Fiction? *Chem. Sci.* **2015**, *6*, 4940−4945.
(349) Willför, S.; Sjöholm, R.; Laine, C.; Holmbom, B. Structural Features of Water-Soluble Arabinogalactans From Norway Spruce and Scots Pine Heartwood. *Wood Sci. Technol.* **2002**, *36*, 101−110.
(350) Kusema, B. T.; Murzin, D. Y. Catalytic Oxidation of Rare Sugars Over Gold Catalysts. *Catal. Sci. Technol.* **2013**, *3*, 297−307.
(351) Mirescu, A.; Prüße, U. A New Environmental Friendly Method for the Preparation of Sugar Acids Via Catalytic Oxidation on Gold Catalysts. *Appl. Catal., B* **2007**, *70*, 644−652.
(352) Min, L.; Tingting, T.; Guoming, Z.; Jiwen, Z.; Xingyong, L. Catalytic Oxidation of Xylose to Xylose Acid Over Pd/C Catalyst. *Chem. React. Eng. Technol.* **2014**, *30*, 352−356.
(353) Amaniampong, P. N.; Li, K.; Jia, X.; Wang, B.; Borgna, A.; Yang, Y. Titania-Supported Gold Nanoparticles as Efficient Catalysts for the Oxidation of Cellobiose to Organic Acids in Aqueous Medium. *ChemCatChem* **2014**, *6*, 2105−2114.
(354) Amaniampong, P. N.; Jia, X.; Wang, B.; Mushrif, S. H.; Borgna, A.; Yang, Y. Catalytic Oxidation of Cellobiose Over TiO_2 Supported Gold-Based Bimetallic Nanoparticles. *Catal. Sci. Technol.* **2015**, *5*, 2393−2405.
(355) Morawa Eblagon, K.; Pereira, M. F. R.; Figueiredo, J. L. One-Pot Oxidation of Cellobiose to Gluconic Acid. Unprecedented High

DOI: 10.1021/acs.chemrev.6b00311
Chem. Rev. 2016, 116, 12328−12368

Selectivity on Bifunctional Gold Catalysts Over Mesoporous Carbon by Integrated Texture and Surface Chemistry Optimization. *Appl. Catal., B* **2016**, *184*, 381−396.
(356) Tan, X.; Deng, W.; Liu, M.; Zhang, Q.; Wang, Y. Carbon Nanotube-Supported Gold Nanoparticles as Efficient Catalysts for Selective Oxidation of Cellobiose Into Gluconic Acid in Aqueous Medium. *Chem. Commun.* **2009**, 7179−7181.
(357) An, D.; Ye, A.; Deng, W.; Zhang, Q.; Wang, Y. Selective Conversion of Cellobiose and Cellulose Into Gluconic Acid in Water in the Presence of Oxygen, Catalyzed by Polyoxometalate-Supported Gold Nanoparticles. *Chem. - Eur. J.* **2012**, *18*, 2938−2947.
(358) Zhang, J.; Liu, X.; Hedhili, M. N.; Zhu, Y.; Han, Y. Highly Selective and Complete Conversion of Cellobiose to Gluconic Acid Over Au/$Cs_2HPW_{12}O_{40}$ Nanocomposite Catalyst. *ChemCatChem* **2011**, *3*, 1294−1298.
(359) Onda, A.; Ochi, T.; Yanagisawa, K. New Direct Production of Gluconic Acid From Polysaccharides Using a Bifunctional Catalyst in Hot Water. *Catal. Commun.* **2011**, *12*, 421−425.
(360) Zanfir, M.; Sun, X.; Gavriilidis, A. Investigation of a Rotating Disc Reactor for Acetone Stripping and Asymmetric Transfer Hydrogenation: Modelling and Experiments. *Chem. Eng. Sci.* **2007**, *62*, 741−755.
(361) Eze, V. C.; Phan, A. N.; Pirez, C.; Harvey, A. P.; Lee, A. F.; Wilson, K. Heterogeneous Catalysis in an Oscillatory Baffled Flow Reactor. *Catal. Sci. Technol.* **2013**, *3*, 2373−2379.
(362) Thomsen, M. S.; Nidetzky, B. Microfluidic Reactor for Continuous Flow Biotransformations With Immobilized Enzymes: the Example of Lactose Hydrolysis by a Hyperthermophilic β-Glycoside Hydrolase. *Eng. Life Sci.* **2008**, *8*, 40−48.
(363) Pei, G. X.; Liu, X. Y.; Wang, A.; Lee, A. F.; Isaacs, M. A.; Li, L.; Pan, X.; Yang, X.; Wang, X.; Tai, Z.; Wilson, K.; Zhang, T. Ag Alloyed Pd Single-Atom Catalysts for Efficient Selective Hydrogenation of Acetylene to Ethylene in Excess Ethylene. *ACS Catal.* **2015**, *5*, 3717−3725.
(364) Lange, J. P. Lignocellulose Conversion: An Introduction to Chemistry, Process and Economics. *Biofuels, Bioprod. Biorefin.* **2007**, *1*, 39−48.
(365) Qi, P.; Chen, S.; Chen, J.; Zheng, J.; Zheng, X.; Yuan, Y. Catalysis and Reactivation of Ordered Mesoporous Carbon-Supported Gold Nanoparticles for the Base-Free Oxidation of Glucose to Gluconic Acid. *ACS Catal.* **2015**, *5*, 2659−2670.
(366) Hermans, S.; Deffernez, A.; Devillers, M. Au−Pd/C Catalysts for Glyoxal and Glucose Selective Oxidations. *Appl. Catal., A* **2011**, *395*, 19−27.
(367) Zhang, H.; Cao, Y.; Lu, L.; Cheng, Z.; Zhang, S. Trimetallic Au/Pt/Rh Nanoparticles as Highly Active Catalysts for Aerobic Glucose Oxidation. *Metall. Mater. Trans. B* **2015**, *46*, 523−530.
(368) Sulman, E.; Doluda, V.; Dzwigaj, S.; Marceau, E.; Kustov, L.; Tkachenko, O.; Bykov, A.; Matveeva, V.; Sulman, M.; Lakina, N. Catalytic Properties of Ru Nanoparticles Introduced in a Matrix of Hypercrosslinked Polystyrene Toward the Low-Temperature Oxidation of D-Glucose. *J. Mol. Catal. A: Chem.* **2007**, *278*, 112−119.
(369) Huisman, G. H.; Van Rens, G. L. M. A.; De Lathouder, H.; Cornelissen, R. L. Cost Estimation of Biomass-To-Fuel Plants Producing Methanol, Dimethylether or Hydrogen. *Biomass Bioenergy* **2011**, *35* (Supplement1), S155−S166.
(370) Sanders, J. P. M.; Clark, J. H.; Harmsen, G. J.; Heeres, H. J.; Heijnen, J. J.; Kersten, S. R. A.; Van Swaaij, W. P. M.; Moulijn, J. A. Process Intensification in the Future Production of Base Chemicals From Biomass. *Chem. Eng. Process.* **2012**, *51*, 117−136.
(371) Stankiewicz, A. I.; Moulijn, J. A. Process Intensification: Transforming Chemical Engineering. *Chem. Eng. Prog.* **2000**, *96*, 22−34.
(372) Brewer, P. Separation Technology: a Solution for the Sugar Industry. *Filtr. Sep.* **2007**, *44*, 15−16.
(373) Jiang, L. Y.; Zhu, J. M. Separation Technologies for Current and Future Biorefineries—Status and Potential of Membrane-Based Separation. *Wires Energy Environ.* **2013**, *2*, 673−690.
(374) Sikdar, S. K.; Burckle, J.; Rogut, J. Separation Methods for Environmental Technologies. *Environ. Prog.* **2001**, *20*, 1−11.
(375) Zhao, L.; Zhao, H.; Nguyen, P.; Li, A.; Jiang, L.; Xia, Q.; Rong, Y.; Qiu, Y.; Zhou, J. Separation Performance of Multi-Components Solution by Membrane Technology in Continual Diafiltration Mode. *Desalination* **2013**, *322*, 113−120.
(376) Towler, G.; Sinnott, R. In *Chemical Engineering Design*, 2nd ed.; Towler, G., Sinnott, R., Eds.; Butterworth-Heinemann: Boston, 2013.
(377) Kiss, A. A.; Bildea, C. S. A Review of Biodiesel Production by Integrated Reactive Separation Technologies. *J. Chem. Technol. Biotechnol.* **2012**, *87*, 861−879.
(378) Schuth, F. *Catalytic Hydrogenation for Biomass Valorization*; The Royal Society of Chemistry: UK, 2015.
(379) Bui, L.; Luo, H.; Gunther, W. R.; Román-Leshkov, Y. Domino Reaction Catalyzed by Zeolites With Brønsted and Lewis Acid Sites for the Production of γ-Valerolactone From Furfural. *Angew. Chem.* **2013**, *125*, 8180−8183.
(380) Gilkey, M. J.; Xu, B. Heterogeneous Catalytic Transfer Hydrogenation as an Effective Pathway in Biomass Upgrading. *ACS Catal.* **2016**, *6*, 1420−1436.
(381) Johnstone, R. A. W.; Wilby, A. H.; Entwistle, I. D. Heterogeneous Catalytic Transfer Hydrogenation and Its Relation to Other Methods for Reduction of Organic Compounds. *Chem. Rev.* **1985**, *85*, 129−170.
(382) Wright, W. R. H.; Palkovits, R. Development of Heterogeneous Catalysts for the Conversion of Levulinic Acid to γ-Valerolactone. *ChemSusChem* **2012**, *5*, 1657−1667.
(383) Palkovits, R. Pentenoic Acid Pathways for Cellulosic Biofuels. *Angew. Chem., Int. Ed.* **2010**, *49*, 4336−4338.
(384) Deng, L.; Zhao, Y.; Li, J.; Fu, Y.; Liao, B.; Guo, Q.-X. Conversion of Levulinic Acid and Formic Acid Into γ-Valerolactone Over Heterogeneous Catalysts. *ChemSusChem* **2010**, *3*, 1172−1175.
(385) Du, X.-L.; He, L.; Zhao, S.; Liu, Y.-M.; Cao, Y.; He, H.-Y.; Fan, K.-N. Hydrogen-Independent Reductive Transformation of Carbohydrate Biomass Into γ-Valerolactone and Pyrrolidone Derivatives With Supported Gold Catalysts. *Angew. Chem.* **2011**, *123*, 7961−7965.
(386) Heeres, H.; Handana, R.; Chunai, D.; Borromeus Rasrendra, C.; Girisuta, B.; Jan Heeres, H. Combined Dehydration/(Transfer)-Hydrogenation of C_6-Sugars (D-Glucose and D-Fructose) to γ-Valerolactone Using Ruthenium Catalysts. *Green Chem.* **2009**, *11*, 1247−1255.
(387) Chia, M.; Dumesic, J. A. Liquid-Phase Catalytic Transfer Hydrogenation and Cyclization of Levulinic Acid and Its Esters to γ-Valerolactone Over Metal Oxide Catalysts. *Chem. Commun.* **2011**, *47*, 12233−12235.
(388) Luo, H. Y.; Consoli, D. F.; Gunther, W. R.; Román-Leshkov, Y. Investigation of the Reaction Kinetics of Isolated Lewis Acid Sites in Beta Zeolites for the Meerwein−Ponndorf−Verley Reduction of Methyl Levulinate to γ-Valerolactone. *J. Catal.* **2014**, *320*, 198−207.
(389) Tang, X.; Hu, L.; Sun, Y.; Zhao, G.; Hao, W.; Lin, L. Conversion of Biomass-Derived Ethyl Levulinate Into γ-Valerolactone Via Hydrogen Transfer From Supercritical Ethanol Over a ZrO_2 Catalyst. *RSC Adv.* **2013**, *3*, 10277−10284.
(390) Iglesias, J.; Melero, J. A.; Morales, G.; Moreno, J.; Segura, Y.; Paniagua, M.; Cambra, A.; Hernández, B. Zr-SBA-15 Lewis Acid Catalyst: Activity in Meerwein Ponndorf Verley Reduction. *Catalysts* **2015**, *5*, 1911−1927.
(391) Kuwahara, Y.; Kaburagi, W.; Osada, Y.; Fujitani, T.; Yamashita, H. Catalytic Transfer Hydrogenation of Biomass-Derived Levulinic Acid and Its Esters to γ-Valerolactone Over ZrO_2 Catalyst Supported on SBA-15 Silica. *Catal. Today* **2016**, 10.1016/j.cattod.2016.05.016.
(392) Tang, X.; Chen, H.; Hu, L.; Hao, W.; Sun, Y.; Zeng, X.; Lin, L.; Liu, S. Conversion of Biomass to γ-Valerolactone by Catalytic Transfer Hydrogenation of Ethyl Levulinate Over Metal Hydroxides. *Appl. Catal., B* **2014**, *147*, 827−834.
(393) Li, H.; Fang, Z.; Yang, S. Direct Conversion of Sugars and Ethyl Levulinate Into γ-Valerolactone With Superparamagnetic Acid−Base Bifunctional Zrfeox Nanocatalysts. *ACS Sustainable Chem. Eng.* **2016**, *4*, 236−246.

DOI: 10.1021/acs.chemrev.6b00311
Chem. Rev. 2016, 116, 12328−12368

(394) Li, H.; Fang, Z.; Yang, S. Direct Catalytic Transformation of Biomass Derivatives Into Biofuel Component γ-Valerolactone With Magnetic Nickel−Zirconium Nanoparticles. *ChemPlusChem* **2016**, *81*, 135−142.
(395) Zhu, S.; Xue, Y.; Guo, J.; Cen, Y.; Wang, J.; Fan, W. Integrated Conversion of Hemicellulose and Furfural Into γ-Valerolactone Over Au/ZrO_2 Catalyst Combined With ZSM-5. *ACS Catal.* **2016**, *6*, 2035−2042.
(396) Titirici, M.-M.; White, R. J.; Brun, N.; Budarin, V. L.; Su, D. S.; Del Monte, F.; Clark, J. H.; Maclachlan, M. J. Sustainable Carbon Materials. *Chem. Soc. Rev.* **2015**, *44*, 250−290.
(397) Lou, L.-L.; Du, H.; Shen, Y.; Yu, K.; Yu, W.; Chen, Q.; Liu, S. Chiral Ir(I) Complex Supported on External Surface Passivated SBA-15 as Heterogeneous Catalyst for Asymmetric Transfer Hydrogenation of Aromatic Ketones. *Microporous Mesoporous Mater.* **2014**, *187*, 94−99.
(398) Gao, J.; Zhang, X.; Yang, Y.; Ke, J.; Li, X.; Zhang, Y.; Tan, F.; Chen, J.; Quan, X. Surface-Passivated SBA-15-Supported Gold Nanoparticles: Highly Improved Catalytic Activity and Selectivity Toward Hydrophobic Substrates. *Chem. - Asian J.* **2013**, *8*, 934−938.
(399) Zang, W.; Li, G.; Wang, L.; Zhang, X. Catalytic Hydrogenation by Noble-Metal Nanocrystals With Well-Defined Facets: A Review. *Catal. Sci. Technol.* **2015**, *5*, 2532−2553.
(400) Pham, T. C. T.; Kim, H. S.; Yoon, K. B. Growth of Uniformly Oriented Silica MFI and BEA Zeolite Films on Substrates. *Science* **2011**, *334*, 1533−1538.
(401) Zhao, S.; Cheng, M.; Li, J.; Tian, J.; Wang, X. One Pot Production of 5-Hydroxymethylfurfural With High Yield From Cellulose by a Bronsted-Lewis-Surfactant-Combined Heteropolyacid Catalyst. *Chem. Commun.* **2011**, *47*, 2176−2178.
(402) Richter, F. H.; Pupovac, K.; Palkovits, R.; Schüth, F. Set of Acidic Resin Catalysts to Correlate Structure and Reactivity in Fructose Conversion to 5-Hydroxymethylfurfural. *ACS Catal.* **2013**, *3*, 123−127.
(403) Dabbawala, A. A.; Mishra, D. K.; Huber, G. W.; Hwang, J.-S. Role of Acid Sites and Selectivity Correlation in Solvent Free Liquid Phase Dehydration of Sorbitol to Isosorbide. *Appl. Catal., A* **2015**, *492*, 252−261.
(404) Nolan, M. R. Graduate Theses and Dissertations, Iowa State University, 2014.
(405) Parlett, C. M. A.; Wilson, K.; Lee, A. F. Hierarchical Porous Materials: Catalytic Applications. *Chem. Soc. Rev.* **2013**, *42*, 3876−3893.
(406) Parlett, C. M. A.; Isaacs, M. A.; Beaumont, S. K.; Bingham, L. M.; Hondow, N. S.; Wilson, K.; Lee, A. F. Spatially Orthogonal Chemical Functionalization of a Hierarchical Pore Network for Catalytic Cascade Reactions. *Nat. Mater.* **2015**, *15*, 178−182.
(407) O'Neill, B. J.; Jackson, D. H. K.; Lee, J.; Canlas, C.; Stair, P. C.; Marshall, C. L.; Elam, J. W.; Kuech, T. F.; Dumesic, J. A.; Huber, G. W. Catalyst Design With Atomic Layer Deposition. *ACS Catal.* **2015**, *5*, 1804−1825.
(408) Christensen, S. T.; Feng, H.; Libera, J. L.; Guo, N.; Miller, J. T.; Stair, P. C.; Elam, J. W. Supported Ru−Pt Bimetallic Nanoparticle Catalysts Prepared by Atomic Layer Deposition. *Nano Lett.* **2010**, *10*, 3047−3051.
(409) Libera, J. A.; Elam, J. W.; Pellin, M. J. Conformal ZnO Coatings on High Surface Area Silica Gel Using Atomic Layer Deposition. *Thin Solid Films* **2008**, *516*, 6158−6166.
(410) George, S. M. Atomic Layer Deposition: an Overview. *Chem. Rev.* **2010**, *110*, 111−131.
(411) Yang, X.-F.; Wang, A.; Qiao, B.; Li, J.; Liu, J.; Zhang, T. Single-Atom Catalysts: A New Frontier in Heterogeneous Catalysis. *Acc. Chem. Res.* **2013**, *46*, 1740−1748.
(412) Thomas, J. M.; Raja, R.; Lewis, D. W. Single-Site Heterogeneous Catalysts. *Angew. Chem., Int. Ed.* **2005**, *44*, 6456−6482.
(413) Sun, S.; Zhang, G.; Gauquelin, N.; Chen, N.; Zhou, J.; Yang, S.; Chen, W.; Meng, X.; Geng, D.; Banis, M. N.; Li, R.; Ye, S.; Knights, S.; Botton, G. A.; Sham, T.-K.; Sun, X. Single-Atom Catalysis Using Pt/Graphene Achieved Through Atomic Layer Deposition. *Sci. Rep.* **2013**, *3*, 1775.
(414) Yan, H.; Cheng, H.; Yi, H.; Lin, Y.; Yao, T.; Wang, C.; Li, J.; Wei, S.; Lu, J. Single-Atom Pd1/Graphene Catalyst Achieved by Atomic Layer Deposition: Remarkable Performance in Selective Hydrogenation of 1,3-Butadiene. *J. Am. Chem. Soc.* **2015**, *137*, 10484−10487.
(415) Jagadeesh, R. V.; Surkus, A.-E.; Junge, H.; Pohl, M.-M.; Radnik, J.; Rabeah, J.; Huan, H.; Schünemann, V.; Brückner, A.; Beller, M. Nanoscale Fe_2O_3-Based Catalysts for Selective Hydrogenation of Nitroarenes to Anilines. *Science* **2013**, *342*, 1073−1076.
(416) Jagadeesh, R. V.; Natte, K.; Junge, H.; Beller, M. Nitrogen-Doped Graphene-Activated Iron-Oxide-Based Nanocatalysts for Selective Transfer Hydrogenation of Nitroarenes. *ACS Catal.* **2015**, *5*, 1526−1529.
(417) Sun, P.; Long, X.; He, H.; Xia, C.; Li, F. Conversion of Cellulose Into Isosorbide Over Bifunctional Ruthenium Nanoparticles Supported on Niobium Phosphate. *ChemSusChem* **2013**, *6*, 2190−2197.
(418) Xi, J.; Zhang, Y.; Ding, D.; Xia, Q.; Wang, J.; Liu, X.; Lu, G.; Wang, Y. Catalytic Production of Isosorbide From Cellulose Over Mesoporous Niobium Phosphate-Based Heterogeneous Catalysts Via a Sequential Process. *Appl. Catal., A* **2014**, *469*, 108−115.
(419) Op De Beeck, B.; Geboers, J.; Van De Vyver, S.; Van Lishout, J.; Snelders, J.; Huijgen, W. J. J.; Courtin, C. M.; Jacobs, P. A.; Sels, B. F. Conversion of (Ligno)Cellulose Feeds to Isosorbide With Heteropoly Acids and Ru on Carbon. *ChemSusChem* **2013**, *6*, 199−208.
(420) Yamaguchi, A.; Sato, O.; Mimura, N.; Shirai, M. One-Pot Conversion of Cellulose to Isosorbide Using Supported Metal Catalysts and Ion-Exchange Resin. *Catal. Commun.* **2015**, *67*, 59−63.
(421) Nicolaou, K. C.; Edmonds, D. J.; Bulger, P. G. Cascade Reactions in Total Synthesis. *Angew. Chem., Int. Ed.* **2006**, *45*, 7134−7186.
(422) Climent, M. J.; Corma, A.; Iborra, S.; Sabater, M. J. Heterogeneous Catalysis for Tandem Reactions. *ACS Catal.* **2014**, *4*, 870−891.
(423) Ordomsky, V. V.; Van Der Schaaf, J.; Schouten, J. C.; Nijhuis, T. A. The Effect of Solvent Addition on Fructose Dehydration to 5-Hydroxymethylfurfural in Biphasic System Over Zeolites. *J. Catal.* **2012**, *287*, 68−75.
(424) Huber, G. W.; Chheda, J. N.; Barrett, C. J.; Dumesic, J. A. Production of Liquid Alkanes by Aqueous-Phase Processing of Biomass-Derived Carbohydrates. *Science* **2005**, *308*, 1446−1450.
(425) Anastas, P.; Eghbali, N. Green Chemistry: Principles and Practice. *Chem. Soc. Rev.* **2010**, *39*, 301−312.
(426) Sheldon, R. A. Green Solvents for Sustainable Organic Synthesis: State of the Art. *Green Chem.* **2005**, *7*, 267−278.
(427) Prat, D.; Hayler, J.; Wells, A. A Survey of Solvent Selection Guides. *Green Chem.* **2014**, *16*, 4546−4551.
(428) Welton, T. Solvents and Sustainable Chemistry. *Proc. R. Soc. London, Ser. A* **2015**, *471*, 20150502.

DOI: 10.1021/acs.chemrev.6b00311
Chem. Rev. 2016, 116, 12328−12368